W-AM-Sy1 STATISTICAL THERMODYNAMICS OF AN ALLOSTERIC PROTEIN: THE HUMAN HEMOGLOBIN MOLECULE

Michael L. Johnson and Gary K. Ackers
University of Virginia and Johns Hopkins University

A large amount of thermodynamic information has recently been obtained on the ligand-linked interactions in human hemoglobin. In particular, recent information which reflects decoupling of the interactions through subunit dissociation provides an important dimension for resolving mechanisms. This thermodynamic information is particularly important since cooperative ligand binding is, in essence, a thermodynamic phenomenon (i.e., the differences in Gibbs free energies at the successive binding steps). The recent results in combination with structural information impose narrow constraints on the range of possible mechanistic models.

We have developed statistical thermodynamic formulations of a number of models, including several previously proposed models, and tested them by numerical analysis against the extensive body of current experimental information. The models describe self-regulation in the hemoglobin system through the coupling between binding of oxygen and protons and the interactions between its subunits. A simple model which is consistent with currently available thermodynamic and structural information will be presented.

W-AM-Sy2 STATISTICAL THERMODYNAMIC ANALYSES OF THE POLYELECTROLYTE PROPERTIES OF DNA, M. Thomas Record, Jr., Department of Chemistry, University of Wisconsin, Madison, Wisconsin 53706.

DNA is a highly charged polyanion and consequently interacts strongly with electrolyte ions in solution, forming steep local gradients in the concentrations of these ions in its vicinity. Any process which modifies the linear charge density of the DNA (e.g. conformational transitions, binding of charged ligands) necessarily affects the extent of the electrolyte-DNA interactions. Consequently large effects of electrolyte concentration on the thermodynamics and kinetics of these processes are observed. Analysis of these electrolyte effects requires a statistical thermodynamic description of electrolyte-DNA interactions. Three such descriptions are available: the classical Poisson-Boltzmann cylindrical cell model, sometimes supplemented by the hypothesis of a local counterion binding equilibrium; Manning's molecular thermodynamic theory, supplemented by the hypothesis of a salt-invariant charge fraction; and Monte Carlo calculations.

Predictions of these theories for the radial distribution functions of electrolyte ions and/or for the thermodynamic properties of the polyelectrolyte solution will be reviewed. Results of cation NMR experiments designed to probe the local concentration and mode of interaction of cations with DNA will be discussed. The applications of these theories to the interpretation of ion effects on the conformational and ligand-binding equilibria of DNA, and related phenomena such as DNA compaction, will then be summarized. (That portion of these investigations originating from the author's laboratory was supported by grants from the NSF (PCM 79-04607) and NIH (GM23467).)

W-AM-Sy3 THE MOLECULAR STRUCTURES OF LIPID BILAYER MEMBRANES AND MICELLES. Ken A. Dill
Chemistry Department, University of Florida, Gainesville, FL 32611.

The amphiphilic chain molecules comprising lipid bilayer membranes and micelles are subject to intermolecular constraints imposed by "hydrophobic" forces, and by steric repulsive forces which prevent a given chain segment from occupying the volume excluded by another. The hydrocarbon chains are otherwise free to adopt statistical disorder, as in a liquid.

Statistical mechanical theory which takes account of these constraints predicts that membranes and micelles resemble "interphases". Interphases are not single phases of matter; the degree of order varies over molecular dimensions. In lipid bilayers, for example, there is a "disorder gradient", in which the hydrocarbon chains of the lipids are highly ordered near the polar head groups, and there is sharply increasing disorder toward the chain tails. Interestingly, theory predicts a reverse disorder gradient in micelles. The greatest disorder in micelles should be near the polar heads, and the order should sharply increase near the crowded center of the micellar core.

Related statistical theory accounts for the solubilities of small hydrophobic molecules in lipid bilayer membranes and micelles. Solute molecules are predicted to concentrate where chain disorder is greatest; at mid-bilayer in planar membranes and in outer regions of micellar hydrocarbon cores. These predictions are supported by neutron diffraction and spectroscopic experiments from other labs.

W-AM-Sy4 STATIC AND DYNAMIC MONTE CARLO CALCULATIONS OF MEMBRANE ORGANIZATION. Ernesto Freire, Department of Biochemistry, Univ. of Tennessee, Knoxville, TN 37916

Statistical mechanical methods have played an important role in the development of our current understanding of the relationships between molecular interactions, physical properties and organization in membrane systems. Unfortunately, analytical statistical mechanical descriptions of biological membranes are, at best, very difficult to obtain due to the intrinsic complexity of these systems. This situation has been alleviated by the development of very accurate numerical methods which take advantage of the availability of fast computers with large storage capacities. For the past few years our laboratory has been engaged in the development of a computer representation of the molecular organization of membrane systems using Monte Carlo techniques. These techniques have allowed us to calculate equilibrium distribution of molecules and time dependent phenomena such as spontaneous fluctuations around equilibrium and relaxation processes triggered by changes in the intermolecular potentials. These "computer experiments" generate the position coordinates of the entire molecular ensemble, thus allowing us to estimate physical or spectroscopic properties which depend on the topological localization of lipid and protein molecules within the membrane. These numerical methods can be used to transform physicochemical or spectroscopic data into organizational parameters of the membrane. (Supported by NIH Grant GM-27244).

W-AM-Min1 FLUORESCENCE AND EPR STUDIES OF BOUNDARY LIPID IN SARCOPLASMIC RETICULUM MEMBRANES. David D. Thomas, Dept. of Biochemistry, University of Minnesota Medical School; and Cecilia Hidalgo, Dept. of Muscle Research, Boston Biomedical Research Institute, Boston, MA 02114.

Previous studies have established a correlation between the fluidity of the lipid environment and the Ca-ATPase activity in sarcoplasmic reticulum. This implies an important role for that fraction of the lipid that is immediately adjacent to the enzyme. In order to investigate the physical state of this lipid population, we have used spin probes to study the hydrocarbon chain mobility (by EPR) and fluorescent probes to study the proximity of labeled phosphatidyl ethanolamine head groups to the protein (by fluorescence energy transfer). Long-chain maleimide spin labels attached covalently to the protein permitted the selective study of boundary lipid, without interference from probes far from the protein. In order to investigate the effect of the lipid environment on the protein's physical state, we monitored the protein rotational mobility by means of a short-chain maleimide spin label (using saturation transfer EPR). Results: Enzymatic activity, protein mobility, and boundary lipid mobility all decrease with decreasing lipid content, although the enzymatic activity shows a more marked decrease as the lipid content is reduced below 40 lipids per protein. A derivative of phosphatidyl ethanolamine, in which fluorescamine is attached to the phospholipid head group, is a potent quencher of trp fluorescence in the protein. Since R_0 for Förster energy transfer is only 24 Å, these probes must be in or near the boundary lipid. At high levels of this probe, the Ca-ATPase activity is unaffected, while Ca uptake is inhibited. These results illustrate several different mechanisms by which boundary lipid may affect the enzyme's physical state and activity.

W-AM-Min2 DYNAMICS OF THE INTERACTION OF BOVINE CYTOCHROME c OXIDASE WITH PHOSPHATIDYLCHOLINES. F.W. Dahlquist, M.R. Paddy, J.H. Davis and M. Bloom. (Intr. by B. Hudson). Inst. of Mol. Biol., U. of Oregon, Eugene, OR , and Physics Dept., U. of British Columbia, Vancouver, B.C. CANADA

^2H NMR and EPR spectra have been obtained as a function of temperature and protein concentration from the same samples of beef heart mitochondiral cytochrome c oxidase reconstituted into 1-(16',16',16'-trideuteriopalmitoyl)-2-palmitoleoyl-sn-glycero-3-phosphocholine. At all temperatures, the EPR spectra show the characteristic "bound" and "free" components, while the ^2H NMR spectra show only a narrow distribution of oreintational order parameters. At temperatures near the phase transition of the pure lipid, the dependence of the ^2H NMR average orientational order on protein concentration fits a two-state model in which the phospholipid molecules exchange rapidly between two states tentatively identified as sites either on or off the protein surface. From this model, the ^2H NMR spectra yield a value of 0.18 mg of phospholipid per mg of protein as necesssary to cover the surface of cytochrome c oxidase, which is the same value as derived from the EPR spectra at -20°C. Both the ^2H NMR and EPR spectra vary markedly with temperature. At temperatures well above the phase transition of the pure lipid, the average orientational parameters derived from the ^2H spectra are independent of protein concentration and are the same as for the lipid alone. Qualitatively, the EPR spectra show large apparent decreases in the average orientational order with increasing temperature. Analysis of ^2H NMR relaxation rates indicates an additional motion in the presence of protein with a correlation time of 10^{-6}-10^{-7} s assuming that the lipids on the protein surface are much more motionally restricted than the rest of the lipid. If this new motion represents exchange between the two states, such an exchange rate is compatible with the observed differences in the ^2H NMR and EPR spectra.

W-AM-Min3 MAGNETIC RESONANCE STUDIES OF LIPID-PROTEIN INTERACTIONS. Sidney Fleischer and J. Oliver McIntyre. Department of Molecular Biology, Vanderbilt University, Nashville, TN 37235.

D-β-hydroxybutyrate dehydrogenase (BDH) is a lipid-requiring enzyme with an absolute and specific requirement of lecithin (PC) for function. The purified enzyme, devoid of phospholipid (PL), inserts into PL vesicles and becomes reactivated. T_1 measurements of [N-$^{13}CH_3$] or [11-^{13}C] PC show that the rotational motion of the polar choline moiety, but not the hydrophobic domain, is slowed by insertion of BDH. This is unique compared with other systems and reflects the high specificity for PC for activation of BDH (Fleischer et al, Biochemistry, 1979). EPR studies using 16 doxyl-sn2 PC (SLI) reflect some perturbation of the PL after insertion of BDH. The motion of the PL in membranes containing the Ca^{++} pump protein (CPP) of sarcoplasmic reticulum (SR) has been studied by NMR and EPR. D-, P-, and H-NMR studies (Seelig et al, Biochemistry,1981; McLaughlin et al, BBA,1981; Deese et al, Biophys. J.,1982) reflect an homogeneous PL environment typical of a PL bilayer, i.e., if more than one PL environment exists, there is rapid exchange between them within the time scale of NMR ($>10^4$/sec). D-NMR studies using reconstituted membranes with high CPP content (RSR) indicate a small (10-20%) decreased motion and increased disorder of the PL. EPR studies using SLI in RSR indicate some perturbation of the PL. Spectral subtraction does not allow an unique interpretation; two extremes are possible, i.e, relatively few PL molecules are appreciably constrained in motion (10^8/sec) vs most or all PL are slightly perturbed (McIntyre et al, Biophys. J.,1982). The motion of BDH has been studied using selective labeling with spin labeled (SL) NADH or SL maleimide. The rotational motion of BDH and CPP are considerably slower than the constrained PL. [Supported by NIH AM 14632 and AM 21987].

W-AM-Min4 LIPID-PROTEIN INTERACTIONS IN MEMBRANES CONTAINING THE ACETYLCHOLINE RECEPTOR.
M.G. McNamee and J.F. Ellena, Dept. Biochem. & Biophys., Univ. of Calif., Davis, CA 95616

Interactions between Torpedo californica acetylcholine receptor and its lipid environment have been studied in native acetylcholine receptor enriched membranes and in reconstituted vesicles prepared from purified receptor and defined lipids. The electron paramagnetic resonance spectrum of 16-doxylstearic acid revealed two spectral components in both native and reconstituted membranes. One component (∿75% of the integrated spectral intensity in native membranes) was characteristic of the spin probe in fluid lipid bilayers. The second component (∿25% of the spectral intensity) was broader and was characteristic of motionally restricted spin probes. The distribution of spin probe between the two spectral environment was independent of temperature over a range of -5 to 25°C although the maximum splittings of both spectral components were temperature dependent. Similar results were obtained in reconstituted membranes at comparable lipid to protein ratios (160:1; mole:mole). The relative amount of the motionally restricted component decreased as the lipid to protein ratio was increased. In parallel studies with phospholipid spin labels containing 16-doxylstearate in the No. 2 position, the amount of motionally restricted label was less than that observed with the free fatty acid (<15% vs. 25%). The results are consistent with the boundary lipid concept and suggest a preferential association of the free fatty acids with the protein. The ion flux properties of both native and reconstituted acetylcholine receptor membranes are very sensitive to the lipid environment and experiments are in progress to determine if functional changes can be correlated with electron paramagnetic resonance spectral changes. (Supported by NIH Grant NS13050).

W-AM-Min5 EQUILIBRIUM CONSTANTS AND NUMBER OF CONTACT SITES IN LIPID-PROTEIN INTERACTIONS IN MEMBRANES. Patricia C. Jost and O. Hayes Griffith, Institute of Molecular Biology, University of Oregon, Eugene, OR 97403

On the basis of compositional and magnetic resonance experiments from several laboratories, the following picture of lipid-protein interactions in membranes has emerged: 1) a significant fraction of membrane lipid must be at the lipid-protein interface (interfacial or boundary region); 2) essentially all lipid at the lipid-protein interface exchanges with the bulk bilayer, as demonstrated both by ESR and by NMR data; 3) there are a large number of contact or binding sites on the hydrophobic protein surface; 4) lipid spin labels at these sites are restricted in motion and spatially disordered by their interaction with the irregular protein surface; and 5) the influence of the protein on lipid dynamics decreases sharply with distance in the plane of the bilayer. The next step in characterizing lipid-protein interactions is to determine the thermodynamics of the interactions, e.g., the number of contact (binding) sites, the value of the relative binding constants for different lipids and the free energies of association. A general multiple equilibria binding treatment has been developed for membranes. With this treatment and ESR data using spin labeled lipids, the total number of contact or binding sites is available for several systems. Cases have been observed for average relative equilibrium binding constants of less than, greater than or equal to unity relative to the unsaturated phosphatidylcholines chosen as the reference state. The experimental plots obtained are in good agreement with the theory and provide methods for determining which lipids are in contact with proteins under physiological conditions, and for characterizing both specific and non-specific lipid-protein associations. Supported by NIH GM 25698.

W-AM-A1 MONODISPERSITY: A CONCEPT IN ALKALINE ELUTION. S.C. vanAnkeren[†], K.W. Kohn[††] and K.T. Wheeler[†], [†]Cancer Center, University of Rochester, Rochester, NY, 14642 and [††]Lab. Mol. Pharmacol., DCT, NCI, NIH, Bethesda, MD, 20014.

The process which governs removal of DNA from filters during alkaline elution is not completely understood. However, the elution kinetics for a given DNA size distribution can be defined mathematically. When the percentage of DNA retained is plotted versus elution time, 1st order kinetics result for random DNA size distributions. Monodispersed distributions should result in linear kinetics; a constant percentage of the DNA elutes with time. The removal kinetics for 9L rat brain tumor cell DNA from 2μm polycarbonate filters were compared to these theoretical models. After irradiation with 0-300 rads, the cells were lysed on the filters with an SDS solution, and the DNA eluted with a solution of tetrapropylammonium hydroxide, SDS, and EDTA at pH 11.0 or 12.3. The DNA on some filters was eluted immediately while the DNA on others was held in eluting solution up to 48 hr before elution. Irradiated DNA, held or unheld, eluted with 1st order kinetics. Unheld unirradiated DNA eluted with complex kinetics. If held at least 24 hr, this DNA eluted with linear kinetics. Both irradiated and unirradiated DNA eluted faster if held for 24 hr at pH 12.3. Holding these DNAs at pH 11.0, below the critical unwinding pH, produced no effect on the elution profiles. Comparison of the experimental data to the theoretical model suggests that after holding at pH 12.3, undamaged DNA molecules elute as a monodispersed distribution while damaged DNA molecules elute as a smaller random distribution. (Supported by CA-21662 and CA-11198. S.C.V. was supported by the DOE Graduate Participant Program.)

W-AM-A2 FIELD REVERSAL TRANSIENT ELECTRIC BIREFRINGENCE OF DNA RESTRICTION FRAGMENTS. Don Eden and John G. Elias, Department of Chemistry, Yale University, New Haven, CT 06511.

We have analyzed the transient electric birefringence response of field reversal experiments performed on DNA restriction fragments in order to characterize the amplitude and temporal behavior of the ionic polarization of the molecules. 64 to 5000 bp monodisperse fragments have been studied at 4°C at neutral pH in sodium phosphate buffer. Contributions to the polarization, both parallel and perpendicular to the molecular axis, have been considered using the theory of Tinoco and Yamaoka. From an analysis of the depth and position of the birefringence minimum upon field reversal we observe, for fragments $\leq$ 267 bp, that the relaxation parallel to the helix is consistent with Mandel's prediction: $\tau = L^2/12D$, where L is the length of the DNA and D is the translational diffusion constant of the counterions. For Na^+=1mM, $D=1.9\times10^{-6}cm^2sec^{-1}$. This is approximately one sixth that of free Na^+, suggesting that the Na^+ interacts strongly with the phosphates. In these fragments we also observe a slow, weak transverse component in the polarization. Typically, the transverse amplitude is less than 10% of the parallel amplitude and the associated relaxation time is 10 times that for rotational diffusion. For fragments larger than 267 bp the shape of the birefringence signal changes dramatically. Local maxima appear and the decays are no longer single expotential. For a 410 bp fragments the ratio of the $\parallel$ to $\perp$ amplitudes of the ionic polarization decreases from 5 to 1 when the Na^+ concentration is increased from 0.2 to 4 mM. Concomitantly there is a five fold decrease in the relaxation time of the perpendicular component. At a constant ionic strength of 1 mM the amplitude ratio, $\parallel:\perp$, approaches 4/3 for large fragments. This work was supported in part by NIH Grant RR-07015.

W-AM-A3 PERSISTENCE LENGTH OF DNA FROM ULTRA-LOW-ANGLE LIGHT SCATTERING. S. A. Ringer, E. S. Sobel, and J. A. Harpst. (Intr. by J. E. Jentoft) Dept. of Biochemistry, Case Western Reserve Univ., Cleveland, OH 44106

An improved Rayleigh light scattering photometer has been used to make reliable measurements at ultra-low angles on high-molecular-weight, native DNA from bacteriophage T7 in a phosphate buffer at 0.195 M Na^+. Light scattering results were obtained from reciprocal-intensity plots and the $P^{-1}(0)$ curve was generated from data in the angular range, 4-70°. Linear extrapolations to zero angle were made only from the limiting 4-9° region of the $P^{-1}(0)$ curve. Measurements on T7 DNA gave a molecular weight of (26.5 ± 0.3) x 10^6 and a root-mean-square radius of (520 ± 20) nm. The experimental $P^{-1}(0)$ curve has been fitted to a theoretical curve, derived from the wormlike coil model for DNA, by the procedure developed recently by Harpst (Biophys. Chem. 11 (1980) 295). Comparison of these curves gave a persistence length for T7 DNA of (45 ± 5) nm and an excluded volume parameter of 0.07. Light scattering measurements have also been made on DNA from T5 bacteriophage. Analysis of these data by the methods noted above gave a molecular weight of (81 ± 2) x 10^6, a root-mean-square radius of (940 ± 60) nm, a persistence length of (40 ± 5) nm, and an excluded volume parameter of 0.07. The persistence length and excluded volume parameter are essentially the same as those derived for T7 DNA. These studies provide reasonable values for the persistence length and the excluded volume parameter for high-molecular-weight DNA. In addition the excellent agreement between experiment and theory has given a direct verification of the wormlike coil model for the behavior of DNA.

(Supported by USPHS, NIH grants GM-21946, GM-14252, and 5T-01-GM-0035).

W-AM-A4 X-RAY SCATTERING FROM THE SUPERHELIX IN DISSOLVED CIRCULAR DNA. G.W. Brady, H. Lambertson, V. Grassian and D. Foos, Rensselaer Polytechnic Institute, Troy, N.Y. 12181 and N.Y. State Department of Health, Albany, N.Y. 12201

Earlier communications (1,2) presented preliminary results in the scattering from superhelical DNA. These were semi-quantitative because of the slit-smearing effects and interference of part of the pattern by scattering from the slits. Using a new apparatus, which will be described, we have succeeded in eliminating these two effects, and have determined updated accurate values for the pitch angle and contour length of the superhelix of circular plasmid COP68 DNA. These are 60° and 1020 A respectively, as contrasted with the preliminary estimates of 45-55° and 920 A. Addition of an intercalator causes a decrease in contour length and radius, and an increase in pitch, although this latter increase is not as great as the radius decrease. This shows that the unwinding of the superhelix is by a rotation mechanism rather than by a simple extension of the duplex axis. The superhelix density can also be directly determined from the measurements. The value found is 0.072, in good agreement with the value 0.069 determined by ethidium bromide (EB) titration and based on an unwinding angle of 26° for EB (3). Since the x-ray value follows directly from the results without any assumptions, it can also be regarded as a confirmation of the 26° EB unwinding angle.

(1) G.W. Brady, D.F. Fein and H. Brumberger (1976). Nature 264, 231-234.
(2) C.J. Benham, G.W. Brady and D.B. Fein (1980). Biophys. J. 29, 351-366.
(3) J.C. Wang, (1974). J. Mol. Biol. 89, 738-801.

W-AM-A5 SELECTIVE INHIBITION OF REPLICON INITIATION AND RELAXATION OF SUPERCOILING IN DNA OF MAMMALIAN CELLS BY NEOCARZINOSTATIN Lawrence F. Povirk and Irving H. Goldberg, Department of Pharmacology, Harvard Medical School, Boston, MA 02115

At low doses the protein antibiotics neocarzinostatin and auromomycin severely inhibited DNA replicon initiation in CHO cells while having no effect on elongation of previously initiated replicons. The selectivity of the effect on initiation was greater than that seen with other chemical agents and comparable to that seen with ionizing radiation. Parallel experiments using the nucleoid sedimentation technique showed that half-maximal relaxation of domains of DNA supercoiling and half-maximal inhibition of replicon initiation required approximately the same dose of neocarzinostatin, 0.05 ug/ml. These results and similar results obtained with auromomycin support the view that relaxation of supercoiling and inhibition of replicon initiation are related phenomena. In contrast, bleomycin appeared to relax supercoils at doses which had no detectable effect on replicon initiation. However, interpretation of results with bleomycin is complicated by the previously reported heterogeneity of DNA damage by this drug. (Z.M. Iqbal, K.W. Kohn, R.A.G. Ewig & A.J. Fornace, Jr., Cancer Res. 36: 3834-3838 (1976)). (Work supported by grant GM 12573 and fellowship 06475 from the National Institutes of Health)

W-AM-A6 SEQUENCE AND SUPERHELICITY DEPENDENCE OF THE HELICAL STRUCTURE OF DNA IN SOLUTION

Lawrence J. Peck and James C. Wang, Depertment of Biochemistry and Molecular Biology, Harvard University, Cambridge, Massachusetts 02138.

Several sequences, including $d(G)_n \cdot d(C)_n$, $d(A)_n \cdot d(T)_n$ and $d(CG)_n \cdot d(CG)_n$ have been cloned into the plasmid pBR322 and their helical structures in solution were examined by the topoisomer band shift method (Wang, J. C., Proc. Natl. Acad. Sci. USA 76, 200-203, 1979). As previously reported (Peck, L. J. and Wang, J. C., Nature 292, 375-378, 1981), under physiological conditions all sequences have right-handed structures. The sequence $d(A)_n \cdot d(T)_n$ is the only one with a tenfold helix; within experimental error all others have helical repeats around 10.6 base pairs per turn. The sequence $d(CG)_n \cdot d(CG)_n$ is unique. We have confirmed the observations of others that in several molar salt this sequence assumes a left-handed helical structure. Furthermore, our results demonstrate that even in a low salt medium such a sequence also assumes a left-handed geometry if the DNA is negatively supercoiled. These results make it possible to determine the difference in free energy between the left and right-handed helices under physiological conditions.
(Supported by a grant PCM 78-05892 from the National Science Foundation.)

W-AM-A7 LOCALIZED VIBRATIONAL MODES OF THE DOUBLE HELIX, E.W. Prohofsky, B.F. Putnam and L.L. Van Zandt. Dept. of Physics, Purdue U., West Lafayette, IN 47907.

Regions of an extended system which are unique have unique vibrational modes. These modes are called localized modes and we have applied methods for calculating such local modes to unique regions of the DNA double helix. Examples of unique regions are melted regions, forks, palindromic regions, bends, kinks, ends and regions of unique base composition. A thorough investigation has been completed for a free end of a poly(dG)·poly(dC)B helix. One result is that the rms amplitude of the vibrations which stretch the hydrogen bonding of the bases is considerably larger near the free end. Other unique resonances near the end have been calculated. The increase in rms hydrogen bond stretch should influence helix melting. This work required a formulation of several elastic parameters of the DNA helix which are consistent with models of helix vibrational modes. We projected out compression, bending, shearing, torsion and elastic force constants from a long range nonbonded interaction model which was based on acoustic velocity measurements. These elastic parameters are in reasonable agreement with other estimates. (This work supported in part by NSF grant DMR 78-20602 and NIH grant GM 24443.)

W-AM-A8 Fe-57 MOSSBAUER AND H-1 NMR STUDIES OF THE SPIN STATES OF IRON IN ITS COMPLEXES WITH THE ANTITUMOR AGENT, BLEOMYCIN-A_2, AND DNA. A. Levy and J.C. Walker, Dept. of Physics, Johns Hopkins Univ., Baltimore, MD 21218; R.P. Pillai, G.A. Elgavish and J.D. Glickson, (Intr. by N. Rama Krishna) Comprehensive Cancer Center, Univ. of Ala. in Birmingham, Birmingham, AL 35294

The putative mode of action of the bleomycins as anticancer agents is degradation of DNA mediated by their iron complexes. However, the detailed mechanism is not yet known. We have been carrying out studies on the complex Fe(III)-bleomycin-A_2 and on the ternary system Fe(III)-A_2-DNA by Mossbauer and NMR spectroscopy to characterize the iron spin states. This might be the key to the role of this complex in DNA cleavage. The Mossbauer spectra in the binary complex demonstrate that the system has a mixture of iron in different spin states. The presence of two different high spin Fe(III), low spin Fe(III) and high spin Fe(II) is manifest. The variation in the hyperfine field and in the quadrupole splittings also indicates that in each of these spin states the iron is surrounded by different ligand field. Variation of the sample pH demonstrates gradual shifts in the relative populations of the different spectral species. Similar effects are observed when the sample is preheated. NMR spectra of the same preheated Fe(III) sample show the emergence of hyperfine shifted signals which are typical of the spectrum of the Fe(II)-bleomycin complex. Preliminary studies indicate that the system Fe-bleomycin-poly(dA-dT) gives rise to an altered Mossbauer spectrum in which the high spin Fe(III) species is predominant. The hyperfine field and quadrupole splitting are significantly enlarged indicating a ligand field distortion upon interaction with the synthetic DNA. This might indicate that interaction of Fe-bleomycin with DNA is accompanied by changes in the equilibria of the different Fe-bleomycin complexes. These changes might turn out to be important in the DNA cleavage processes.

W-AM-A9 KINETIC MEASUREMENTS OF E. COLI RNA POLYMERASE ASSOCIATION WITH T7 MAJOR AND MINOR PROMOTERS. Carol L. Cech, Dennis E. Prosen, Chris J. Dayton, Kathryn L. Parker, Department of Chemistry, University of Colorado, Boulder CO 80309.

During infection of E. coli by bacteriophage T7, E. coli RNA polymerase utilizes only three promoters (A1,A2,A3.) In vitro, the A promoters predominate at very low polymerase concentration, but at higher concentration the minor B,C,D, and E promoters are used with equal efficiency. The binding constant for the initial association of polymerase with promoters and the forward rate of isomerization to an "open" complex capable of initiation have been independently measured for the A1, A3, D, and C promoters using the abortive initiation reaction. Reactions were measured at 80mM KCl, 10mM $MgCl_2$, pH8, 37° using restriction fragments 470 to 1500 base-pairs in length. Both major and minor promoters isomerize rapidly ($t_{1/2}$=11 to 27 sec.) The minor complexes isomerize less than two times slower than the major complexes. In contrast, initial binding to the minor promoters ($K_I=10^7$) is at least 10-fold weaker than binding to major promoters ($K_I \geq 10^8$), suggesting promoter selectivity in the T7 system occurs at the point of initial binding. No evidence was found to indicate that initiation itself is ever rate-limiting in T7. Kinetic measurements of the A1 and C promoters on intact T7 gave identical results. The rate of association to open complex thus appears to be independent of template length for DNA fragments 500 base-pairs or longer. All open complexes dissociated with halflives longer than one hour. Overall equilibrium binding constants estimated from kinetic measurements ranged from 10^{10} to $\geq 10^{11}$ for minor and major promoters, respectively. Kinetics of association to the C promoter at 10° were also measured.

W-AM-A10 MOLECULAR MECHANISM OF PROMOTER SEARCH BY RNA POLYMERASE. Cheng-Wen Wu and Chan-Suk Park, Department of Pharmacological Sciences, State University of New York at Stony Brook, New York 11794.

The rapid-mixing photocrosslinking technique, in conjunction with an immunoprecipitation assay developed to measure the change in the distribution of Escherichia coli RNA polymerase molecules bound to T7 DNA, has been applied to investigate the molecular mechanism of promoter search by RNA polymerase. The binding of RNA polymerase to the DNA template can be divided into at least two steps. The initial binding is rapid and occurs at nonspecific sites randomly distributed throughout the DNA molecule. This is followed by a relatively slow promoter search in which RNA polymerase is transferred from nonspecific sites to promoter sites through a series of intramolecular processes. The rate of polymerase loss from a segment of DNA which does not contain promoter sites is a function of the distance from this segment to both the promoter sites and the ends of the DNA molecule. The kinetic data are consistant with a molecular mechanism in which RNA polymerase undergoes a net bidirectional linear diffusion along the DNA template to search for the promoter site. This interpretation is supported by the computer simulation which correctly predicts the relative rates of polymerase loss from various DNA segments. The mechanism derived from these studies is in accordance with the notion that the whole DNA molecule serves as an effective sink for trapping and guiding polymerase molecules during promoter search. (Supported by NIH grant GM 28069 and ACS grant NP 309).

W-AM-A11 TRANSCRIBABLE AND NON-TRANSCRIBABLE DNA CONFORMATIONS. G.L. Eichhorn, Y.A. Shin, J.J. Butzow, and B.F. Hughes. National Institutes of Health, National Institute on Aging, Gerontology Research Center, Baltimore, MD 21224.

We have previously shown that metal ions can influence the conformation of nucleic acids either by stabilizing one or another conformation or even by becoming a part of the nucleic acid structure. Recently the discovery of "Z-DNA" - a left-handed double helix - has caused much excitement; the formation of this structure is also dependent on metal ions. If Z-DNA or any other DNA conformation has any importance in biological phenomena, one would expect that conformation to affect biological information transfer involving DNA acting as a template. We have therefore investigated the conversion of poly(dGdC) from B to Z-DNA by $Co(NH_3)_6Cl_3$ and discovered that this conversion has very little effect on the transcription of poly(dGdC) by E. coli RNA polymerase. We also discovered that $Co(NH_3)_6Cl_3$ under certain experimental conditions leads not only to the conversion of B to Z-DNA, but to further conversion of Z-DNA to a form which we call X-DNA, which resembles A-DNA in its CD characteristics, and which does have a much lower ability to be transcribed. Under somewhat different conditions Z-DNA is also converted to ψ-DNA, the highly compacted structure with a very large CD intensity. Under these conditions RNA synthesis is also inhibited. Thus Z-DNA itself is not significantly different in template activity from B-DNA, but it can act as an intermediate for the conversion of DNA into non-transcribable template forms. The fact that the very different B and Z forms are approximately equally well transcribed is in accord with the possibility of localized conformational changes in DNA molecules being transcribed.

W-AM-A12 QUANTITATIVE ASSESSMENTS OF GENOMIC RELATEDNESS DERIVED FROM DNA THERMAL DENATURATION DATA. A. T. Ansevin and D. L. Vizard, Department of Physics, University of Texas System Cancer Center, Houston, Texas 77030.

High resolution methods of DNA thermal denaturation frequently provide remarkably detailed profiles of the extent of denaturation versus temperature. Comparison of such profiles for DNAs from two different sources gives an immediate qualitative impression of the extent to which they may be related. When the general match is good and deviations can be ascribed to a particular region of the profile, subtraction may be used to quantitate the amount of inserted or deleted DNA in mutant viruses or constructed plasmids. However, the subtraction technique loses much of its applicability when DNA profiles are sufficiently dissimilar. In an effort to quantitate the relationship among different genomes using the wealth of information present in high resolution denaturation profiles, we have developed two systematic comparison methods, one yielding a similarity index and the other a dissimilarity index. The similarity index, with a scale from 0 to 1, takes account of the detailed shape of profiles and is appropriate for relatively closely related genomes. The dissimilarity index, which has a scale from 0 (identity) to infinity, does not directly evaluate shape but can be used in estimating the minimum degree of sequence divergence between distantly related DNA populations, assuming that the sequence departure is linearly related to differences in melting temperature and to the number of base pairs involved. Computer programs have been written in Basic to calculate both indices and the evaluations are applied to a series of bacteriophages infecting B. subtilis. The validity of these approaches is assessed by comparison to previously published restriction fragment data and clasic genetic tests for the same DNAs. Supported by NIH grant GM23067.

W-AM-A13 PHYSICAL CHARACTERISTICS OF THE RECONSTITUTION INTERMEDIATES OF 30S RIBOSOMAL SUBUNITS
Ming F. Tam and Walter E. Hill, Chemistry Department, University of Montana, Missoula MT 59812

The isolated reconstitution intermediates (RI_{30} and RI^*_{30}) from the 30S ribosomal subunit of Escherichia coli were physically characterized by sedimentation, diffusion and density measurements. The characteristics of these particles, each having 10 proteins bound, were compared with the characteristics of 16S RNA and the reconstituted 30S subunit. The results show that binding of the 10 proteins on the 16S RNA at 4°C does not markedly affect the folding of the RNA molecule. However, upon heating at 40°C to form the RI^*_{30} particle, significant folding of the RNA took place giving a structure significantly more compact than that of the 16S rRNA or the RI_{30} particle. There is no further conformational change between the RI^*_{30} particle and the reconstituted 30S subunit formed by addition of the remaining proteins. (Research supported in part by Grant #GM27201 from the National Institutes of Health)

W-AM-B1 RECOVERY OF INTRACELLULAR pH (pH_i) IN FROG SKELETAL MUSCLE: EFFECTS OF MEMBRANE VOLTAGE AND OF INHIBITORS. R.F. Abercrombie and A. Roos, Department of Physiology & Biophysics, Washington University School of Medicine, St. Louis, MO 63110.

The pH_i (Thomas-style microelectrodes) of frog semitendinosus muscle in normal 2.5 K^+ Ringer falls from 7.18 ± .03 to 6.8 ± .03 when, at pH_o 7.35, HEPES is replaced by 5% CO_2-HCO_3^-. The CO_2-depressed pH_i does not recover in 2.5 K^+ Ringer but does in 50 K^+-normal Cl^- (Biophys. J. 33: 62a, 1980). Measurements were made 40 min after contracture. Recovery rate is 40-50% less (a) when depolarization is achieved by 50 K^+ at normal K^+.Cl^- product (Cl_o reduced to 5.9); (b) when 0.1 mM 4-acetamido-4'-isothiocyanostilbene-2,2'-disulfonic acid (SITS), an inhibitor of anion transport, is added to the 50 K^+-normal Cl^- superfusate; or (c) with acid loading (50 K^+-normal Cl^-) by 5,5-dimethyl-2,4-oxazolidinedione (DMO) in the nominal absence of HCO_3^-. Amiloride (0.5 mM) reduces pH_i recovery by about one-half, and in combination with SITS by ~70%. Na replacement by N-methyl-D-glucamine abolishes recovery. In hypertonic medium (250 mM mannitol), depolarization also evokes a Na-dependent pH_i recovery after acid loading. However, the amiloride sensitive component now predominates, and SITS has a small effect. Also, there is less difference between depolarization in normal Cl^- and in normal K^+.Cl^-, and recovery is only slighly reduced by removing HCO_3^-. These results suggest that two, normally dormant, Na-dependent mechanisms for pH_i regulation are set in motion upon depolarization. One is SITS-sensitive and probably involves Cl^- and HCO_3^-. The other is SITS-insensitive but amiloride-sensitive and predominates in hypertonic medium. Supported by NIH Grant HL00082 to A.R.

W-AM-B2 EXTERNAL Na (Na_o) INHIBITION OF K EFFLUX FROM HUMAN RED CELLS. Isabel Bize*, Daniel C. Tosteson, and Mitzy Canessa; Department of Physiology & Biophysics, Harvard Medical School, Boston, MA 02115.

K efflux from fresh cells into Na medium containing 0.1 mM ouabain is 2.3 ± 0.16 mmol/l cells x hr (n = 7). The replacement of Na_o by choline, TEA, TMA and methylglucamine markedly increased K efflux to 4.02 ± 0.15 mmol/l cells x hr. The effect of Na_o is specific since it cannot be replaced by external Rb, Cs, or Li. K efflux into a Na-free medium is inhibited by external Ca or Mg to similar values as measured in Na medium. The concentration for half-maximal inhibition of K efflux was 0.5 mM for Mg and Ca.

In cells loaded by the nystatin procedure to contain only cellular K, the K efflux is not inhibited by Na_o or external Mg. The requirement for internal Na excludes the Gardos effect, and suggests a role for Na-K cotransport or the Na pump. To assess the effect of Na in outward Na-K cotransport, we investigated the effect of 1 mM furosemide. Although Na_o inhibited up to 50% of the outward K cotransport, the furosemide-resistant Na_o-inhibited K efflux was 5 times higher than the cotransport component. The Na_o-inhibited K efflux was also observed in the presence of ouabain plus bumetamide, DIDS, amiloride, oligomycin, and nitrate in the medium.

In fresh cells loaded with 1 mmol/l cells of Li, K efflux into Na-free medium was markedly inhibited (2.5 ± 0.1 mmol/l cells x hr) and became insensitive to Na_o and external Mg. These results suggest the presence of a passive movement for K specifically inhibited by Na_o and by therapeutic concentrations of cellular lithium. The relationship of this passive movement of K to a proton-conductive pathway and/or to K channels is under investigation. Supported: NIH GM-25686.

W-AM-B3 THE RELATIONSHIP BETWEEN Na COUNTERTRANSPORT AND Na-K COTRANSPORT IN HUMAN RED CELLS. Mitzy Canessa, Norma Adragna, and Daniel C. Tosteson; Department of Physiology & Biophysics, Harvard Medical School, Boston, MA 02115.

Several experimental findings indicate that Na countertransport and cotransport can be operationally defined as two different Na transport systems. They differ in their apparent affinity for intracellular Na or Li as well as in their sensitivities to bumetamide, to replacement of chloride by nitrate, in their response to external divalent ions, and in their capacity to couple the energy of the K gradient to drive the uphill movement of Na.

Studies in different populations of hypertensive patients seem to indicate that, despite differences in their functional properties, Na countertransport and Na-K cotransport are similarly regulated. In a Caucasian population, we found that elevated countertransport correlated significantly with elevated cotransport in patients with essential hypertension. In Black hypertensive patients with reduced Na-K cotransport, countertransport was not significantly elevated as previously found in Paris. Indeed, the discovery of these demes of red cell Na transport may be an important tool for research in the genetic epidemiology of human hypertension. In order to determine whether these two transport systems are under genetic control, we have studied intrafamiliar correlations for parent-child, mother-child, and sib-sib for both transport systems in 30 families. These data suggest that Na cotransport and countertransport might be related by gene-environment interactions.

This work was supported by NIH grant HL-25064.

W-AM-B4 INTERNAL PROTONS ARE COMPETITIVE INHIBITORS OF CHLORIDE EXCHANGE IN HUMAN ERYTHROCYTES.

GUNN, R.B. AND M.A. MILANICK. Dept. of Physiology, Emory University, Atlanta, GA 30322 and Dept. of Biophysics and Theoretical Biology, Univ. of Chicago, IL 60637.

We measured the effect of internal protons on chloride exchange across resealed human red cell ghost membranes containing less than 1/20th of the hemoglobin concentration within normal red cells. The results were qualitatively the same using either ghosts with a constant internal ionic strength (KCl substituting for K-gluconate) or ghosts with increasing ionic strength (KCl only). The efflux media contained either 22 mM KCl, 128 mM K-gluconate, 27 mM glycylglycine pH 6.8 or 50 mM KCl, 27 mM glycylclycine and sufficient sucrose to balance the internal osmolarity, pH_o=6.8 and pH_o=7.8. A Lineweaver-Burke plot of the flux values obtained at low intracellular chloride concentrations (<150 mM) was linear and extrapolated to the same maximum flux value at several fixed internal pH values between 5.7 and 7.8. This suggest that the internal proton is primarily competitive in this pH range. The slopes of the Dixon plots (1/flux vs. H^+_{in}) obtained at 100, 200, 400, and 600 mM internal chloride tend to zero as Cl increases. This indicates competitive inhibition by the internal proton and the formation of only TCl_{in} and TH_{in} complexes between the transporter(T) and Cl_{in} and H_{in}, and excludes the formation of $TClH_{in}$ when pH_{in}>5.7. At high intracellular chloride concentrations (>400 mM) the flux decreased as the concentration of chloride increased although the extracellular concentration was fixed. Thus the anion transport mechanism shows substrate inhibition by internal chloride. Supported by USPHS grants HL-20365 and GM-28393.

W-AM-B5 EVIDENCE FOR SPECIFIC SH-GROUP PARTICIPATION IN Cl^-DEPENDENT K^+ FLUXES OF LK SHEEP RED CELLS. P.K. Lauf, Department of Physiology, Duke University Medical Center, Durham, N.C. 27710.

In low potassium (LK) sheep red cells a part of the ouabain-insensitive passive K^+ flux requires the obligatory presence of Cl^- or Br^- anions and can be stimulated by osmotic cell swelling (Dunham & Ellory, 1980) or by N-ethylmaleimide (NEM) in isosmotic media (Lauf & Theg, 1980). As Cl^- dependent K^+ flux exists in reticulocytes of both high potassium (HK) and LK sheep, but disappears in mature HK red cells (Lauf, 1981), this K^+ transporter is of interest with respect to the origin of the HK/LK dimorphism. This study addresses further the specificity of the NEM effect and its relationship to the hyposmotically induced K^+ fluxes. When LK cells were exposed to NEM in NO_3^- media of pH values increasing from 6.8 to 8.2, Cl^- dependent K^+ efflux measured at pH 7.4 in Cl^- media was at a maximum in cells NEM-treated around pH 7 but in cells NEM-treated around pH 8 the K^+ efflux fell to values of untreated controls. Hence the K^+ efflux stimulation caused by NEM may be due to adduct formation with acidic thiol groups, i.e. SH groups with neighboring positive charges which may modulate the Cl^- dependence or the flow of K^+ ions across the LK membrane. Surprisingly, exposure of LK cells to iodoacetamide or iodoacetic acid prior to NEM treatment abolished the stimulatory effect of NEM indicating that SH group alkylation may result in a carrier conformationally different from that after NEM treatment alone and/or that there are other SH groups with different pK values controlling the reactivity of the NEM susceptible SH residues. That NEM still was capable to enhance K^+ influx by 3 fold in osmotically swollen or shrunken LK cells means that the NEM and volume stimulated K^+ fluxes are rather independent of each other. However, participation of one and the same carrier cannot be excluded at present time. (Supp. by NIH grant AM 28236/HEM).

W-AM-B6 VOLUME REGULATION BY AMPHIUMA RED BLOOD CELLS: THE ROLE OF CA^{+2} AS A MODULATOR OF ALKALI METAL/PROTON EXCHANGE. Peter M. Cala, Ph.D., Department of Human Physiology, School of Medicine, University of California, Davis, California 95616.

Following osmotic perturbation the Amphiuma red blood cell regulates volume back to normal levels. This response to cell swelling (regulatory volume decrease, RVD) is characterized by net loss of K^+, Cl^- and H_2O. Subsequent to osmotic shrinkage the Amphiuma RBC regulates volume (regulatory volume increase, RVI) by gaining Na^+, Cl^- and H_2O. Previous studies have shown that the alkali metal and chloride fluxes responsible for volume regulation are electrically silent (Cala 1980. J. Gen. Physiol. 76:685-708), the former being obligatorily counter coupled to H^+ while Cl^- exchanges for HCO_3^-. When exposed to the Ca^{+2} ionophore A23187 the Amphiuma RBC loses K^+ in excess of that observed during RVD. In addition to the effects upon ion flux A23187 produced membrane hyperpolarization which in some cells resulted in membrane potentials equal to the potassium equilibrium potential. Known inhibitors of the Ca^{+2} activated K^+ conductance blocked membrane hyperpolarization and K^+ fluxes associated with both A23187 and RVD. Further, the same fractional inhibition was obtained regardless of whether K^+ flux was clue to osmotic swelling or ionophore. The above studies suggest that Ca^{+2} at the internal aspect of the membrane activates parallel K^+ flux pathways, one conductive and the other electrically silent with the latter being the only contributor to net K^+ flux. It was concluded that Ca^{+2} plays an important role in the control and activation of the K^+/H^+ exchange responsible for RVD and based upon studies with amiloride that the K^+/H^+ exchange (RVD) and the Na^+/H^+ exchange (RVI) represent different operating modes of the same transport moiety. (USPHS NIH Grant HL-21179)

W-AM-B7 DIRECT HIGH-RESOLUTION NMR STUDIES OF METAL CATION TRANSPORT ACROSS MODEL AND CELL MEMBRANES: ^{23}Na AND ^{39}K NMR.

Charles S. Springer, Jr., Martin M. Pike, and James A. Balschi, Department of Chemistry SUNY at Stony Brook, Stony Brook, N.Y. 11794.

Paramagnetic anionic coordination complexes (ex. $Dy(DPA)_3^{3-}$, where DPA^{2-} is the dipicolinate ion) have been developed for use as shift reagents for the magnetic isotopes of the physiological metal aquo cations (Na^+, K^+, Mg^{2+}, and Ca^{2+}). Studies with large unilamellar lecithin vesicles (LUV) and whole cells (yeasts, erythrocytes) show that the presence of the water soluble shift reagent on only one side of the membrane allows the simultaneous observation of distinct resonances corresponding to cations outside and inside the cells (or LUV). These observations have been made in ^{23}Na, ^{39}K, and ^{7}Li natural abundance NMR spectra. Facilitated transport of these cations (introduction of ionophores in the case of LUV) can be observed by monitoring the time course of the NMR spectrum.

W-AM-B8 FLUX RATIO ANALYSIS OF THE AMILORIDE-SENSITIVE NA^+ ENTRY SITE IN FROG SKIN. D.J. Benos and R. Latorre, Department of Physiology and Biophysics, Harvard Medical School, 25 Shattuck Street, Boston, MA 02115

Net sodium movement across the apical membrane of most high resistance epithelia appears to be driven by its electrochemical potential gradient. This pathway is facilitated, is rate-limiting for transepithelial Na^+ transport, and is specifically inhibited by amiloride. Fuchs et al (J. Physiol. 267:137, 1977) first proposed that Na^+ entry through these amiloride sensitive channels occurs via electrodiffusion where passive Na^+ movements obeys independence. One necessary criterion of independence is that the ratio of unidirectional ionic fluxes through a specific pathway obeys the Ussing flux ratio equation. We here report a flux ratio analysis for the amiloride-sensitive Na^+ entry pathway in R. catesbeiana skin.

Unidirectional ^{22}Na fluxes were performed on skins whose basolateral membranes were depolarized with 100 mM $[K^+]$ in the serosal bathing solution. The fluxes were determined under all experimental conditions in the presence and absence of $10^{-4}M$ amiloride to ascertain Na^+ flow through the amiloride sensitive sites. 'Reversed' Na^+ flow through the amiloride-sensitive pathway was induced by pre-equilibrating the serosal surface of the frog skins with either nystatin or amphotericin B. The external $[Na^+]$ was varied from 20 to 300 mM and the transepithelial potential was clamped to either -50, 0, +50, or +100 mV. Apical membrane potential under all experimental conditions was assessed with microelectrodes. Our results indicate that the flux ratio of Na^+ through the amiloride pathway is very close to that predicted by electrodiffusion theory. Supported by N.I.H. Grants AM25886 and GM-25277.

W-AM-B9 HIGH CONDUCTANCE PLASMA MEMBRANE AS CAUSE OF DECREASE IN RESISTANCE WITH ONSET OF SECRETION IN IN VITRO FROG STOMACH. W. Rehm, G. Carrasquer, M. Schwartz, and T. C. Chu*, Dept. of Medicine, University of Louisville, Louisville, KY 40292.

The resistances (R) of the resting and the secreting mucosae are 350 and 150 ohms cm^2 respectively ($R \simeq 200$ ohms cm^2). The area of the lumen-facing membrane of the acid-secreting cells markedly increases (Δarea) in going to the secretory state. We have shown (unpublished work) that ΔR is not due to Δ area; hence, ΔR is primarily a result of the establishment of high conductance pathways in the plasma membrane and/or to the increase in conductance of the lumen fluid. The increase in $[H^+]$ in the luminal fluid would result in a decrease in R. However, as the following analysis shows, this could account for only a fraction of ΔR. The $[H^+]$ of the secreting mucosa was estimated by use of the following equation: $Q = -DA\, dc/dX + vAC$, where Q = H^+ rate; D, Fick's diffusion coefficient; A, area of lumina for gross area of 1 cm^2; $C = [H^+]$; X, distance from bottom of tubule; and v, velocity of bulk flow. We used a distributed parameter model where $Q = PX$ and $v = SX$ (P and S constant) from $X = 0$ to $X = 2 \times 10^{-2}$ cm, i.e., for the length of the tubular lumina. It is assumed that Q and v remain constant from $X = 2 \times 10^{-2}$ cm to the end of the pit lumina at 3×10^{-2} cm. With the final $Q = 10^{-9}$ Eq sec^{-1}, the $[H^+]$ at $X = 0$ is 17 mM and at $X = 2 \times 10^{-2}$ cm is 9 mM. The NaCl conc. at $X = 0$ is 83 mM. The $[H^+]$ is very low at the end of the lumina, and for calculations we assumed it to be zero. The ΔR due to the $[H^+]$ in the lumina was calculated and found to be about 15 ohms cm^2, i.e., only a fraction of ΔR. Therefore, ΔR is due to the establishment of highconductance channels in the plasma membrane of the acid-secreting cells with small contributions from Δarea and $\Delta[H^+]$. (NIH and NSF support)

W-AM-B10 AN ACIDIFYING ATPase IN VESICLES FROM THE TURTLE URINARY BLADDER EPITHELIUM. Steven J. Youmans, Howard Worman, and William A. Brodsky; Mt. Sinai Med. Sch., New York, NY 10029 and Univ. Chicago Sch. Med., Chicago, IL 60637.

Urinary bladders of Pseudemys scripta are known to acidify the urine. We report the first evidence of ATP-dependent acid transport in cell-free membrane preparations of this tissue. A fraction of mixed apical and basolateral epithelial cell membranes was prepared by differential centrifugation as described elsewhere (Biochim. Biophys. Acta 556:490, 1979). This fraction was osmotically active: 90° scattering of 500 nm light dropped 15-22% 6 min. after K salts were added to a suspension of 45 µg membrane protein/ml in 125 mM sucrose buffer. This is consistent with re-swelling of closed vesicles. Relative rates of change were: 150 mM KNO_3 = 150 mM KCl > 100 mM K_2SO_4. The Steck and Kant method (Meth. Enzymol. XXXI(A):172, 1974) indicated inside-out vesicle orientation. Studies were done with the fluorescent pH-sensitive dye quinacrine (λ_{excite} = 420, λ_{emit} = 500 nm). Vesicles containing 1 mg protein were suspended to 600 µl in (mM): sucrose, 250; $MgCl_2$, 3; ouabain, 0.1; HEPES, 10; KCl, 100; valinomycin, 10^{-3}; quinacrine-HCl, $4x10^{-3}$; and oligomycin, 7.5 µg; pH 7.3. When 1 mM Tris-ATP was added, fluorescence decreased 19.0 ± 1.6 % (Mean ± SE, n = 9. Different from zero, $P < .001$) in 3 min., indicative of internal acidification. The protonophore FCCP (2µM) returned fluorescence to near baseline in 10 sec. Further ATP or FCCP additions caused only small decreases. Without FCCP, fluorescence returned to baseline in 10 min. The results indicate the presence of an oligomycin- and ouabain-resistant function that acidifies the interior of inside-out vesicles in the presence of ATP. (Supported by NIH grant 16928. S.J.Y. is the recipient of HEW National Research Service Award 1 F32 AM06559-01.)

W-AM-B11 REGULATION OF APICAL POTASSIUM CONDUCTANCE IN THE ISOLATED EARLY DISTAL TUBULE OF THE AMPHIUMA KIDNEY. W.B. Guggino, B.A. Stanton, and G. Giebisch. Dept. of Physiology, Yale University, New Haven, CT 06510.

Early distal tubules of Amphiuma kidney were perfused in vitro and apical cell membrane potential (V_a), the basolateral cell membrane potential (V_{bl}), the transepithelial potential (V_{te}) and the ratio of apical to basolateral cell membrane resistances (R_a/R_{bl}) were measured. The effect of luminal and basolateral pH changes on luminal potassium conductance was examined. In control perfusions, V_a was -68 ± 3 mV, V_{bl}, -63 ± 3 mV, V_{te}, +5 ± 1 mV, and R_a/R_{bl}, 4.0 ± 1.5. Increasing K^+ in the luminal solution to 15 mM caused a significant decrease in V_a, to -42 ± 2 mV, V_{bl}, to -37 ± 2 mV and R_a/R_{bl}, to 2.7 ± 1.1. Luminal perfusion with 0.5 mM Ba^{++}, also decreased from control values, V_a to -49 ± 4 mV, and V_{bl} to -43 ± 5 mV. Ba^{++} increased R_a/R_{bl} to 14.7 ± 1.1. These data are consistent with a K^+ selective apical cell membrane. Acidifying the basolateral solution from pH 7.6 to 6.6 by lowering HCO_3^- at constant pCO_2 decreased, V_a to -39 ± 5 mV, V_{bl} to -34 ± 4 mV and increased R_a/R_{bl} to 7.4 ±2.5. Luminal perfusion of 15 mM K^+ in the presence of an acid basolateral solution resulted in a small reduction of V_a to -33 ± 3 mV, and V_{bl} to -28 ± 2 mV indicating that acidifying the basolateral solution diminishes the K^+ selectivity of the apical cell membrane. V_{te} remained unchanged in all experimental conditions. In contrast, reduction of pH of the apical perfusion solution from pH 7.6 to 6.6 did not alter either cell membrane potentials or apical cell membrane K^+ selectivity. Conclusions: 1. The apical cell membrane of the early distal tubule of the Amphiuma kidney is K^+ selective. 2. The K^+ selectivity of the apical cell is reduced by lowering the pH of the basolateral solution but not the apical solution.

W-AM-B12 EFFECT OF UREA HYPEROSMOLARITY ON ACID SECRETION IN FROG AND DOGFISH STOMACH IN VITRO George W. Kidder III, Dept. of Physiology, Univ. of Maryland Sch. of Dentistry, Baltimore, MD and Mt. Desert Island Biological Laboratories, Salisbury Cove, ME

The secretion of HCl into the secretory tubules and its subsequent osmotic equilibrium with H_2O is believed to account for the production of the primary secretion. Raising the osmolarity of the secretory cells should therefore increase the osmolarity and decrease the pH of the primary secretion, increasing the gradient up which H^+ must be transported and decreasing the secretory rate. On the assumption that urea would enter the cells from the serosal side and exert its osmotic effect across the mucosal membrane without other effects on the cells, the gastric mucosae were subjected to urea hyperosmolarity. In frog, increasing osmolarity from 214 mOsM (salts only) by addition of urea to both solutions produces a decrease in acid secretory rate, which reaches zero at about 800 mOsM, for a calculated pH of 0.4 in the primary secretion. In dogfish, whose plasma normally contains 350 mM urea, omission of urea depresses secretion as compared to normal (850 mOsM) solutions. Secretory rate also declines at higher urea concentrations, reaching zero near 1500 mOsM (pH 0.12).

This calculated pH depends on H^+ and Cl^- being the only transported species, lack of significant mixing between the tubule ends and the bulk mucosal solution, and a mucosal-facing membrane essentially impermeable to urea. Experiments with urea efflux from dogfish mucosae into urea-free solutions indeed show higher permeability of serosal than mucosal membranes, but also reveal an apparent variation in permeability with urea concentration, which remains to be explained. The calculated pH values should therefore be taken as starting points for further experimentation.

Supported by NSF PCM-77-03336 to GWK and NSF DEB-78-36821 to MDIBL.

W-AM-B13 THE CATALYTIC CYCLE OF THE GASTRIC (K^++H^+)-ATPase. W.W. Reenstra, J. Poulter* and J.G. Forte. Dept. of Physiology-Anatomy, University of California, Berkeley CA 94720 (USA)

In order to more fully understand the mechanism of the (K^++H^+)-ATPase, the hydrolysis of *p*-nitrophenyl phosphate (pNPPase) was studied in hog gastric microsomes. The pNPPase activity was activated by K^+, which increased both V_{max} and V_{max}/K_m. The free enzyme bound K^+ (K = 1.4mM). ATP was a potent inhibitor of pNPPase; plots of 1/V vs. [ATP] were non-linear. At high concentrations, ATP was competitive with pNPP. After adjusting the data for the competitive inhibition, ATP inhibition was shown to reduce pNPPase from V_0^{ATP}, at [ATP] = 0, to a limiting non-zero value, V_∞^{ATP}. Increasing [K^+] decreased V_∞^{ATP}-V_0^{ATP}, increased the [ATP] needed to obtain V_∞^{ATP} and had no effect on the competitive K_I. The non-phosphorylating analog AMPPNP was competitive with pNPP and its K_I was increased by increasing [K^+]. Poorly hydrolyzed analogs (e.g., CTP) displayed inhibition similar to that of ATP but with much lower affinity constants. The results at low [ATP] are consistent with 1) ATP hydrolysis occurring by scheme I and 2) pNPP hydrolysis being catalyzed by E·K.

$$E_1 + ATP \rightleftarrows E_1\cdot ATP \rightleftarrows E_1\sim P \rightleftarrows E_2\text{-}P\cdot K \rightleftarrows E_2\cdot P\cdot K \rightleftarrows E_1\cdot K \rightleftarrows K_1 + E \qquad (I)$$

Since a steady state [E·K] is formed by ATP hydrolysis, phosphorylating compounds cannot reduce the pNPPase to zero. Moreover, if ATP hydrolysis were to increase [E·K], this mechanism would predict stimulation of pNPPase by ATP; the mechanism could thus account for published data for the (Na^++K^+)-ATPase. ATP binding to E·K with a low affinity is proposed to account for the competitive inhibition. Rapid conversion of E·K·ATP to E·ATP is shown to be consistent with the previously observed biphasic kinetics of ATP hydrolysis. (Supported by U.S.P.H.S. Grant AM 10141)

W-AM-B14 EFFECT OF SPHINGOMYELINASE (SPH-ase) ON NaKATPase. Edward S. Hyman Touro Research Institute, New Orleans, Louisiana 70115

Phosphatidylcholine and phosphatidylserine are essential to the function of NaKATPase. Sphingomyelin (SPH) is also present in NaKATPase and its function has not been determined. In vitro SPH forms a matrix with an acidic phospholipid. In a thin or black membranes in vitro this matrix selectively conducts K^+ and K^+ sized cations (E.S. Hyman, Fed. Proc., 33, 279, 1974), and it is occluded by divalent cations except Mg^{++} (E.S. Hyman, Biophys. J., 17, 185a, 1977). Thus this matrix has been proposed as the K^+ selection device of membranes and as the gate for K^+ access to the E·P site of NaKATPase. If so, then destruction of SPH may be expected to remove the gate. SPH-ase derived from the human placenta splits phosphorylcholine selectively from the basic phospholipid optimally at pH 5 but usably at pH 6. In vitro ATPase activity is progressively destroyed by SPH-ase at pH 6 as a function of time and concentration. In the range of incomplete destruction of ATPase the enzyme loses its requirement of K^+ and the Pi production and the turnover rate (S^{-1} or $\Delta Pi/E\cdot P$) without K^+ approaches (or under certain conditions even exceeds) that in the presence of K^+. As a control the same ATPase preparation was incubated in the same pH 6 buffer without SPH-ase, and SPH-ase was added after the pH was raised to 7.5 to assay the ATPase. The control ATPase was unaffected by those conditions. These preliminary findings support the theory that a SPH containing K^+ selective phospholipid pore gates access of K^+ to the active site of ATPase.
Supported by the Glazer Medical Fund

W-AM-B15 ESTIMATION OF HETEROGENEITY AND INITIAL VELOCITY OF TRANSPORT IN VESICLES BY INVERSE LAPLACE TRANSFORMATION OF TRANSPORT DATA. Ulrich Hopfer and Stephen W. Provencher. Dept. Anatomy, Case Western Reserve University, Cleveland, OH, Max-Planck-Institute for Biophysics, Frankfurt, Germany, and EMBL, Heidelberg, Germany.

The equation describing isotope exchange of a solute between a large reservoir and an ensemble of vesicles, is given by: $f(t)=\Sigma a_i \exp(-k_i t)$ for a discrete model, or: $f(t)=\int_0^\infty f(k)\exp(-kt)\,dk$ for a continuous distribution of rate constants. f(t) is defined as: 1-fractional exchange, which is time dependent. a_i and f(k) are the weighting factors for the contribution of vesicles with a given rate constant k. Provided the rate constant is time-independent, the distribution of rate constants {f(k)} may be estimated by numerical inverse Laplace transformation of transport data with the method of Provencher (Makromol.Chem.180,201(1979)). The distribution was evaluated for Na-dependent D-glucose transport in rabbit renal cortical and small intestinal brush border membranes from transport data of 2-7200 sec. The results indicate considerable heterogeneity of transport rates in different vesicles with a spread of at least 2 orders of magnitude. Knowledge of f(k) plus the intravesicular volume available for exchange, allows estimation of initial steady-state rates (i.e. for t=0). For D-glucose, maximal initial rates at 25°C and 0.2M NaCl were (in nmol/sec/mg protein): ∿0.6 in intestinal, and ∿2.6 in renal membranes. >90% of the rate was determined by the Na-dependent glucose carrier. The specific initial rates, estimated in this manner, are dependent only on the number of transport sites and their intrinsic activity. Thus, the renal membranes were 4times more active than the intestinal ones. The advantages of the new treatment of transport data are information on vesicle heterogeneity and reliable estimates of initial rates.

W-AM-C1 FROG MUSCLE MEMBRANE: AN IONIC CHANNEL BLOCKED BY MICROMOLAR EXTERNAL [Ca]. P.T. Palade, E. McCleskey and W. Almers. Dept. Physiology & Biophysics, U. of Washington, Seattle, WA.

Using the vaseline gap, we voltage-clamped frog semitendinosus fibers in external media of various pCa, containing 130 TMA^+, 32 Na^+, 22 MOPS pH 7, 1 μM TTX with the main anion being appropriate amounts of the Ca^{++}-buffers EGTA, HEDTA or diglycolate, partially complexed with Ca^{++}. Ends were cut in intracellular medium containing 40 TMA, EGTA and (32 CS + 28 TMA)-aspartate at pH 7. At 22° C, HP = -100 mV and external pCa = 7.3, steps to between -80 and +30 mV gave currents that were inward at negative and outward at positive potentials (upper). Inward (and not outward) currents vanish when TMA replaces external Na^+; however, Li, K, Rb and Cs can carry inward current. Inward currents depend on external pCa, being diminished or abolished at pCa = 4.7 (lower), increased by 10-30% at pCa = 8-8.3, and half-maximal at pCa ≅ 6.3. Raising pCa speeds kinetics. Ca^{++} blocks outward current less strongly than inward currents. Other divalent cations (Sr, Ba, Mn, Co, Cd, Ni) also block, though less effectively than Ca^{++}. Mg^{++} is much less effective, with a half-blockage concentration in the milimolar range. (Supported by USPHS #AM17803.)

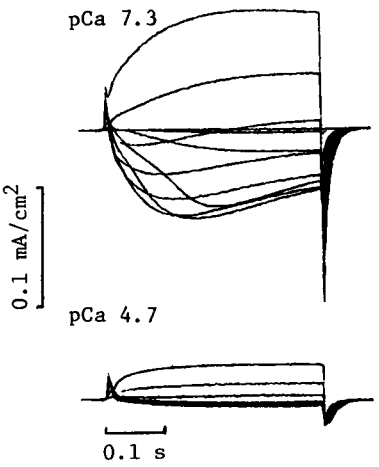

W-AM-C2 CALCIUM CURRENTS IN MAMMALIAN SKELETAL MUSCLE. P. Lynn Donaldson & Kurt G. Beam, Dept. of Physiology and Biophysics, Univ. of Iowa, Iowa City, IA 52242.

The three microelectrode voltage clamp was used to measure slow ionic currents in rat skeletal muscle at 20°C. The bathing solution contained (mM) TEA (146), Na (5), Cs (5), Ca (10), Mg (1). Br was the predominant anion; the solution was buffered to pH 7.4 with HEPES (10). Contraction was blocked with sucrose (350-400 mM); sodium currents were blocked by TTX (1uM). The holding potential was -90 mV. Test currents were elicited by steps to potentials ranging from -50 to +50 mV. A small correction for linear ionic and capacitative currents was made. The threshold for appearance of net inward current varied from -20 to 0 mV. (Fibers depolarized below this threshold displayed small outward currents which appeared to be residual delayed rectifier currents not blocked by TEA). The currents continued to be net inward over at least part of their time course for potentials up to about +30 mV, with peak inward current of up to 150 uA/cm^2. The inward currents were reversibly abolished by the addition of 10 mM Ni or 0.5 mM Cd; substitution of Ba for Ca increased the size of the currents. These similarities to Ca currents in other tissues argue that this inward current in rat muscle is a calcium current. Inward current was not maintained during a depolarization. In some fibers the inward current decayed to zero. In other fibers the inward current was succeeded by a maintained net outward current. The kinetics of the inward current were strongly voltage-dependent. Thus, in a representative fiber the current at -10 mV reached half its maximal inward level in about 200 msec, whereas at +10 mV the half-maximal time was about 25 msec. At physiological temperatures the channel may activate sufficiently fast to allow significant calcium entry into the cell during one or a few spikes. Supported by MDA & NIH (NS 14901).

W-AM-C3 A COMPARISON OF PACEMAKER MECHANISMS OF EMBRYONIC VENTRICULAR AND ATRIAL CHICK HEART CELL AGGREGATES. A. Shrier[1] and J.R. Clay[2]. [1]Department of Physiology, McGill University, Montreal, P.Q., Canada H3G 1Y6; [2]Lab of Biophysics, NINCDS, MBL, Woods Hole, MA, USA 02543.

We have investigated the pacemaker properties of aggregates of cells dissociated from the atria and ventricles of 10-14 day old embryonic hearts. These preparations usually beat spontaneously and rhythmically in tissue culture medium containing 1.3 mM potassium with a beat rate typically in the range of 15-60 beats per minute. The beat rate results show considerable variability, which precludes any statistically significant comparison between the spontaneous activity of the two cell types at this developmental stage. However, the shapes of the pacemaker potential changes are different, which reflect differences in the underlying membrane currents. Ventricular preparations have a time dependent potassium ion pacemaker current which is activated between -90 and -70 mV (I_{K_2}); a second time dependent component which is activated at potentials positive to -70 mV (I_x); and a background current (I_{bg}) which displays inward rectification (Clay and Shrier, J. Physiol. 312, 491, 1981). Atrial preparations lack a time dependent pacemaker current activated negative to -70 mV; they possess a time dependent current which is activated at potential positive to -50 mV (I_x); and a linear I_{bg}. We have successfully simulated the pacemaker voltage changes from the above voltage clamp measurements and from those of Ebihara et al. (J. Gen. Physiol. 75, 437, 1980) of the fast inward current (I_{Na}). An outcome of the analysis is the role in pacemaking of the steady state amplitude of I_{Na} (the "window current"). This component has negative slope conductance which effectively increases the slope resistance of the preparation in the vicinity of threshold. Consequently, it tends to prolong the interbeat interval. (Supported by the MRC, Canada).

W-AM-C4 AN OUTWARD CURRENT IN HEART CELLS THAT RECTIFIES BY DECREASING MEAN CHANNEL OPEN TIME. L. J. DeFelice, Anatomy Department, Emory University, Atlanta, GA 30322 and D.E. Clapham, Brigham and Women's Hospital, Boston, MA 02115.

We have used single channel recording techniques to study voltage-dependent currents in aggregates of embryonic chick heart. We have recorded four different kinds of channels by observing their mean open time and the direction of the current. In this paper we describe only one of these channels. The channel was recorded from 7 day ventricular aggregates at room temperature and in medium containing 1.3 or 3.5 mM external K and TTX. The open channel has a linear i(V) curve with a reversal potential of -45 mV and a single channel conductance of 71 pS. The mean channel open time increases with depolarization according to the equation $\tau_o = 14 \exp (V/47)$ msec for V between -40 and +20 mV. For V > 20 mV, τ_o decreases. The steady state open channel probability (p), defined from single channel records as τ_o times rate of opening, goes through a maximum as the membrane is depolarized. The maximum value of p is about 1/3 for V = 20 mV; at V = -20 mV and +40 mV, p is 1/10 its maximum value. Thus, the activation variable for this current is not a monotonically increasing function of voltage. In a limited voltage range, these results describe an inward rectifier that works by decreasing mean channel open time, not single channel conductance. The relationship of this current to macroscopic currents described previously in heart cell membranes will be discussed. Supported by NIH #1-PO1-HL27385.

W-AM-C5 SPONTANEOUS VOLTAGE FLUCTUATIONS IN CULTURED HEART CELLS: ROLE OF INTRACELLULAR CALCIUM. M. L. Bhattacharyya and R. D. Nathan. Department of Physiology, Texas Tech University School of Medicine, Lubbock, TX 79430.

Enzymatic release of sialic acid residues from the sarcolemma of cultured chick heart cells produces spontaneous 2-10 mV fluctuations in the membrane potential (Life Sci. 29: 1071-1078, 1981). In the present study we found that such perturbations could be blocked by intracellular injection of EGTA and could sometimes be mimicked by intracellular injection of Ca^{++}. When 50-85% of the extracellular Na^+ was replaced by Li^+ (but not by choline or TRIS), myocytes exhibited spontaneous voltage fluctuations like the ones produced by neuraminidase. During either condition, the perturbations were enhanced by 1 mM caffeine or 5-8 mM Ca^{++} and blocked by 3-5 mM caffeine but not by TTX (10^{-5} g/ml) or D600 (5 x 10^{-6} g/ml). Other manipulations that enhance intracellular Ca^{++}, such as removal of extracellular K^+ or the addition of strophanthidin (5 x 10^{-6} M), 10-20 mM Ca^{++} or 5 x 10^{-5} M A23187 (a Ca^{++} ionophore), failed to induce similar voltage fluctuations; rather, slower and more periodic perturbations were produced. In the presence of TTX and neuraminidase (0.5 U/ml), the amplitude of voltage fluctuations decreased as the membrane became hyperpolarized during current injection through a second intracellular electrode. Preliminary voltage clamp experiments demonstrated that when heart cell aggregates were treated with neuraminidase and the membrane potential held constant (-30 to -52 mV), the holding current exhibited 1-5 nA fluctuations which were never seen in untreated controls. We conclude that enzymatic release of sialic acid residues from cultured chick heart cells leads to an increase in intracellular Ca^{++} via Na-Ca exchange. Calcium-induced Ca^{++} release from the sarcoplasmic reticulum may be the process that triggers the current fluctuations. Supported by NIH grants HL 07289 and HL 20708.

W-AM-C6 DISTINCTION IN THE MODES OF ACTION OF THE CALCIUM CURRENT INHIBITORS D600, DIPHENYLHYDANTOIN, AND NISOLDIPINE IN CARDIAC PURKINJE FIBERS. T. Scheuer and R.S. Kass, Department of Physiology, University of Rochester, Rochester, N.Y. 14642.

In the cardiac Purkinje fiber, the calcium current I_{si} is inhibited by D600, nisoldipine and diphenylhydantoin (DPH), three compounds with marked differences in structure and potency. We have begun to investigate distinctions between the modes of action of these compounds using a two microelectrode voltage clamp arrangement in shortened calf and dog cardiac Purkinje fibers. Experiments were carried out in fibers which had been injected with tetrabutylammonium ion to block overlapping outward currents and permit quantitative analysis of the calcium current. When depolarizing test pulses are imposed from holding potentials near -40 mV, each of these agents blocks I_{si}, but differences in the actions of these drugs become apparent when the holding potential is changed. The block of I_{si} by D600 can be substantially removed by holding the membrane at negative potentials for long (150 sec) periods without stimulation. When the membrane is returned to the more positive holding potential, complete block of I_{si} redevelops with the first 5-10 pulses of a .4 to .67 Hz train. Like D600, inhibition of I_{si} by DPH is also removed at negative holding potentials, but, in this case, blockade redevelops much more slowly (on the order of 1 min). In contrast, when this protocol is repeated in the presence of nisoldipine, little, if any, effect is observed on the amount of I_{si} blocked by this compound. Thus, even simple studies of these agents suggest substantial differences in their modes of action.

Supported by NIH HL-21922.

W-AM-C7 COMPARISON BETWEEN Ca^{2+} CHANNEL BLOCK BY Cd^{2+} AND D600 IN SINGLE MAMMALIAN HEART CELLS
Kai S. Lee, Esther W. Lee and Richard W. Tsien, Department of Physiology, Yale University School of Medicine, 333 Cedar Street, New Haven, Connecticut 06510.

In many excitable cells, Ca^{2+} entry can be inhibited by inorganic ions such as Cd^{2+} or organic Ca^{2+}antagonists such as D600. Do these agents act by blocking Ca^{2+} channels, or by displacing Ca^{2+} from the external membrane surface? Using the suction pipette method, we studied Ca^{2+} channel in single cells freshly isolated from adult guinea pig ventricles. With 1mM Ca^{2+} Tyrode outside, 150mM K^{+}inside, I_{si} seemed to reverse above +65mV. The reversed outward current was mostly eliminated by replacing K_i with Cs_i, but was not abolished by removal of Ca_o^{2+}, Na_o^{+}, Na_i^{+}, or by exposure to TTX, 4-AP, or internal TEA. Outward and inward currents inactivated similarly by depolarizing potentials, but current at E_{rev} remained unchanged, supporting a genuine I_{si} reversal potential as proposed by Reuter & Scholz. Likewise, Cd^{2+} and D600 reduced currents in both directions, leaving current at E_{rev} unaffected. Thus both agents act by blocking channels, not by simply reducing available charge carriers for inward current. Do the inhibitors compete with permeant ions for a site within the channel? For ions like Cd^{2+}, Hagiwara's model predicts that I_{Ca} should be harder to block than I_{Ba} if Ca^{2+} binds more strongly than Ba^{2+} to a channel site. This was true for Cd^{2+}, but D600 gave the opposite result: I_{Ca} was much more sensitive than I_{Ba}. Apparently, D600 and Cd^{2+} do not block Ca channel by competition for the same site in heart.

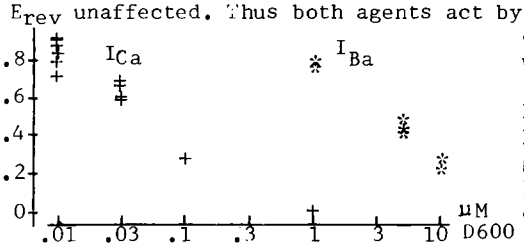

W-AM-C8 DELAYED RECTIFICATION IS NOT A CALCIUM ACTIVATED CURRENT IN CARDIAC PURKINJE FIBERS.
Robert S. Kass, Department of Physiology, University of Rochester, Rochester, N.Y. 14642.

Voltage clamp studies of plateau currents in the Purkinje fiber have revealed three overlapping time- and voltage-dependent membrane currents. These include the calcium current I_{si}, the transient outward current (I_{to}) and the delayed rectifier (I_x). I_{to} is, at least in part, a calcium-sensitive current, and several properties of I_x have suggested that it too may be activated by intracellular calcium. Activation of I_{si} preceeds the slower onset of I_x, and inhibition of I_{si} by previously studied blockers is accompanied by reduction of I_x. In addition, catecholamine-induced increases in I_{si} are accompanied by marked increases in I_x. In the present series of experiments, the relationship between I_x and I_{si} was investigated using a novel calcium channel blocking agent: nisoldipine. The experiments were carried out in shortened calf or dog cardiac Purkinje fibers. Membrane current was measured with a conventional two-microelectrode arrangement, and tension was monitored optically. Nisoldipine blocks calcium current in these preparations in a dose-dependent manner. When the holding potential is maintained near -40 mV, nisoldipine (10 μM) occludes the effects of D600 (10 μM) on I_{si}, and completely inhibits contractile activation. Despite this block of I_{si} and contraction, nisoldipine does not reduce activation of the delayed rectifier. In contrast, reduction of I_x by D600 persists even when I_{si} is completely blocked by pretreatment with nisoldipine. Finally, calcium channel blockade by either nisoldipine or D600 completely prevents any norepinephrine-induced increase in measured calcium current, but does not block I_x enhancement by this catecholamine. All of these results provide strong evidence that I_x is not a calcium activated current. Supported by NIH HL-21922.

W-AM-C9 EFFECT OF STROPHANTHIDIN ON INTRACELLULAR Na ION ACTIVITY AND TWITCH TENSION OF BEATING DOG CARDIAC PURKINJE FIBERS.
C.O.Lee and M. Dagostino*, Department of Physiology, Cornell University Medical College, N.Y., N.Y. 10021

We have performed simultaneous and continuous measurements of intracellular Na ion activity (a_{Na}^{i}), twitch tension (T) and action potential of beating (60/min) dog cardiac Purkinje fibers during onset and recovery of the effect of strophanthidin (stro). The fibers were exposed to strophanthidin of 10^{-8}, $5x10^{-8}$, 10^{-7}, $5x10^{-7}$, and 10^{-6} M for 5 min. No detectable changes in a_{Na}^{i} and T were observed in the fibers exposed to 10^{-8} M strophanthidin and the threshold concentration of strophanthidin appeared to be around $5x10^{-8}$ M. At concentrations $>5x10^{-8}$ M strophanthidin produced dose-dependent increases in a_{Na}^{i} and T in a linear fashion. The time course of change in a_{Na}^{i} was similar to that of change in T as shown in the Figure. A plot of T versus a_{Na}^{i} during onset and recovery showed a linear relationship between T and a_{Na}^{i}. The results indicate that the positive inotropic effect of strophanthidin is closely associated with the increase in a_{Na}^{i}. (Supported by USPHS HL 21136).

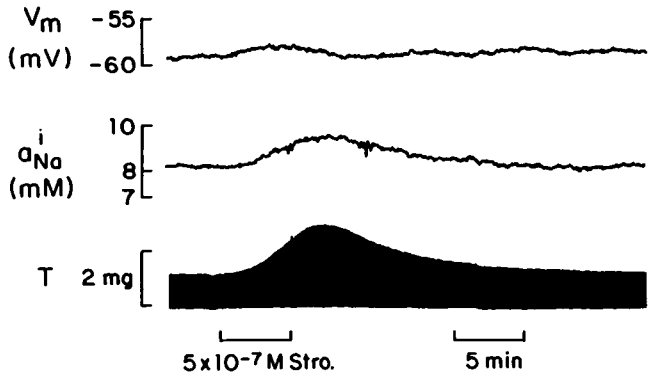

W-AM-C10 QUINIDINE BLOCK OF CARDIAC SODIUM CHANNELS IS RATE- AND VOLTAGE-DEPENDENT. T.J.Colatsky, Department of Physiology, Cornell Medical College, New York, NY 10021.

Quinidine is believed to exert its antiarrhythmic action in heart by blocking sodium channels. The mechanism of cardiac sodium channel block was investigated in short (0.5-0.8 mm) rabbit Purkinje fibers using the two-microelectrode voltage clamp technique. Low external sodium (7-15mM) and temperature (15-20°C) were used to improve voltage control and temporal resolution of the current. Application of 5 μg/ml (13.4 μM) quinidine produced little (< 5%) resting block of sodium currents elicited from holding potentials near -85 mV. Inactivation curves measured with 1-10 sec prepulses were shifted slightly (1-5 mV) toward more negative potentials. Use-dependent block was observed when brief (50 msec) depolarizing pulses were applied repetitively at intervals of 0.2-5 sec; under these conditions, quinidine reduced the sodium current to less than 50% of the initial (rested) value. The amount of use-dependent block decreased as the holding potential during the pulse train was made more negative. Double pulse experiments revealed that block is greatly enhanced by positive conditioning pulses. Prolongation of the conditioning pulse from 50 msec to 5 sec produced little additional block. Repetitive pulses generated substantially greater inhibition of sodium current than a single pulse that depolarized the membrane for a comparable period of time. These results indicate that (1) quinidine has a higher affinity for the activated (open) cardiac sodium channel, than for the resting or inactivated channel, and (2) the binding of quinidine to the open channel is voltage-dependent.

W-AM-C11 HOW DOES LIDOCAINE REDUCE THE OSCILLATORY TRANSIENT INWARD CURRENT IN SHEEP CARDIAC PURKINJE FIBERS? By S-S. Sheu, W.J. Lederer & *D.A. Eisner. Dept. Physiology, Univ. Maryland, Baltimore, MD 21201 and *Dept. Physiology, University College London, England.

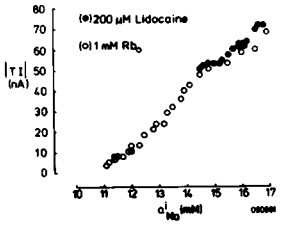

An arrhythmogenic oscillatory transient inward current (TI) is seen in heart muscle when intracellular calcium activity (a^i_{Ca}) is elevated. Following Na pump inhibition (produced by 0 mM K_o in these experiments), intracellular sodium activity (a^i_{Na}) rises and leads to an increase in a^i_{Ca} by means of the Na/Ca exchange mechanism and TI currents can be seen. Local anesthetics reduce TI magnitude (|TI|) and could act by decreasing Na entry. The results shown in the figure were obtained from voltage-clamped sheep cardiac Purkinje fibers (two-microelectrode technique) while using a liquid ion-exchanger Na-sensitive microelectrode. The same relationship between a^i_{Na} and |TI| is seen upon stimulating the Na pump with 1 mM Rb_o (open circles) or upon adding 200 μM lidocaine (filled circles). This result is consistent with a^i_{Na} mediating the reduction of |TI| by lidocaine and suggests that lidocaine does not act directly to alter calcium release. On removing Rb_o or lidocaine, a hysteresis in the a^i_{Na}-|TI| relationship is seen that is similar for both substances. Such a hysteresis may reflect the same underlying factors that produce the a^i_{Na}-tension hysteresis recently reported (see Eisner, Lederer & Vaughan-Jones, 1981, J. Physiol.,317, 163-187).

Support from NIH (HL-25675) and the National Foundation for the March of Dimes. This work was done during the tenure of an established Investigatorship of the American Heart Association and with funds contributed in part by the Maryland Affiliate.+

W-AM-C12 DETECTION OF SINGLE CHANNELS FROM CARDIAC MUSCLE IN PLANAR PHOSPHOLIPID BILAYERS. Roberto Coronado and Alan Williams* (Intr. by Christopher Miller). Department of Physiology & Biophysics, Harvard Medical School, Boston, MA 02115 and Section of Biochemistry*, Molecular and Cell Biology, Cornell University, Ithaca, NY 14853.

Channels from bovine heart sarcolemma were incorporated into planar phospholipid bilayers. Incorporation was accomplished by Ca^{++}-mediated fusion of purified sarcolemma vesicles with bilayers containing acidic phospholipids. Bovine heart sarcolemma was purified essentially as described by Jones et al. (JBC 255:9971, 1980).

Several types of channels can be incorporated when a KCl gradient is established across the bilayer. Using 200 mM cis KCl and 100 mM trans KCl (cis refers to the chamber where sarcolemma and Ca^{++} are added), we have detected a 25 pS cation-selective channel and a 240 pS anion-selective channel. Both types of channels (i) are Nernst-selective for cations over anions or vice-versa; (ii) have apparently only one open state; and (iii) are sensitive to membrane voltage.

Inside-out sarcolemma vesicles, prepared by affinity chromatography (Reinlib et al., FEBS Lett. 126:74, 1981), have a marked preference over right-side out vesicles to fuse with planar membranes. The total number of fusion events at any given time is ten times higher for inside-out vesicles than for right-side out vesicles. The preferential fusion of inside-out vesicles can be used to interpret the voltage dependence and the role of these channels in the electrical events of cardiac muscle.

Supported by Postdoctoral Fellowship from the Muscular Dystrophy Association, Exchange Fellowship from British Heart Foundation-American Heart Association*, and NIH grant GM-25277.

W-AM-C13 A STUDY OF THE INFLUENCE OF STATIONARY MAGNETIC FIELDS ON THE ELECTROCARDIOGRAPHIC INDICES AND BLOOD PRESSURE OF MONKEYS. C. T. Gaffey, T. S. Tenforde, T. F. Budinger, and B. R. Moyer. Biology and Medicine Division, Lawrence Berkeley Laboratory, Berkeley, CA 94720. Electrocardiogram (ECG) and direct blood pressure measurements were made on male monkeys (Macaca cynomolgous) exposed to DC magnetic fields. Monkeys were lightly anesthetized with ketamine hydrochloride and blood pressure measurements were made by cannulation of the femoral artery. The ECG was detected with platinum electrodes subdermally implanted in the chest and back. Each monkey was oriented in an electromagnetic gap with its spinal axis perpendicular to the lines of magnetic induction. Continuous records of the ECG and blood pressure were made before, during and following magnetic field exposures. A homogenous DC magnetic field could be adjusted up to strengths of 1.5 Tesla. A magnetically-induced increase in the T-wave amplitude was observed in monkeys, as previously reported for rats, dogs and baboons. The T-wave amplitude rose above the non-exposed (control) value of 100 μV by factors of about 5 and 8 in magnetic fields of 1.0 and 1.5 Tesla, respectively. The enhancement of the T-wave amplitude was completely and immediately reversible upon removal of the field. Magnetic field exposures up to 1.5 Tesla had no effect on the P wave, the QRS complex, the heart rate or the respiratory rate. The systolic and diastolic blood pressures remained unchanged in fields up to 1.5 Tesla. These results are consistent with the view of an absence of cardiac stress during magnetic field exposures, even though blood-flow potentials appear in the ECG traces. (This research was supported by the U.S. Department of Energy).

W-AM-D1 THE STRUCTURE AND MOLECULAR WEIGHT OF 30S DYNEIN FROM TETRAHYMENA. Kenneth A. Johnson and Joseph S. Wall. (Intr. by W. D. Taylor) Biochemistry Program, The Pennsylvania State University, University Park, PA and Dept. of Biology, Brookhaven National Lab, Upton, NY

Dynein was obtained by high salt extraction of Tetrahymena cilia, and was purified by ion exchange chromatography and sucrose gradient sedimentation. The 30S dynein species was examined by scanning transmission electron microscopy (STEM). Diluted samples were applied to carbon films, freeze-dried and were examined as unstained specimens. The images revealed that 30S dynein consists of a group of 3 globular heads on 3 separate strands which are joined at a common base, similar to a bouquet of 3 flowers. The molecular weight of each globular head was ∿300 kdaltons and the entire particle exhibited a molecular weight of ∿ 1.7 x 10^6 daltons, as obtained by integration of electron scattering intensities in the STEM. The polypeptide composition of 30S dynein observed by SDS-PAGE (Porter and Johnson, this volume) suggests the following stoichiometry: 3 or 4 polypeptides of > 300 kd, 1 each of 100 kd, 85 kd, and 70 kd polypeptides and a group of 3-4 20 kd polypeptides. The amplitude of the phosphate burst (Johnson and Porter, this volume) is consistent with ∿ 2 ATP binding sites per dynein molecule but further work will be required to establish the number of ATP binding sites. The nature of the dynein mechanochemical cycle must now be reconsidered in terms of this new dynein arm structure. (Supported by NIH GM 26726 to K.A.J.)

W-AM-D2 ATP SENSITIVE BINDING OF 30S DYNEIN TO BOVINE BRAIN MICROTUBULES. Mary E. Porter and Kenneth A. Johnson. (Intr. by R. A. Deering) Dept. of Biology, Univ. of Penn., Philadelphia, PA, M.B.L., Woods Hole, MA and Biochemistry Program, Penn State University, University Park, PA.

Dynein was isolated by high salt extraction of Tetrahymena cilia and was purified by chromatography on DEAE Sephacel. The binding of 30S dynein to bovine brain microtubules has been characterized as follows: (1) Titration of dynein with microtubules showed a linear increase in turbidity up to an equivalence point of 3 mg dynein/mg tubulin with apparently tight binding. (2) The increase in turbidity was reversed by the addition of ATP. (3) Electron microscopy revealed dynein arms which were spaced at 24 nm along the microtubule and were quantitatively removed following the addition of ATP. (4) SDS-PAGE analysis showed that the 30S dynein polypeptides cosediment with microtubules in the absence but not in the presence of ATP. (5) Stopped-flow measurements showed a rapid (msec time scale) decrease in light scattering due to dissociation of the dynein-microtubule complex following the addition of ATP. (6) After ATP-induced dissociation, the dynein rebound to the microtubules following a lag, the duration of which was proportional to the concentration of ATP. (7) 14S dynein did not decorate microtubules as seen by E.M., did not cosediment with microtubules, and did not alter the kinetics of ATP-induced dissociation of the 30S dynein-microtubule complex. These studies demonstrate that 30S dynein under our conditions (50 mM PIPES, 4 mM $MgCl_2$, pH 6.96) interacts with bovine brain microtubules through the ATP-sensitive site of the dynein molecule with a stoichiometry of 3 mg dynein/mg tubulin. (Supported by NIH GM 26726 to K. A. Johnson. M.E.P. was supported by NIH training grant GM 07229 and NIH GM 20644 to R. E. Stephens.)

W-AM-D3 THE PATHWAY OF ATP HYDROLYSIS BY THE DYNEIN-MICROTUBULE COMPLEX. Kenneth A. Johnson and Mary E. Porter. Biochemistry Program, The Pennsylvania State University, University Park, PA and M.B.L., Woods Hole, MA and Dept. of Biology, Univ. of Penn., Philadelphia, PA.

Dynein was obtained by high salt extraction of Tetrahymena cilia, was purified by ion exchange chromatography and was recombined with bovine brain microtubules as described by Porter and Johnson (this volume). The kinetics of ATP-induced dissociation of the 30S dynein from the dynein-microtubule complex was investigated by stopped flow light scattering measurements. The rate of ATP-induced dissociation increased linearly with increasing ATP concentration until loss of signal amplitude precluded accurate measurement of the rate (> 400 s^{-1}). The apparent second order rate constant for ATP binding to the dynein-microtubule complex was 4.8 x 10^6 M^{-1} s^{-1} (50 mM PIPES, pH 6.96, 4mM Mg Cl_2, 28 C). The kinetics of ATP binding and hydrolysis were measured by chemical-quench flow methods. The amplitude of the ATP binding transient gave one ATP site per 1 x 10^6 daltons (± 20%). At 30 μM ATP, the ATP became tightly bound at a rate of 140 s^{-1}, which equals the rate of ATP-induced dissociation of the dynein-microtubule complex. Hydrolysis occurred at a rate of 60 s^{-1} with an amplitude of 0.6 relative to the ATP binding amplitude. The following pathway is thus established.

$$M{\cdot}D + ATP \xrightarrow{1} M{\cdot}D{\cdot}ATP \xrightarrow{2} D{\cdot}ATP \underset{}{\overset{3}{\rightleftharpoons}} D{\cdot}ADP{\cdot}P_i \xrightarrow{4} D{+}ADP{+}P_i$$

where k_1 = 4.8 x 10^6 $M^{-1}s^{-1}$, k_2 > 1000 s^{-1}, $k_3 + k_{-3}$ = 60 s^{-1}, K_3 = 1.5 and k_4 = 6 s^{-1}. This is the first demonstration that ATP binding induces rapid dissociation of the dynein-tubulin complex and that ATP hydrolysis occurs at a slower rate on the free dynein molecule. (Supported by NIH GM 26726 to KAJ. MEP was supported by NIH GM 20644 to R. E. Stephens.)

W-AM-D4 VANADATE-INDUCED INHIBITION OF DYNEIN ATPASE FROM TETRAHYMENA. Takashi Shimizu and Kenneth A. Johnson. (Intr. by F. C. Wedler) The Pennsylvania State University, Department of Biochemistry, University Park, PA 16802.

The effects of vanadate on the dynein ATPase were investigated by transient state kinetic analysis of nucleotide-induced dissociation of the dynein-microtubule complex and by analysis of the presteady state phosphate burst. Dynein was isolated and recombined with bovine brain microtubules as described by Porter & Johnson (this volume) and the kinetics of ATP-induced dissociation of the complex were determined by stopped-flow light scattering measurements. Vanadate, up to a concentration of 0.05 mM, did not alter the rate of ATP-induced dissociation of the dynein-microtubule complex. Neither ADP (0.5 mM) nor vanadate (0.25 mM) alone induced the dissociation of the dynein-microtubule complex; however, together they induced the dissociation of the complex with a maximum rate of ca 0.5 sec^{-1} at saturating ADP and vanadate. Half maximal rates were obtained with ca .01 mM vanadate (saturating ADP) or with ca 0.1 mM ADP (saturating vanadate). The kinetics of the ATP binding and hydrolysis were examined by chemical-quench flow methods. Vanadate (0.05 mM) did not affect the rate or amplitude of the phosphate burst. These studies suggest that vanadate associates at the phosphate site of the catalytic center of dynein in the presence of ADP to form a dynein-ADP•V complex but does not inhibit a single turnover of ATP binding and hydrolysis in the absence of ADP. (Supported by NIH GM 26726 to K.A.J.)

W-AM-D5 EVIDENCE THAT INTERMEDIATE-FILAMENT-LIKE PROTEINS FORM INTEGRAL COMPONENTS OF MICROTUBULES. R.W. Linck, D.F. Albertini*, D.M. Kenney*†, G.L. Langevin* & A.W. Vogl.*¶ Departments of Anatomy, Harvard Medical School, Boston, MA, USA 02115 and the University of British Columbia¶, Vancouver, B.C., Canada V6T 1W5 and the Center for Blood Research†, Boston, MA, USA 02115.

Microtubule structure and chemistry have been studied using sea urchin sperm flagella (S. droebachiensis) as the model system. Extraction of purified flagellar axonemes and doublet microtubules with NaSCN or urea yields stable filaments which in negative stain measure 5-7 nm in diameter. Electrophoretic analysis of these filaments indicates that they are essentially devoid of tubulin and are composed instead of several proteins with molecular weights ranging from 47 to 56 kilodaltons and with isoelectric points from 6.0 to 7.0. Tentatively we refer to this set of proteins as "flagellar tektins" and the stable filaments composed thereof as "tektin filaments." Flagellar tektins are distinctly different from the tubulins in terms of their solubility properties, molecular weights, isoelectric points and negative stain filament structure; however, flagellar tektins are strikingly similar to several types of intermediate filaments (IFs) and IF proteins by these same criteria. These results support and more precisely define our "tektin filament hypothesis" (cf. Biophys. J. (1981) 33:215a) which suggests that polymers of certain IF proteins (i.e., tektins) form integral components of the microtubule wall. Our data suggest two possible models for the general structure of microtubules: In one case tektins form one or more of the 13 protofilaments of a microtubule; in the second case, all 13 protofilaments are composed of tubulin, but certain of these are stabilized by adjoining tektin polymers. Our models are consistent with a wide range of published observations. Supported by NIH grants GM 21527, HD 11769 and HL 24311.

W-AM-D6 CELLULAR DISTRIBUTION OF MICROTUBULES IN ADULT RAT HEART ISOLATED MYOCYTES BY INDIRECT IMMUNOFLUORESCENCE. L. RAPPAPORT, J.L. SAMUEL, F. MAROTTE, M. BORNENS and K. SCHWARTZ. Unité 127 INSERM, 41 Bd de la Chapelle, PARIS 75010 FRANCE.

The cellular distribution of tubulin has been studied by immunochemical techniques in numerous cells. Myocytes were poorly studied probably because of the thickness of the cells and their relatively low concentration of tubulin.

- Cardiac myocytes were isolated by Powells's method (1).
- Antibodies were purified from sheep or rabbit antitubulin serum by affinity chromatography made up of electrophoretically "MAP_s" - free pure rat brain tubulin.
- Presence of tubulin in myocytes was estimated by immunoenzymatic procedures.
- For microscopy studies cells were treated with triton X-100. Microtubules were visualized by an indirect immunofluorescence technique. Microtubules were distributed among three regions :

1) They concentrate in the perinuclear region ; a special intensity being observed at the poles of the nucleus. In this area they form a network between the two nuclei which could indicate an association with golgi apparatus and/or rough endoplasmic reticulum.

2) A microtubular network appears sparsely distributed in the cell, perhaps associated with myofibrils as suggested by Golstein and Entman (2) by E.M. study.

3) Fluorescence is visualized at the periphery, perpendicularly to the axis of the cell.

Microtubule networks were destroyed by either colchicine or cold treatment. They were, on the other hand, protected by treatment with taxol.

(1) T. Powell et al. J. Physiol. (1980) 302 131 (2) M.A. Golstein and M.L. Entman (1979) 80 183-95

W-AM-D7 EFFECTS OF LASER DAMAGE TO THE EUGLENA PHOTORECEPTOR ON THE CONTROL OF FLAGELLAR MOTILITY. Kathleen M. Nichols, Biology Dept. Russell Sage College, Troy, N.Y. 12180 and Robert Rikmenspoel, Dept. Biological Sciences, SUNY, Albany, N.Y. 12222.

Euglena impaled on a microelectrode were irradiated with an infrared laser beam aimed at the stigma-paraflagellar swelling. Cells were then exposed to light restricted to a 530-700 nm wavelength band or injected with negative direct current. In the absence of externally supplied Mg^{2+}, 60% of cells exhibited reversed flagellar waveforms after irradiation of the photoreceptor area with approximately 0.4 mJ of energy. Only 10% of unirradiated cells had reversed flagellar waveforms. Flagellar reversal increased to 90% when the illumination was restricted to a 530-700 nm band after irradiation. The flagellar frequency of irradiated cells was ½ the frequency of unirradiated cells in the absence of external Mg^{2+}. The irradiated and light restricted cells were non motile without externally supplied Mg^{2+}. In the presence of 3 mM Mg^{2+} the forward flagellar waveform occurred in 90% of irradiated cells under full illumination and in 83% of irradiated and wavelength restricted cells. Pre-irradiation flagellar frequencies were restored after radiation in the presence of 3 mM Mg^{2+}. The injection of 0.15 μA of negative direct current caused 100% flagellar reversal and OHz flagellar frequency after laser irradiation in the absence of external Mg^{2+}. In the presence of 3-5 mM Mg^{2+} externally supplied, Euglena exhibited 100% flagellar reversal and OHz flagellar frequency with the injection of approximately 0.45 μA. Irradiation of the Euglena photoreceptor depletes the cell of Mg^{2+} necessary for the control of flagellar motility. The irradiation of any other area of the Euglena cell with 0.4 mJ of energy did not alter the control of flagellar waveform or frequency. Supported by NIH grant HD-6445.

W-AM-D8 PRECISION MEASUREMENTS OF THE MOVEMENT OF SEA URCHIN SPERM FLAGELLA. Cheryl A. Isles and Robert Rikmenspoel, Department of Biological Sciences, SUNY, Albany, N.Y. 12222.

High speed films at 400 frames/sec were made of sea urchin sperm on Kodak 2415 emulsion. Dark field illumination, using stroboscopic flashes of 100 μsec each, and a NA = 0.85 microscope objective were employed to ensure good definition of the flagellar waveforms. At a fixed location on the flagellum, 20 μm from the head, the amplitude and the local curvature of the flagellum were measured. A grid of fine glass wires mounted in the field diaphragm of the microscope eyepiece, and illuminated from the side, served as fiducial markers for the amplitude measurements, enabling the position of the flagellum to be defined to better than 0.1 μm (s.d.). The local curvature was measured by computer from the coordinates of the flagellar position around the location at 20 μm from the head. The accuracy of the curvature measurement was close to 50 cm^{-1} (s.d.). The flagellar movements were followed for 4 to 5 periods of motion. Fourier spectra of the variation of the amplitude and of the curvature with time were computed. The results obtained so far show no Fourier components above the fundamental frequency in the amplitude measurements. The spectra for the curvature have a slight indication of a 3rd harmonic component just detectable above the background noise of approximately 3% of intensity of the fundamental frequency. The fundamental frequency was found to vary by close to 10% over the course of 4 to 5 periods of motion. These results suggest that theoretical models for the contractile events for sea urchin sperm flagella should be formulated so that the time course of the amplitude of the resulting flagellar motion is purely sinusiodal (within approximately 1%), and the time course of the local curvature does not deviate more than approximately 3% from purely sinusoidal. Supported by NSF grant PCM 8003700.

W-AM-D9 PRESSURE-INDUCED DEPOLYMERIZATION OF GFA INTERMEDIATE FILAMENT PROTEIN. James S. Huston, Linda B. Cooley, Dept. of Biochemistry, Albany Medical College, Albany, NY 12208, David C. Rueger and Amico Bignami, Dept. of Neuropathology, Harvard Medical School, and Spinal Cord Injury Research, West Roxbury VA Medical Center, Boston, MA 02132.

Glial fibrillary acidic (GFA) protein forms 8 to 10 nm filaments in astroglial cells of the CNS. These intermediate filaments are similar to those generally present in the eukaryotic cytoskeleton. Our velocity sedimentation studies of purified bovine GFA protein reveal marked depolymerization as rotor speed increases. In low speed runs utilizing a UV scanner, protein turbidity decreases monotonically with increasing radial position until it drops precipitously to zero near the base of the solution column. In 50mM NaCl + 2mM Tris + 0.5mM dithiothreitol, pH 7.8 at 20°C, apparent S values range from 65 to 375 S at 8,000 rpm, while they span 5 to 47 S at 40,000 rpm. This behavior is clearly indicative of pressure-induced depolymerization of GFA protein aggregates in solution. The low speeds at which this effect manifests itself emphasize that caution must be exercised in experimental manipulations of GFA and perhaps other intermediate filament proteins. For example, in purification schemes that alternate between high and low speed centrifugations, GFA-like species will cycle between small and large aggregates that can copurify with other filamentous proteins isolated. This would not derive from specific interactions between different proteins, but from pressure effects on self-association of the intermediate filament protein. Likewise, use of ultracentrifugation to quantitate the fraction in filamentous states could be problematical, in that pressures generated during fractionation would depolymerize aggregates normally present at 1 atm pressure.

Supported by grants from NSF (BNS 80-19867), NIH (NS 13034, BRSG#S07RR07394-20), and the VA.

W-AM-D10 "COMPUTER-LIKE" INFORMATION PROCESSING IN CYTOSKELETAL PROTEINS. SR Hameroff, RC Watt, Department of Anesthesiology, University of Arizona, Tucson, AZ 85724

Cellular functions including neural axonal transport depend on cytoskeletal proteins such as microtubules (MT) and associated ATPase proteins. Mechanisms of spatial and temporal control remain unknown in axonal transport and similar MT functions. The cylindrical grid-like MT structure and connecting proteins could provide programmable switching matrices for information transfer resulting in temporal and spatial control of axonal transport and other functions. Media of information transfer among the 4 nm, 55,000 dalton subunits could include conformational states coupled to Ca^{++}, energy state, or electron occupancy/excitation in aromatic hydrophobic regions. Tubulin switching programming regulating intracellular functions could ensue from genetically-controlled primary protein structure or post translational effects. Pulsed reading, switching, and transduction could be driven by membrane depolarization or calcium ion fluxes. Key intra-protein hydrophobic environments could thus integrate and transduce several input modes to determine conformational state and mechanical activities. Aspects of this model are analogous to information and computer technologies including programmable Boolean switching matrices, transistor circuits, bubble memory, charge transfer devices, and/or surface acoustic wave resonators.

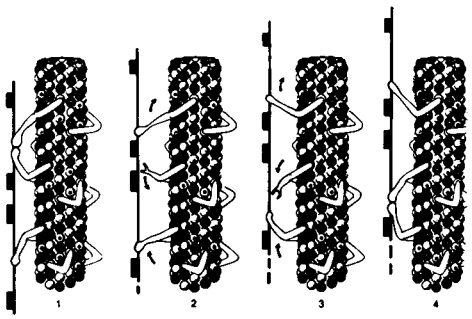

W-AM-D11 INITIATION OF ADH-INDUCED WATER FLOW: ROLE OF MICROTUBULES, L.M. COLUCCIO, R.J. BRADY, R.H. PARSONS (Intr. by, W.H. JOHNSON). BIOL. DEPT. R.P.I., TROY, N.Y. 12181

Use of microtubule-disrupting drugs, specifically colchicine, has previously demonstrated a need for microtubules in the initiation of the increased water permeability which occurs in response to ADH stimulation. To investigate the role of microtubules we have used a combination of the microtubule-disrupting drug colchicine and high hydrostatic pressure to determine whether formed or growing microtubular structures are required for initiation of the ADH response. Other systems have shown pressure-induced disassembly of microtubules to be reversible followed by reassembly in 15-20 minutes following release. When ADH and 8000 psi are administered simultaneously, the initiation of the ADH-induced increase in water flow is inhibited by 71% $\pm$ 9.03 (6) during the time the bladders are under pressure, supplying further evidence that microtubules, depolymerized by the pressure, are required for initiation of the response. 8000 psi applied 10 minutes prior to ADH results in an increased rate of initiation compared to control (ave. increase during first 3 minutes 1.25 $\pm$ 0.27 (6) water flow units, $(mg \cdot cm^{-2} \cdot min^{-1})$ per minute vs. 0.43 $\pm$ 0.12 (6) wfu's/min). These results indicate that the process of reassembly has accelerated the ADH response since polymer formation is favored upon release of pressure. The inhibition of the ADH initiation brought about by colchicine (ave. 3 min increase, colchicine treated 0.18 $\pm$ 0.04 (6) wfu's/min.) is released with pretreatment with 8000 psi for 10 minutes (ave. 3 min increase colchicine + pressure 1.13 $\pm$ 0.06 (6) wfu's/min.). Repeating the experiments with dibutyryl cAMP gave similar results. These data can be interpreted as suggesting that the growing structure, i.e. the assembly of the tubulin dimers into microtubules, is required for ADH-induced initiation.

W-AM-D12 A MODEL OF DEOXYGENATED SICKLE HEMOGLOBIN FIBERS DERIVED FROM X-RAY DIFFRACTION DATA by B.M. Fairchild & L.S. Rosen. St. Luke's-Roosevelt Hospital Center, Columbia University, College of Physicians and Surgeons, New York, N.Y. 10025.

The basic structural unit of the fiber, the protofilament, is similar to the double filament formed by the 64Å repeat of the asymmetric unit of a monoclinic crystal, form I. Comparison of the fiber pattern to that of a second monoclinic crystal, form II, suggests that the fiber structure resembles more closely the structure of both these crystalline forms combined than either one alone. A fiber model comprising both monoclinic crystals, where one form is displaced along the fiber axis by 5Å with respect to the other, yields a minimal residual of .33 when the fiber pattern is compared with calculated structure factors of the model. An extension of this model consists of a combination of 3 monoclinic unit cells, with their 6 protofilaments in the appropriate juxtapositions, to which is added a single unpaired protofilament transposed from the structure of a newly described triclinic crystal, form III. These 7 protofilaments pack in a pseudo-hexagonal arrangement as seen in the projection down the fiber axis, similar to that suggested by reconstruction from electron micrographs. In our preliminary model, the pairing of single filaments that form the 6 protofilaments, and their respective polarities, are the same as in the monoclinic crystals; the polarity of the unpaired protofilament is not yet known. This pairing scheme based on crystalline structures does not agree with that derived from electron microscopy of incomplete fibers in which 2 or 4 protofilaments are absent. Because of the persistent resemblance of fiber to crystalline structure, the intermolecular interactions that stabilize the fiber possess quasi-equivalences not expected from such a complicated architecture. (Supported by NIH grant HL 23984)

W-AM-E1 ELECTRON FLOW IN THE CHLOROPLAST CYTOCHROME b_6f COMPLEX DRIVEN BY THE PHOTOCHEMICAL REACTION CENTER OF THE BACTERIUM RHODOPSEUDOMONAS SPHAEROIDES R.C.Prince,K.Matsuura,E.Hurt*, G.A. Hauska* and P.L.Dutton. Department of Biochemistry and Biophysics,University of Pennsylvania,Pa 19104 and (*) Department of Botany,University of Regensburg,West Germany.

The cytochrome b_6f complex of chloroplasts functions both between the photosystems,as a plastoquinol-plastocyanin oxidoreductase,and in a cyclic pathway around photosystem 1.This diversity of function,together with the high chlorophyll content in vivo,has made it difficult to study. The recent isolation of a chlorophyll-free,functional b_6f complex (EJB 117 591) allows in vitro studies,and here we report a construction with the well characterized reaction center of Rps. sphaeroides.In the presence of equine cytochrome c and ferrocyanide as electron donors to the RC, electrons are delivered from the RC to the b_6f complex,but only at high ambient redox potentials. Nothing happens on flash 1,but on flash 2 both cytochromes b_6 and f are seen to go reduced.If f is prereduced,b_6 is still seen to go reduced,but if the Rieske iron-sulfur center is prereduced,no b_6 reduction occurs.We interpret this as oxidant-induced reduction of b_6;flash 1 generates an impotent Q_B semiquinone in the RC,and flash 2 produces Q_B quinol.This delivers both electrons to the b_6f complex.One goes,via Rieske,to f,the other to b_6,in reactions sensitive to DBMIB and DNP-INT.We do not yet know whether the Q_B quinol migrates to the b_6f complex,or whether it reduces a Q_Z quinone in the complex,but in either case the reaction is quite rapid,for b_6 reduction is complete within 35 ms.

This work was supported by NSF grants 79-19598 and 79-09042,and DFG SFB 43/C2

W-AM-E2 QUANTITATIVE MEASUREMENT OF THE ELECTROCHEMICAL PROTON GRADIENT IN CELLS OF A PHOTOSYNTHETIC PURPLE SULFUR BACTERIUM. Victor L. Davidson and David B. Knaff, Department of Chemistry, Texas Tech University, Lubbock, TX 79409.

Cells and chromatophores of the photosynthetic purple sulfur bacterium Chromatium vinosum generate a transmembrane electrochemical proton gradient ($\Delta\bar{\mu}_H+$) outside acidic and positive upon illumination. The magnitudes of $\Delta\bar{\mu}_H+$ and its components ΔpH and the membrane potential ($\Delta\psi$) have been determined under a variety of conditions. ΔpH and $\Delta\psi$ vary considerably as a function of both the pH and cation composition of the external medium. These effects can be explained by the presence of cation-proton antiports and cation dependent transport systems. Either ΔpH or $\Delta\psi$ can be selectively eliminated using specific ionophores and uncouplers. Elimination of one component of $\Delta\bar{\mu}_H+$ often results in dramatic changes in the magnitude of the other component. Knowing the values of ΔpH and $\Delta\psi$ and having the ability to manipulate the relative contributions of each to $\Delta\bar{\mu}_H+$ has enabled us to perform experiments which more clearly define the nature of the driving force for several cation and amino acid transport systems in C. vinosum.

This research was supported by grants (PCM 78-17304 and PCM 81-09635) from the National Science Foundation to D.B.K.

W-AM-E3 STUDIES ON RECONSTITUTED BACTERIAL COUPLING FACTORS AFTER LABELING WITH THE TRIPLET PROBE EOSIN.Rita Casadio'and Richard Wagner''.'Institute of Botany,University of Bologna,Italy and''Leherstuhl Biophysik,Universität Osnabrück ,Germany(FRG).

Eosin-isothiocyanate was covalently bound to bacterial coupling factors(BF1) isolated from cromatophores of Rhodopseudomonas sphaeroides.Isolation of the enzyme was performed by means of usual techniques(either by sonication or chloroform treatment of chromatophores).The crude extract was purified on a Sephadex G-200 gel.In contrast to other methods(1),the latter procedure yielded a 95% pure enzyme with a molecular weight of about 300 KD and both Mg^{++} and Ca^{++}dependent ATPase activities which contained 5 subunits.Eosin-labeling impaired neither the activities of the isolated enzyme,nor its functional reconstitution into depleted membranes.This was analogous with the behaviour of chloroplast CF1(2).Photoselection experiments were carried out with chromatophores reconstituted with eosin-labeled BF1.The eosin probe was used as a spectroscopic tool to measure the rotational mobility and domain flexibility of the enzyme in relation to the extent of the transmembrane electrochemical potential difference and in the presence of its substrates as in previous work with CF1(2) and with the ferredoxin-NADP-oxidoreductase(3).

1)Baccarini-Melandri ,A. and Melandri,B.A.(1980)Methods in Enzymology 69,313-321.
2)Wagner,R.and Junge,W.(1980)FEBS Lett.114,327-332.
3)Wagner,R.,Carrillo,N.,Junge,W.and Vallejos,R.(1981)FEBS Lett.131,335-340.

W-AM-E4 ATP FORMATION RESULTING FROM SINGLE TURNOVERS OF THE ELECTRON TRANSPORT CARRIERS IN CHLOROPLASTS. Donald R. Ort, and Thomas Graan (Intr. by D. DeVault), Dept. of Botany, University of Illinois, Urbana, Illinois 61801, U.S.A.

Two saturating single-turnover flashes spaced 100 ms apart is sufficient to achieve ATP formation in isolated chloroplast thylakoids. Two turnovers of the electron carriers result in the accumulation of about 7 nmoles of H^+/mg chlorophyll. Under the same conditions (i.e. ΔG_{ATP}=40 KJ/mol) a solitary flash is inadequate to produce ATP. The electron flux from the third or any subsequent flash is coupled to ATP formation as efficiently as is observed in continuous light (i.e. ATP/2e > 1.0). The yield of ATP per flash increases with declining temperature being largest near 4° C the lowest value tested. The number of H^+ accumulated per flash is independent of temperature so the greater yields of ATP near 4° C indicate that fewer protons are exiting the membrane via nonproductive pathways. The yield of ATP per flash near 4° C is largely independent of flash frequency between 1 and 30 Hz.

When the formation of an electrical potential difference is prevented by adequate amounts of valinomycin and potassium the accumulated effects of 10 flashes are required before ATP formation is achieved. In the presence of the exchange carrier Nigericin, the electrical component of the driving force for ATP formation is enhanced at the expense of the ΔpH. In this case ATP formation is efficiently coupled to electron flux only at flash frequencies rapid enough to allow a summation of the electrical field. These results clearly demonstrate that any processes which are prerequisites to ATP synthesis (i.e. activation of coupling factor or generation of Δ P) are fulfilled by a remarkably small number of charge separations.

W-AM-E5 THE IMPORTANCE OF ADENYLATE KINASE ACTIVITY IN DEVELOPING A QUANTITATIVE MODEL FOR H. HALOBIUM PHOTOPHOSPHORYLATION. S.L. Helgerson, Carol Requadt, and Walther Stoeckenius, CVRI and Dept. of Biochemistry and Biophysics- UCSF, San Francisco, CA 94143.

When H. halobium R1 cells containing bacteriorhodopsin are illuminated under anaerobic conditions, both the rate of photophosphorylation and the steady state ATP level are controlled by the light intensity (i.e., the energy input to the system). The rate and extent of ATP synthesis saturate at approximately 25 mW/cm^2 and 2.5 mW/cm^2 (500-700 nm illumination), respectively. The intracellular ATP, ADP, AMP and P_i concentrations have been measured at various light intensities. From these data the phosphorylation potential and the energy charge (E.C. = (ATP + ½ ADP)/(ATP + ADP + AMP) were calculated. We found that (a) [P_i] is in three fold excess over the total adenosine nucleotide pool; (b) both [ADP] and [AMP] decrease as ATP is synthesized; (c) the rate and relative increase in the E.C. and ATP show a similar dependency on illumination intensity; and (d) the relative concentration of each nucleotide varies smoothly with the E.C. This result indicates that an intracellular adenylate kinase activity (2ADP $\leftrightarrow$ AMP + ATP; K_{app} = 0.5) is present. The adenylate kinase acts to buffer the cellular phosphorylation potential against changes in the energy input. Thus, any quantitative energy coupling model must take into account the chemical energy stored in the total adenosine nucleotide pool, not just in the measured phosphorylation potential. (Supported by NIH Program Project Grant GM 27057).

W-AM-E6 INVESTIGATIONS INTO THE WATER-OXIDIZING ENZYME: CHOLATE-SOLUBILIZED PROTEINS. Daniel Abramowicz, Sarah Tabbutt, and G. Charles Dismukes, Department of Chemistry, Princeton University, Princeton, NJ 08544 USA

Isolated spinach thylakoids have been extracted with cholate, which releases a mixture of 15-20 proteins. Applying isoelectric focusing in a sucrose gradient and chromatofocusing techniques, we have achieved analytical separation and high resolution of the cholate-extracted mixture. The effect of this extraction upon the O_2 evolution rate is partially reversible, as shown by a restoration of up to 40% original activity upon dialysis to remove cholate. We have isolated a 65kD protein with a pI of 5.9-6.1. This protein contains a significant amount of Mn (@ 0.5 atom $\pm$ 0.5), although the overwhelming majority of the Mn appears in the protein fraction containing the coupling factor (CF) subunits. This 65kD protein has not been reconstituted to extracted membranes. If CF is extracted prior to the cholate-solubilization (NaBr, dithyiothreitol, EDTA), O_2 evolving capacity is destroyed and most of the Mn no longer migrates with the protein between pI 8.5-5.0. Some of the protein bound Mn is labile and conditions are being optimized to reduce the loss of native Mn from the proteins. Further experiments, including attempts at reconstitution and spectroscopic studies (UV-Vis and low temperature EPR), are under way.

These preliminary results lend support to some previous experiments. SPECTOR and WINGET (PNAS 77, 957-959) have isolated a 65kD protein containing 2 Mn atoms which they report is capable of reconstituting significant O_2 evolution to depleted membranes. This protein has subsequently been shown to photodimerize. Also, DISMUKES and SIDERER (PNAS 78, 274-278) have shown the enzyme contains at least 2 and probably 4 Mn ions with in vivo EPR experiments on broken chloroplasts.

W-AM-E7 CHLORIDE EFFECTS IN PHOTOSYSTEM II REACTIONS OF CHLOROPLASTS FROM SALT-TOLERANT HIGHER PLANTS. C. Critchley, Govindjee, I. C. Baianu, and H. S. Gutowsky, University of Illinois, Urbana, Illinois 61801.

Chloride is an essential cofactor in photosynthetic O_2 evolution. The O_2 evolving complex appears to be the only site in the linear electron transport chain responsible for this effect. In thylakoids from spinach, peas and maize 10 to 20 mM Cl^- is required to restore fully the O_2 evolution. In thylakoids isolated from leaves of salt-tolerant species, however, maximal O_2 evolution activity and chlorophyll a fluorescence induction require 250 to 500 mM Cl^-, in the pH range between 7.4 and 8.2, where rates of O_2 evolution and fluorescence induction in the absence of added Cl^- are extremely low or zero. The effect is specific for Cl^- since other halides, i.e., Br^- or I^-, or complex anions like NO_3^- do not or only poorly substitute for Cl^-. F^- and SO_4^{2-} are inhibitory in all systems tested. Only electron transport including PS II is adversely affected by the absence of Cl^- from the assay medium. PS I activity is almost entirely insensitive to Cl^-. The loss of chlorophyll fluorescence induction, observed in Cl^- deficient samples, indicates loss of activity on the donor side of PS II, i.e., a block in the water splitting reaction. Addition of electron donors to PS II in samples without added Cl^- restores the fluorescence transient, indicating that the O_2 evolving complex is the site for Cl^- action. ^{35}Cl-NMR measurements on thylakoid pellets and suspensions from some of the salt-tolerant species in the presence of 1M NaCl show a pH dependence of $1/T_2^*$, which correlates with that of O_2 evolution. The marked broadening of the ^{35}Cl line is indicative of Cl^- binding and this is indeed observed in the pH range where maximal O_2 evolution occurs. The results suggest that in chloroplasts from halophytic higher plants, the reversible, pH dependent binding of Cl^- is necessary to activate the O_2 evolving system.

W-AM-E8 PHYSIOLOGICAL STUDIES OF P_{588} IN A BACTERIORHODOPSIN-DEFICIENT *HALOBACTERIUM HALOBIUM* MUTANT STRAIN. H. Jurgen Weber*, S.L. Helgerson* and I. Probst+, *C.V.R.I., UCSF, San Francisco, CA 94143. +Physiol. Chem. Inst., Univ. Gottingen, W.Germany.

We present evidence that *Halobacterium halobium* mutant strains can be isolated which - when rigorously characterized - can be used for a dissection of complex light-mediated ion fluxes in these bacteria. One of these strains JW-1 (formerly called ET-15) lacks the light-driven proton pump bacteriorhodopsin (BR) but contains another pigment, P_{588}. Envelope vesicles or whole cells of this mutant display only uniphasic, light-mediated proton uptake which is enhanced by uncouplers and suggests that the driving force for proton uptake in this strain is a light-generated membrane potential. Such potentials (80 mV, inside negative) can indeed be measured in envelope vesicle preparations. In contrast, measurements of membrane potentials in JW-1 cells did not reveal changes in the light, although light-mediated, uncoupler-enhanced proton uptake by the same cells was again observed. In addition, no change of internal ATP levels could be detected in the light. Another strain, JW-11, is a mutant which lacks retinal biosynthesis and light-induced proton translocation. Supplementation of the medium with all-trans retinal during cell growth restored the capability for uncoupler-stimulated proton uptake mediated by P_{588}, thereby suggesting a retinal requirement for this pigment. These data and the action spectrum of proton uptake suggests that P_{588} is identical or part of a recently proposed light-driven Na^+-pump in *Halobacterium halobium*. (Supported by NIH Grant GM 28767, and NIH Program Project Grant GM 27057).

W-AM-E9 PHOTOSYNTHETIC PERTURBATIONS IN STRESSED PLANT LEAVES: VISUALIZATION BY DELAYED LIGHT EMISSION IMAGE INTENSIFICATION. James L. Ellenson, Boyce Thompson Institute, Ithaca, New York.

Image intensified detection of delayed light emission (DLE) is being used to investigate perturbations in photosynthetic activity of intact plant leaves exposed to physiological stress. The stress studied in the present investigation is that due to leaf exposure to sulfur dioxide (SO_2). Because SO_2 inhibits electron transport through the Photosystem II (oxygen-evolving) portion of the photosynthetic electron transport chain, and because DLE is a sensitive indicator of Photosystem II activity, the presence of SO_2 in leaf tissues is detected by alterations in DLE intensities. Upon initiation of SO_2 exposure ($\leq$2 ppm) dramatic, local increases in leaf DLE are initially detected. Prolonged exposure, however, results in a characteristic diminution of DLE in leaf areas which will eventually show visible injury. The pattern of these DLE emission intensities has been found to be a very sensitive indicator of metabolic injury prior to any evidence visible to the naked eye. Combined with more conventional measurements of leaf gas exchange phenomena, DLE imagery provides a new and more detailed means to study how photosynthetic activity in intact plant systems behaves under both normal and stressed conditions.

W-AM-E10 PHOTOSYNTHETIC EFFICIENCY, TIME DOMAINS, AND THERMODYNAMICS. Harold J. Morowitz and Alan Bearden, Dept. of Biophysics and Biochemistry, Yale University, New Haven, CT 06520, and Dept. of Biophysics and Medical Physics, Univ. of California, Berkeley, CA 94720.

Over the past 30 years, a series of discussions on photosynthetic efficiency has been based on assigning a "temperature" to a beam of light and then applying the Carnot formalism. While the Planck analysis allows one to assign temperature and entropy to equilibrium radiation in a cavity, the use of these constructs in the far from equilibrium domain is unjustified and leads to numerical values of unknown validity. First we establish that the early events of photosynthesis are adiabatic because they occur in a time domain very short compared with collision equilibrium times. Secondly we establish the experimental irreversibility of the light reactions. Thirdly we prove that assigning temperatures and entropies to a light beam (as distinguished from a cavity containing radiation) leads to a clear violation of the second law of thermodynamics. These three results make it clear that thermodynamics and near to equilibrium irreversible thermodynamics are the wrong conceptual tools for the study of photosynthetic efficiency. Trying to develop more appropriate theoretical tools leads to an analysis of time domains and the relationship of processes that occur with very widely different time constants. Classical thermodynamics was not faced with this kind of problem, but students of phenomena in the picosecond range must deal with this type of irreversibility in an explicit fashion.

A.B. wishes to acknowledge support through the Biophysics Program of the NSF (PCM 78-22245) and from the Department of Energy through the Lawrence Berkeley Laboratory of the University of California.

W-AM-F1 A ^{13}C NMR STUDY OF GLYCOGEN METABOLISM IN THE PERFUSED RAT LIVER. Laurel O. Sillerud*, Carl W. Westphal*, Takashi Ogino*, and Robert G. Shulman. Yale University, New Haven, CT 06511 (introduced by R. J. Gillies).

The synthesis and degradation of glycogen by the liver plays a fundamental role in the regulation of the blood glucose level in mammals. Glycogen metabolism is controlled by several means, one of which involves the polypeptide hormone glucagon. It has been shown that the [1-^{13}C] peak of liver glycogen synthesized from ^{13}C labeled glycerol can be identified in perfused mouse livers, and it was shown that glucagon will hydrolyze the glycogen (1). We now show how carbon-13 nuclear magnetic resonance spectroscopy can be used to follow glycogen synthesis and degradation in the perfused rat liver. The concentrations of glycogen in the livers from fed rats is high enough so that we have measured it by natural-abundance ^{13}C NMR. This eliminates the need to use ^{13}C-labeled compounds, at least when glycogenolysis by glucagon was followed at the natural abundance level of ^{13}C NMR. At 31°C the half life of glycogen decreased from 500 min to $\sim$ 80 min upon the addition of 10 nM glucagon. Under this stimulation the rate of glucose formation was 0.7 μ moles/g-liver/minute. Perfusion of the liver with 25 to 30 mM [1-^{13}C] glucose led to net glycogenesis with a glucose consumption rate of 0.6 μ mole/g-liver/minutes. Quantitative interpretation of the results was facilitated through the utilization of ^{13}C NMR difference spectroscopy by means of which it was possible to completely remove the natural-abundance background ^{13}C spectrum of the liver. Under these circumstances the mobilization or deposition or other endogenous substances could also be observed. [1]Cohen, S.M., Rognstad, R., Shulman, R.G. & Katz, J. (1981) J. Biol. Chem. 256: 3428.

W-AM-F2 HUMAN PLATELET CYTOPLASMIC pH AND ITS STIMULUS-INDUCED INCREASE. Nancy E. Norman, David B. Schwartz and Elizabeth R. Simons. Boston University School of Medicine, Boston, MA 02118.

We have shown earlier that stimulation of washed human platelets by α-thrombin leads to a dose-dependent depolarization of their membrane, measured via the distribution of a fluorescent or of a tritium-labelled lipophilic cation. We can now demonstrate that a similarly thrombin dose-dependent alkalinization of the platelet's cytoplasm accompanies such a stimulation. The pH gradient change has been monitored fluorimetrically via adaptations of the techniques of Deamer *et al.* (Biochim. Biophys. Acta 274: 323, 1972) and of Thomas *et al.* (Biochemistry 18: 2210, 1979). They are based on different principles depending, respectively, on the distribution of the weak fluorescent base 9-aminoacridine between the buffer and the platelet and on the *in situ* formation via esterolysis of 6-carboxyfluorescein in the cytoplasmic compartment. With 6-carboxyfluorescein, intracellular pH can be probed either in pre-equilibrated platelets or via analysis of the kinetics of hydrolysis of 6-carboxyfluorescein diacetate in the cytoplasm. These techniques indicate that the normal platelet's transmembrane potential decreases and its cytoplasmic pH increases within less than 5 seconds after exposure to thrombin. At a saturating dose, ≥ .025 U/ml, the cytoplasmic pH has risen by 0.27 units from a resting pH of 7.0 (when cells are equilibrated at pH 7.35 in Hepes buffer). A parallel drop in membrane potential, from -52 to -15 mv, occurs. These techniques are also applicable to studies of the effects of drugs on the stimulus response of a human platelet. (Supported by NIH grant HL 15355).

W-AM-F3 THE PLATELET AGGREGOMETER -- AN ANOMALOUS DIFFRACTION EXPLANATION

Paul Latimer, Physics Department, Auburn University, AL 36849

The *in vitro* aggregation of blood platelets is normally followed with a visible light transmittance photometer (aggregometer) and platelets in plasma from which the erythrocytes and leucocytes have been removed. It is generally supposed that aggregation leads to a simple increase in transmittance although no supporting optical explanation has been offered. We used a basic anomalous diffraction relation to access the influence of various elements of structural detail on scattering by an aggregate. It is found that a given aggregate can be realistically modeled with a certain heterogenous population of spheres of suitable size and refractive index. As a test, the effects of the aggregation of latex spheres on suspension transmittance were measured and successfully accounted for with this theoretical approach. When applied to platelets, the theory predicts that if transmittance is measured with a photometer with a highly collimated optical system, the initial stages of aggregation will cause transmittance to decrease and that the later ones cause it to increase. If the optical system is not highly collimated, aggregation is predicted to always cause transmittance to increase. The implications of these findings are two-fold. Some reported aggregometer time curves need to be reinterpreted. Discrepancies between some results from different laboratories are probably due to differences in the designs of their photometers, not as has been supposed to differences in the morphological behaviors of the platelets.

W-AM-F4 A HIGH RESOLUTION TELEVISION DETECTOR FOR X-RAY DIFFRACTION AND ELECTRON MICROSCOPY. Kenneth Kalata (Intr. by W. Phillips), Rosenstiel Basic Medical Sciences Research Center, Brandeis University*, Waltham, MA 02254.

A versatile television detector system has been built for X-ray diffraction and electron microscope studies in structural biology. A camera head consisting of a thin phosphor convertor, an image intensifier, and an SIT vidicon tube generates a real-time video image which is processed digitally and integrated in a large, high-speed memory system. Active areas from 4 to 80mm square can be selected and easily changed. For rates of up to 10^4 or 10^5 events/sec the location of each event can be computed, while rates of up to 10^{12}/sec can be accommodated by continuously digitizing and storing the video signal at each pixel. All scan and data acquisition parameters and operating modes are under software control to allow the detector system to be optimally configured for each application. The spatial resolution depends on the active area and operating mode and ranges from 10 to 150μ. Array sizes of up to 4000x4000 pixels can be selected to match the detector resolution and the available memory. Data can be collected 10 to 20 times faster than with film and a dynamic range greater than 10^3 to 10^4 can be obtained.

Supported by the author and by NSF Grant PCM-7922766.

*Also Harvard/Smithsonian Center for Astrophysics, Cambridge, MA 02138;
and Mimbres Research Institute, Mimbres Hot Springs Ranch, San Lorenzo NM 88057.

W-AM-F5 THE THREE-DIMENSIONAL RECONSTRUCTION OF BIOLOGICAL MACROMOLECULES. Jonathan Seymour, Rosenstiel, Brandeis University, Waltham, MASS 02254.

The application of image analysis techniques to electron micrographs of negatively stained macromolecules has yielded low resolution (2-3 nm) structural information on a variety of biological macromolecules. A method has been developed to calculate reconstructions of particles with a one-dimensional repeat from a series of micrographs, where the specimen is tilted at different angles around the crystallographic axis. The resolution is limited by the restricted range of tilt angles available (usually ±60) and is approximately inversely proportional to the particle diameter (for example spacings out to 1/3.3 nm^{-1} can be used if the particle diameter is 7 nm). Transform data are collected on a series of layer planes and reconstructed using Fourier-Bessel inversion methods. The method provides an objective measure of symmetry elements that may be present in the particle. Tilt series of TMV and F-actin paracrystals have been recorded and the equatorial layer plane of data analysed. The profile of the stain envelope surrounding these particles has been determined, yielding information on the extent of flattening in negative stain and the packing of filaments within F-actin paracrystals. This technique tests the validity of assuming that helical particles retain their symmetry in negative stain and also can potentially improve the powerful helical reconstruction method, by providing additional information on the equatorial layer plane and allowing filament components that donot obey helical symmetry, but do obey the one-dimensional repeat, to be included in the reconstruction. (This work was supported by a Fellowship from the Muscular Dystrophy Association).

W-AM-F6 DIFFERENTIAL-WAVELENGTH DECONVOLUTION OF TIME-RESOLVED FLUORESCENCE INTENSITIES: A NEW METHOD FOR ANALYSIS OF EXCITED STATE REACTIONS by Joseph R. Lakowicz and Aleksander Balter, University of Maryland, School of Medicine, Department of Biological Chemistry, Baltimore, Maryland 21201.

We present a new method for the analysis of time-resolved decays of fluorescence intensity. This procedure was used to resolve the initially excited and the solvent relaxed states of N-acetyl-L-tryptophanamide (NATA) in propylene glycol and to determine the kinetic constants for the excited state acid-base reactions of 2-naphthol. Time-resolved decays of fluorescence were collected at wavelengths across the emission spectra. Instead of the usual procedure of deconvolving these data using the lamp pulse, we deconvolved these data using the response observed on the short wavelength side of the emisssion. The advantages of this procedure are twofold. First, the spectral contribution due to the initially excited state appears as a zero-decay time component which is easily measured. For NATA in propylene glycol at -20°C the resolved spectra displayed emission maxima at 320 and 350 nm. Secondly, this deconvolution procedure greatly simplifies the analysis of reversible excited state reactions, as we illustrated for 2-naphthol. When the usual deconvolution procedure is used one finds two wavelength-independent decay times. Both decay times are dependent upon the forward and reverse reaction rates. In contrast, by using differential-wavelength deconvolution, the non-zero decay time is characteristic of only the emission rate and reverse reaction rate of the reacted state. The zero-decay time component reveals the extent of spectral overlap. Since no additional data acquisition is required by our procedure, we expect that this method will enhance the usefulness of time-resolved data for analysis of excited state processes.

W-AM-F7 DERIVATIVE RAMAN SPECTROSCOPY APPLIED TO BIOMEMBRANE SYSTEMS Martin Van de Ven and James P. Sheridan, Optical Probes Branch, Code 6510, Naval Research Laboratory, Washington, D.C. 20375, USA This paper describes the first application of derivative Stokes-Raman light scattering to biomembrane systems. The technique offers an extremely promising method for the rejection of high fluorescence backgrounds to yield increased signal-to-noise ratios together with improved detection of weak shoulders in spectral lines and/or small shifts in the peak of a spectral line. In this technique, when the wavelength of the exciting light is modulated, the wavelength of the Raman scattered light, but not the broad luminescent background, is correspondingly modulated. The exciting source consists on an Ar^+ laser-pumped CW Rhodamine dye laser. Tuning of the dye laser is carried out with an electro-optic birefringent tuner. The wavelength is sinusoidally modulated with a stable audio-oscillator. The wavelength-modulated Raman signal is converted into an amplitude modulation via a scanning Spex double monochromator. The signal is demodulated via a phase-sensitive lock-in-amplifer. The output is proportional to the first derivative of a Raman spectrum if the modulation bandwidth is small compared to the width of a Raman line. The biomembrane systems studied include multilamellar liposomes composed of mixtures of phospholipids and cholesterol with and without the polyenes β-carotene or Amphotericin B. These model membrane systems, containing highly fluorescent components, are shown to yield accurate Raman data while substantially supressing sample fluorescence. In particular, the initial results indicate that the modulation technique, when properly used, can offer improvements in Raman signal/noise ratios of up to an order of magnitude for the conformationally sensitive phospholipid acyl chain vibrations.

W-AM-F8 SURFACE BINDING RATES OF NON-FLUORESCENT MOLECULES MAY BE OBTAINED BY TOTAL INTERNAL REFLECTION / FLUORESCENCE CORRELATION SPECTROSCOPY (TIR/FCS). Nancy L. Thompson and Daniel Axelrod, Biophysics Research Division, University of Michigan, Ann Arbor, Michigan, 48109.

The combination of total internal reflection with fluorescence correlation spectroscopy (TIR/FCS) can measure the association and dissociation rates of fluorescent-labeled solubilized biomolecules at a solid surface (Thompson et.al., Biophys.J. 33: 435). Conventional TIR/FCS does not require an extrinsic perturbation from chemical equilibrium or a spectroscopic or thermodynamic difference between the solubilized and surface bound states, but it does require the molecules to be fluorescent. We demonstrate theoretically that TIR/FCS can also measure the surface binding rates of a non-fluorescent chemical species.

In TIR/FCS, fluorescent molecules bound to a solid/liquid interface are selectively excited by the evanescent wave of a totally internally reflecting laser beam. As molecules bind and unbind in chemical equilibrium, the fluorescence collected from the surface fluctuates at random; the rapidity of these fluctuations determined by on-line photon autocorrelation is related to the kinetic rates of binding. In the new version of TIR/FCS, non-fluorescent molecules (whose kinetic rates are of interest) compete in equilibrium with fluorescent analogs for surface binding sites. We show how the autocorrelation function of fluorescence fluctuations depends on the binding and unbinding rates of both molecular types.

The competition approach also allows the investigation of chemical kinetics at surfaces whose binding sites are nearly saturated. By mixing fluorescent-labeled and unlabeled solute, the normalized variance of the fluorescence signal can be increased to an experimentally practicable level.

W-AM-F9 AUTOMATIC RECORDING APPARATUS FOR π-A ISOTHERMS OF MONOLAYERS, Y. Hifeda and G. W. Rayfield, Physics Department, University of Oregon, Eugene, Or 97403.

A simple π-A automatic recording apparatus is described which is inexpensive, simple to build and operate. An 11" x 14" x-y recorder and an inexpensive linear motion transducer are the main ingredients of the apparatus aside from the sheet of teflon used for the trough. The x-y recorder both records and drives the surface barrier while the linear motion transducer was used to construct a vertical pull surface balance utilizing a glass Wilhelmy plate (sensitivity .022 dyne/cm per mV). Bath temperature is regulated by using a fish aquarium pump to circulate water from a large reservoir through glass tubing in the aqueous substrate.

Extensive π-A measurements were carried out on palamitic, myristic, stearic, oleic, arachidic and behenic acids in order to test both the procedure and apparatus. The effect of contaminates, compression rate, temperature, aqueous substrate and calcium ion concentration were investigated in detail. These results will be presented with reference to previous work by other investigators on these same fatty acid monolayers. The meaning of π-A isotherms measured with a vertical pull surface balance will also be discussed.

W-AM-Po1 CONTRACTION BAND BEHAVIOR IN INTACT & CHEMICALLY SKINNED, ISOLATED CARDIAC MUSCLE CELLS.
John W. Krueger and Barry London. Albert Einstein College of Medicine, Bronx, New York 10461.

We used Jamin-Lebedeff interference (n.a.=1.0) and phase contrast (n.a.≥1.25) microscopy to observe the appearance of the sarcomere at short lengths (1.4-1.7μm) in enzymatically isolated, unattached ventricular cells from the rat. A television system maximized image contrast. This enabled visualization of t-tubules in intact cells bathed in refractive index matching solutions, z bands at SL∿1.9μm in cells skinned with 0.5% Brij, and H zones in skinned cells stretched to SL>2.3μm. Iontophoretic activation of skinned cells (relative sensitivity: $Sr^{+2}>>Ca^{+2}$) elicited sarcomere shortening from rest lengths of 2.0-1.9μm to form: 1) C_m contraction bands at SL∿1.7μm; 2) phase brightening of A bands at SL∿1.6μm; and 3) dense C_z contraction bands at shorter SLs. These observations are totally consistent with previous expectations of the sliding filament mechanism and very uniform myofilament lengths (Huxley & Hanson; Huxley & Niedergerke (1954)). This behavior did not characterize the sarcomeres in electrically stimulated, intact cells where individual A bands could be followed without phase brightening or contraction band formation despite equivalent sarcomere shortening. Contraction bands could be seen in intact cells shortened with Ba^{+2} in low Ca^{+2} solutions. Individual skinned cells shortened with full contraction band formation when washed with a solution containing no ATP, Mg^{+2} or Ca^{+2} and 10 mM EGTA and 3 mM EDTA. Addition of ATP and Mg^{+2} to these preshortened cells restored sarcomeres to rest length indicating an energetic requirement of relengthening in unattached heart cells. These results suggest that the physical morphology of the shortened sarcomere may depend upon the nature of activation in intact heart muscle.
Supported, in part, by the NYHA and HL 21325-05.

W-AM-Po2 STIFFNESS OF MAXIMALLY ACTIVATED SKINNED FIBRES FROM FROG MUSCLE AT LOW MgATP CONCENTRATIONS
B.B. Hamrell, J. Rondinone and R.M. Simmons, (Intr. by David R. Harder) Department of Physiology, University College London, London, England

The stiffness of skinned fibres from frog muscle was measured during maximal contractions (pCa 4.5) at 0-2°, using MgATP concentrations ranging from 1 uM to 5 mM. The "instantaneous" stiffness was obtained from the length and tension records during rapid (200 us) length changes of about 0.5%, according to the procedure of Ford, Huxley and Simmons (J. Physiol. 269: 441-515, 1977).

As the MgATP concentration is increased from 1 uM, tension rises to a peak at about 30 uM and then declines smoothly to about 70% of the peak value at 5 mM MgATP (Ferenczi, Ph.D. Thesis, University College London, 1978). The stiffness remains approximately constant from 1 uM to 30 uM MgATP and declines at higher MgATP concentrations in much the same way as tension. Using stiffness as a measure of the number of attached crossbridges, the results suggest that the average tension exerted per attached crossbridge rises sharply between 1 and 30 uM MgATP and remains constant at higher concentrations.

Supported in part by the Medical Research Council (Dr. Simmons), the NIH (Senior (Fogarty) International Fellowship No. TW00375)(Dr. Hamrell) and the Muscular Dystrophy Association (Dr. Rondinone)

W-AM-Po3 IMPEDANCE MEASUREMENTS AT THE PELVIC END OF FROG SARTORIUS MUSCLE FIBERS.
R.L. Milton, R.T. Mathias, and R.S. Eisenberg. Dept. of Physiology, Rush Medical College, 1750 West Harrison, Chicago, Illinois 60612.

Impedance measurements were made at the pelvic end of frog sartorius muscle fibers using a three microelectrode technique similar to the three microelectrode voltage clamp used by previous investigators (Adrian, Chandler, and Hodgkin, J. Physiol. 186: 51-52P, 1966). These measurements were used to generate curves of the propagation constant and longitudinal resistance of the fiber as a function of frequency. The sensitivity of these results to random errors in the data was also determined. A mathematical model of the fiber was curve fit to the data to obtain values for membrane capacitances and conductances (Mathias, Eisenberg, and Valdiosera, Biophys. J. 17: 57-93, 1977). The results of these measurements were compared to similar measurements made at the center of the fiber. Discrepancies between the results obtained in the center and those obtained at the end were investigated. Particular attention was given to the effects of current flow out the end of the fiber and to the effects of non-uniform sarcomere spacing at the end of the fiber. The implications of these artifacts for voltage clamp studies at the end of the fiber was examined.

W-AM-Po4 EPR STUDIES OF CROSSBRIDGE ROTATION IN INSECT FLIGHT MUSCLE IN RIGOR AND RELAXATION.
David D. Thomas*,Roger Cooke†, Vincent A. Barnett*, and Mark S. Crowder†, *Dept. of Biochemistry, University of Minnesota Medical School, Minneapolis,MN 55455; †Dept. of Biochemistry and Biophysics and the CVRI, University of California, San Francisco, CA 94143.

We have used electron paramagnetic resonance (EPR) to measure the orientation (by conventional EPR) and rotational motion (by saturation transfer EPR) of spin-labeled myosin heads in glycerinated muscle fibers and purified myosin. An iodoacetamide spin label reacts selectively with myosin heads in glycerinated insect fibers, but the reaction is much slower than for rabbit fibers, indicating a significant chemical difference between SH groups in myosin heads in insect and rabbit. Nevertheless, EPR spectra of insect fibers in rigor are very similar to those of rabbit. The heads are highly oriented and immobile and the mean angle between the probe axis and the fiber axis is virtually identical (within 1 degree) for insect and rabbit. Labeled heads show slightly less order and more motion in insect than in rabbit. ATP (in the presence of 1mM EGTA) induces considerable rotational disorder and sub-millisecond mobility in labeled heads. However, this disorientation and motion is less than in relaxed rabbit fibers. Thus, though results are similar for rabbit and insect, myosin heads in insect fibers show less order (more motion) in rigor and more order (less motion) in relaxation. This suggests that myosin is less flexible in insect than in rabbit, in agreement with our previous findings for purified myosin.

W-AM-Po5 HYPERTONICITY AND FORCE DEVELOPMENT IN FROG SKELETAL MUSCLE FIBRES. B.H. Bressler, L. Dusik, M. Trotter, P. Vaughan, Departments of Anatomy and Physiology, University of British Columbia, Vancouver, Canada.

Is the force inhibition observed in skeletal muscle fibers, placed in a hypertonic solution, due to excitation-contraction uncoupling or to a specific effect on the contractile proteins? Mechanical experiments have been performed on isolated fibre bundles of frog semitendinosus and point voltage clamp studies on isolated sartorii. Solutions were made hypertonic by the addition of sucrose or NaCl (the latter in electrical experiments only). Instantaneous stiffness values were obtained with 1 msec step changes of length from the plateau of an isometric tetanus. Within 20 minutes in 2.04 NR, isometric tetanus tension fell by at least 50% and then remained constant over a 2 hour period. By contrast the instantaneous stiffness remained closer to values recorded in isotonic Ringer. Under point voltage clamp, in the period during which the twitch time was visibly slowing (correlating with reduction in developed tension) the stimulus strength-duration curve was identical to that for controls. The possibility that the inward spread of activation is limited cannot be completely obviated. However, the stiffness observations suggest that the increased intracellular ionic strength produced when fibers are placed in hypertonic Ringer interferes with the force production per individual cross-bridge. While there may be a moderate reduction in the total number of formed cross-bridges, excitation-contraction uncoupling is not a major factor in the inhibition of force production. Supported by the M.R.C. and the M.D.A.C.

W-AM-Po6 HIGH PERFORMANCE INSTRUMENT FOR MYOFIBRILLAR MECHANICS.
Tatsuo Iwazumi, Dept. of Physiology & Biophysics, Univ. of Texas Medical Branch, Galveston, TX 77550

Precise measurement of myofibrillar mechanics has been unsuccessful because of the minute size and extremely small forces of the preparation. A new instrument has been developed which offers unprecedented performance. The force transducer has a resolution better than 0.1μg and a frequency response from DC to 30KHz in water. The length control servo has a step response of 10μs in water and the length resolution of about 2nm. Two very fine wires (16μm) are suspended in parallel, and a magnetic field is applied perpendicularly to the plane which includes both wires. The magnified image (50X) of each wire is projected onto a dual photodiode, and the wire position is derived from the normalized difference of two photo-currents. One of the wires serves as a force transducer and another as a length control actuator. A myofibril is mounted onto and perpendicular to the two wires by means of the thermal fusion of wax which is coated on the wires. The force is measured by a servo loop in which the wire position is held stationary by passing a current through the wire to counteract the muscle tension. The high speed small length control is performed by a similar servo loop as the force transducer except that it has a position control input. The wire currents are chopped at 500KHz and fed alternately to prevent mutual interaction between them.

The real time sarcomere length is measured by first converting the sarcomere image video signals from a 1024 element photodiode array to power spectral densities, then taking the inverse of the distance between two first orders. Supported by AHA Texas Affiliate.

W-AM-Po7 Ca^{++} EFFECTS ON THE UNLOADED SPEED OF SHORTENING (V_{max}) OF MAMMALIAN SKELETAL MUSCLE FIBERS. D.G.S. Stephenson and F.J. Julian, Dept. Zoology, LaTrobe Univ., Melbourne, Australia, 3083; Boston Biomedical Res. Inst., Muscle Dept., 20 Staniford St., Boston, MA 02114.

There is disagreement concerning the relation between pCa and V_{max} of vertebrate skeletal muscle fibers (Julian, J.Physiol., 218: 117, 1971; Podolsky and Teichholz, 211: 19, 1970) and it is not clear whether the role of Ca^{++} in contraction can be simply reduced to that of a "switch". In these experiments we used both chemically and mechanically skinned muscle fibers of rabbit and rat which were activated in solutions of various pCa's containing (mM); Na 36; K^{+} 70; Mg^{++} 1; ATP 8; TES 70; creatine phosphate 10; EGTA + Ca EGTA 20; creatine kinase 15 U/ml, temp 15° C; pH 7.10; ionic strength$\sim$150 mM. Previous to the activation step the preparations were equilibrated in a relaxing solution (pCa$>$ 8) in which 19.5 mM EGTA was replaced with 19.5 mM HDTA. This allowed rapid activation of the skinned muscle fibers (Moisescu, Nature, 262: 610, 1970) with minimal deterioration of the steady state force level. No residual force could be detected in relaxing solutions. V_{max} at given pCa was determined using the slack-test method (Julian & Moss, J. Physiol. 311: 179, 1981). Results obtained on individual preparations indicate that V_{max} gradually rises when Ca^{++} increased from values close to the force threshold to about 10^{-5} M. Fast-twitch muscle fibers of both rat and rabbit shortened (3-11%) much faster at pCa 5 ($V_{max}>10$ Muscle lengths/s (ML/s)) than at pCa 6.3 ($V_{max}\sim 0.5$ ML/s). Slow-twitch muscle fibers also showed a clear Ca^{++} dependency of V_{max} (see also Moss, Biophys. J. 33: 28a, 1981). These results support the idea that Ca^{++} ions play an important role in determining the kinetics of the cross-bridge cycle. (Supported by USPHS HL 16606, MDA and ARGC).

W-AM-Po8 SHORTENING STEPS IN UNSTIMULATED MUSCLE. J.W. Lacktis, F.V. Brozovich and G.H. Pollack. Dept. of Anesthesiology and Div. of Bioengineering (RN-10), University of Washington, Seattle, WA 98195.

Previous studies of sarcomere dynamics in single muscle fibers have shown that sarcomere shortening during contraction occurs in steps, and that the size of the steps may be related to the repeat spacing of the actin monomer (1). In the present experiments, we observed sarcomere dynamics in passively shortening muscle fibers to determine whether the preferred step size was similar to that found in stimulated muscle. Single, unstimulated frog toe muscle fibers were made to shorten at a constant velocity at rates between 0.4 and 1.0 L/sec by feeding a length ramp into the moveable lever arm of a Cambridge servo-motor. Due to the presence of end compliance, smooth, constant velocity length ramps do not necessarily constrain the fiber to an identical shortening pattern. Fibers were illuminated with a xenon lamp and sarcomere length was computed from the striation image using an on-line phase locked loop measuring device (2). Preliminary results show a preferred SL decrement between 3.8 and 4.2 nm/half sarcomere in fibers shortening passively. This is somewhat less than the 5.5 nm/half sarcomere reported for actively shortening fibers. The discrepancy may be related to differences of shortening velocity. We are currently developing histograms of step size distribution at several rates of active and passive fiber shortening to pursue this question further.

1. Jacobson, R.C., Tirosh, R., Delay, M. and Pollack, G.H. (1981) Biophys. J. 33, 223a.
2. Meyers, J.,Tirosh, R., Jacobson, R.C. and Pollack, G.H. IEEE Trans. BME. In press.

W-AM-Po9 CROSSBRIDGE COOPERATIVITY IN ACTIVE MUSCLE. Y.Matsumoto. Emory Univ., Atlanta, Ga. 30322

The assumption that the molecular dynamics in active muscle is an ordered process to generate vector force requires examination. The system reaction kinetics can be ordered if there exists an autocatalytic step. If we consider a chemical system involving two variable intermediates together with a substrate and final products whose concentrations are assumed to be controlled throughout the reaction process, a trimolecular or higher order step is necessary for the onset of cooperative behavior in time (Hanusse, 1972). Thus the system is open, driven far from equilibrium and subjected to feedback. We consider a three state kinetic model of actomyosin ATPase, a detached and two attached states: let Z = M**P, detached state; X = $A(x_o)$M*P, non-force generating attached state; Y = $A(x_o+\Delta x)$MP, force-generating attached state; S = ATP; P = ADP+P_i; A(x) = actin site at x; and M = myosin. The Lohmann reaction favors the above requirement that the S and P are controlled. Approximation of A(x) and S indicates that these are in excess over X+Y+Z. Thus we assume $k_{-1}= k_{-2}= k_{-3}= k_{-4}= 0$.

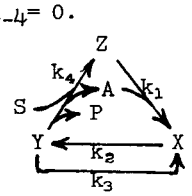

$$A(x) + Z \overset{k_1}{\rightarrow} X$$
$$2X \overset{k_2}{\rightarrow} 2Y$$
$$Y + 2X \overset{k_3}{\rightarrow} 3X$$
$$Y + S \overset{k_4}{\rightarrow} A(x_o+\Delta x) + P + Z$$

$$A(x) + S \rightarrow A(x_o+\Delta x) + P$$

The rate equations for the kinetic system reduces to:

$$X = -k_1AX - k_1AY + k_1A + k_3X^2Y - k_2X^2,$$
$$Y = -k_4SY + k_3X^2Y + k_2X^2,$$

where $X + Y + Z = 1$. In view of determining k'_s, preliminary study in progress is directed towards stability and energy flux analyses. More importantly we seek experimental test.

W-AM-Po10 RELAXATION IN ISOLATED SINGLE FROG ATRIAL CELLS. J. W. Trank, M. Tarr and K. K. Goertz,* Physiology Dept., Univ. of Kansas College of Health Sciences & Hospital, Kansas City, KS. 66103.

The characteristics of auxotonic relaxation were investigated in isolated single frog (Rana catesbeiana) atrial cells. Force decay during auxotonic relaxation occurred at a relatively constant rate (dF/dt) which depended on the peak force (F) developed during the contraction. The equation $dF/dt = AF + B$ describes the relationship between the rate of auxotonic force decay and peak auxotonic force in any given cell. Values for A ranged from about 3-5/sec and B ranged from about 20-80 nN/sec. The value of A was contractile activation dependent: increasing with increased activation. In these experiments there is a direct relationship between dF/dt, cell velocity and average sarcomere velocity. Thus, the results indicate that sarcomere velocity during relaxation is directly related to the peak force developed during the contraction, and this relationship is activation-dependent. The direct effect of external force (load) on relaxation velocity is also confirmed by the observation that rapid force changes imposed during relaxation immediately alter the velocity of the extending cell from any given cell length. Our results demonstrate that relaxation in the single frog atrial cell is not only activation-dependent; it is also highly load-dependent. (Supported by NHLI Grant 18943).

W-AM-Po11 A RELAXATION MODEL FOR CARDIAC MUSCLE. M. Tarr, J.W. Trank, and K.K. Goertz*. Physiology Dept., Univ. of Kansas College of Health Sciences and Hospital, Kansas City, KS. 66103.

Computer simulations of cardiac relaxation are presented based on a model in which it is assumed that 1) Hill's force-velocity relationship, $V=B(P_o-P)/(P+A)$, applies during relaxation, 2) internal force increases linearally as sarcomere length decreases below 2.4 μm, 3) P_o declines exponentially with time during relaxation and increases linearally as sarcomere length increases above 1.4 μm, and 4) A is proportional to P_o. Sarcomere extension during relaxation is highly dependent on external force in this model. However, the paradoxical finding of rapid sarcomere extension during relaxation with small external force (unpublished observation in single frog atrial cells) is predicted by the model and results from the combined effects of internal force, rapid decay of P_o, and a small A/P_o ratio. Also, coincidence of the isometric relaxation phases of isotonic afterloaded contractions (characteristic of relaxation in frog heart) is predicted by the model if B is large (e.g., 20 μm/sec-sarcomere) and the time of onset of P_o decay is independent of sarcomere length. Coincidence does not occur (characteristic of mammalian heart) if the time of onset of P_o decay decreases as sarcomere length decreases. The computer simulations suggest that a similar load-dependent mechanism may underlie relaxation in both mammalian and frog cardiac muscle in which relaxation has been described as being primarily dependent on either a load-dependent (mammalian) or activation-dependent (frog) mechanism (see Brutsaert et al., J. Physiol. 283:469, 1978). (Supported by NHLI Grant 18943).

W-AM-Po12 ANALYSIS OF RADIONUCLIDE GASTRIC EMPTYING STUDIES. Richard P, Spencer, Mozafareddin K. Karimeddini, Fazle Hosain, Howard A. Levy. Department of Nuclear Medicine, University of Connecticut Health Center. Farmington, CT 06032.

Upon ingestion of foods, pooling occurs in the stomach. Emptying then happens as the components of the meal pass into the duodenum and lower small bowel. Although there are complex events occurring (fluid entry, mixing and digestion plus bulk flow), the process can be approximated by an emptying half-time (based on the assumption of a first order process). Differences between the emptying of solids and liquids are usually emphasized, with little effort to find common factors. The pressure-volume relationship of Nelson-Kohatsu is: $dV/dt = (Ps - Pd)/R$, where the volume change with time is given as the difference between gastric and duodenal pressures, divided by the resistance of the pylorus. It can be shown that, since pressure is force/area, a meal of constant size would have less effect on a large stomach than on a small stomach. Such an observation does exist in the literature. While the coupling constants are not known apriori, gastric emptying studies must be standardized for stomach size (usually based on height, weight, or estimated body surface area; males and females are considered separately). We studied a meal of known composition (solid meal with a tracer in the liquid phase) at 2 different volumes, and found the characteristic normal slope. This permitted assay of literature data on gastric emptying. A preliminary conclusion is that the stomach does not empty solids, but only "gruel". Much of the difference between solid and liquid emptying is likely accounted for in terms of the digestive process. We have also studied the effects of medications on gastric emptying by measuring changes in the slope. A reasonable quantitative approach is thus likely available for analyzing gastric emptying data.

W-AM-Po13 SARCOMERE RELAXATION MECHANISMS IN ISOLATED HEART MUSCLE. J.W. Krueger and K. Tsujioka. (Spon: J.B. Wittenberg). Albert Einstein College of Medicine, Bronx, New York 10461

Thin heart muscles were isolated from the right ventricles of rats and electrically stimulated to contract (24/min., 27°C, 1.9 mM Ca^{+2}). Sarcomere length (S.L.) was measured using a light diffraction method which does not depend upon a unique angle of incident illumination. S.L. was servo-controlled by negative feedback. Rapid, controlled S.L. stretches-sufficient to break all contractile bonds-increased isometric tension at all times in relaxation. On the other hand, quick shortening by as little as 2% S.L. completely prevented redevelopment of isometric tension at the same times. Slowing the speed of controlled sarcomere shortening while keeping the degree of total shortening constant enhanced redevelopment of isometric tension. Increasing the velocity of controlled sarcomere lengthening always increased tension. Similarly, quick increments in isotonic load always increased the velocity of sarcomere lengthening. Three step lengthening and supraisometric tension were seen in muscle length but not in sarcomere length. Isotonic and isovelocity sarcomere Force-Velocity relations were normalized to the isometric tension occuring prior to the load or velocity steps at various times in contraction. The results showed that during iosmetric relaxation, the sarcomeres become progressively more resistant to lengthening at any relative load and less able to shorten. Isotonic velocity transients resembling those reported in skeletal muscle (refer to Civan & Podolsky, J. Physiol. 184: 511) were often seen but only if the sarcomeres were held isometric before the isotonic quick release. The character of the isotonic transient appears to change during relaxation. The results indicate that those active sites which form or persist in isometric relaxation may have altered dynamic properties. Supported, in part, by the NYHA and HL 21325-05.

W-AM-Po14 LIGHT DIFFRACTION, POLARIZATION AND A-BAND CHANGES OF STRIATED MUSCLES by B. G. Pinsky and Y. Yeh, Dept. of Applied Science, University of California, Davis, California 95616.

The diffraction spectra of laser light of single fibers of skeletal muscle exhibit a large degree of optical depolarization. When the linearly polarized incident laser source is oriented at polarization angles between $0 < \Theta < \frac{\pi}{2}$ radians with respect to the fiber axis, the diffracted light is elliptically polarized. In the initial experiments, both the amplitude change and the phase shift of detected light has been measured for passive stretches from resting length to beyond overlap. These results show that whereas the amplitude changes are minimal, the phase angle of the ellipse does rotate by as much as 20° when the fiber is stretched from 2.4 microns to 3.8 microns. To further ascertain that the observed phenomenon is diffraction related, an experiment monitoring the spectra of scattered light in between diffraction orders showed this signal to be significantly less depolarized. Studies of changes of this optical depolarization signal on the rigor-to-relaxed transition in glycerinated fiber will be reported. These results suggest that the degree of depolarization of the diffraction spectra is a sensitive probe of A-band dynamics: Changes in the ellipticity and phase angle may be related to intrinsic anisotropy and attitudinal changes of the S-2 moiety. (Supported in part by NIH grant #AM26817.)

W-AM-Po15 MUSCLE SOUNDS: A WIDESPREAD PHENOMENON? F.V. Brozovich and G.H. Pollack, University of Washington, Department of Anesthesiology and Bioengineering (RN-10) Seattle, WA 98195

Last year, at this meeting, we reported that muscle shortening was accompanied by the generation of a series of discrete sound bursts. We have since improved the resolution of our system, increasing the signal to noise ratio, and now report additional properties of these sounds. Approximately 70 frog sartorius muscles were stimulated to twitch isotonically against a load of 5-10 g. The sounds were recorded with a piezoelectric transducer resonant at 899 kHz placed 0.5cm from the muscle. Shortening of 20-30% was accompanied by a series of sharp, discrete sound bursts of various amplitudes. Some bursts were repeatable from contraction to contraction. For a group of 4 muscles, at 4.0°C the interval between successive sound bursts averaged 35.9 msec; when the temperature was raised to 12.5°C the average interburst interval decreased to 22.5 msec, yielding a Q_{10} of 2.0; this is expected for muscle shortening. The main frequency component of each burst was 2.5 kHz, suggesting that step duration at the molecular level may be 400 μsec.

It has recently come to our attention that the sounds produced by the heart are thought to originate, at least in part, from the contracting cardiac muscle. The possibility that such sounds and the discrete bursts recorded from frog muscle are generated by a similar mechanism is heightened by the observation that sarcomere shortening in both skeletal and cardiac muscle is stepwise (Pollack, et al, Nature 1977). We placed the sound transducer on the chest wall and recorded heart sounds. Preliminary analysis shows a frequency content comparable to that of the bursts generated by shortening skeletal muscle. Thus, heart sounds may originate from discrete, synchronous bursts of shortening in the myocardium.

W-AM-Po16 THE MECHANICAL PROPERTIES OF SKINNED FAST AND SLOW FIBRES ISOLATED FROM FISH MYOTOMAL MUSCLE. J.D. Altringham* and I.A. Johnston, Dept. of Physiology, St. Andrews, Fife, Scotland.

The pCa-tension relation and force-velocity characteristics of skinned fibres from cod (Gadus morhua) and dogfish (Scyliorhinus canicula) myotomal (segmental trunk) muscles were investigated. The higher maximum isometric tensions generated by fast fibres ($\sim$ 1.9 kg cm^{-2} in both species) relative to those of slow fibres ($\sim$ 0.85 kg cm^{-2}) are not fully explained by their higher myofibrillar fractional volumes. The $[Ca^{++}]$'s for half maximal tension were lower in the slow fibres of both species (see also (1), on rabbit). Maximum contraction velocities were 1.01 and 0.53 Ls^{-1} for cod, and 2.34 and 0.68 Ls^{-1} for dogfish fast and slow fibres respectively. Interestingly, the fast fibre P-V relationships exhibit the greater curvature (lower a/Po) in both species, in contrast to results obtained from other vertebrates (e.g (2,3)). Woledge (4) proposed that the lower a/Po observed in the slow muscles of Testudo, relative to frog sartorius, was associated with a greater energetic efficiency. The present results do not appear to fit into this scheme, possibly due to the rather different energetic and mechanical constraints placed on the muscle by its environment, and myotomal arrangement. (All experiments carried out at 8°C.)

(1) Kerrick, W.G.L., Secrist, D., Coby, R. and Lucas, S. (1976) Nature 260, 440-441.
(2) Lannergren, J. (1978) J. Physiol. Lond. 283, 501-521.
(3) Close, R. (1964) J. Physiol. Lond. 173, 74-95.
(4) Woledge, R.C. (1968) J. Physiol. Lond. 197, 685-707.

*current address: Dept. of Anesthesiology and Bioengineering RN-10, University of Washington, Seattle, Washington 98195.

W-AM-Po17 IMPROVED SARCOMERE LENGTH DETERMINATION FROM ISOLATED CARDIAC CELLS. K.P. Roos and A.J. Brady. Dept. of Physiology, UCLA School of Medicine, Los Angeles, CA 90024

Calcium tolerant isolated cardiac muscle cells were prepared by the enzymatic digestion of perfused adult rat myocardium (Brady et al., Nature 282:728, 1979). The characteristic A-I band striation pattern was monitored from these isolated cells (myocytes) with an improved direct image system. The small size (≈15μm x 120μm) and functional integrity of this myocyte preparation make it well suited for study with a light microscope where the striation pattern of an entire cell can be monitored as a complete and independent contracting unit free of extracellular elastic elements. The upgraded direct image system incorporates high-resolution immersion Nomarski type differential interference contrast (DIC) optics coupled to a 1728 element CCD photodiode detector. The image performance characteristics of this DIC optical system have been determined empirically from calibrated parallel bar test grids with various abrupt changes in periodicity. The A-I band periodicity or sarcomere length of myocytes can be determined with a precision of at least ±.05μm with this system. Analog data from the detector corresponding to the light-dark striation pattern is rapidly digitized and stored in the memory of a computer for later digital image processing. Up to 108 sequential frames of sarcomere length data can be acquired with the new ultra-high-speed direct memory access (DMA) interface at a maximum rate of 692 KHz (2.55 ms/data frame) though 12-15ms frame rates provide sufficient speed to freeze sarcomere motion with improved signal to noise ratios. This high-speed, high-resolution acquisition system has been utilized to quantitatively measure individual sarcomere lengths along the length of dynamically contracting myocytes. (Supported by USPHS HL 11351-15 to AJB & Grant-In-Aid & Equipment grant from the Am. Heart Association to KPR).

W-AM-Po18 MODE OF SARCOMERE SHORTENING AT THE MYOFIBRILLAR LEVEL. T. Tameyasu, J.D. Altringham and G.H. Pollack. Dept. of Anesthesiology and Div. of Bioengineering (RN-10), University of Washington, Seattle, WA 98195.

Stepwise sarcomere shortening has been recorded in striated muscle fibers using several techniques: Laser diffraction (Pollack et al., Nature, 1977), high speed cinematography of the striation pattern (Delay et al., Science, 1981), and analysis of the microscopic image by a phase-locked loop device (Jacobson et al., Biophys. J., 1981). In intact fibers, lateral translation during contraction may be responsible for masking more discrete step/pause events. In order to obtain more accurate information about the steps, we are studying sarcomere shortening in very small skinned preparations (< 15 μm diameter, 100-200 μm long), to monitor the behavior of a small population of sarcomeres. Preparations are made by manually teasing glycerinated frog twitch and fish fast myotomal fibers. The later exhibit a very high degree of sarcomere registration. One end of the preparation is attached to the tip of a rigid glass capillary, the other end to a flexible capillary. The striation image obtained by phase or modulation contrast microscopy is projected onto a photodiode array, capturing a 5 μm wide strip of 15-20 sarcomeres (a second array has a capture width < 1 μm). Array output is fed into a phase-locked loop device, which computes mean sarcomere length every 5 msec. Local application of a high $[Ca^{++}]$ solution caused the short length of myofibril under study to shorten, stretching the remaining sarcomeres and/or the flexible capillary. Preliminary results clearly show that sarcomere shortening is non-smooth, but it is too early to be certain the pattern is stepwise. Experiments are being continued, with recently improved optics. (Supported by MDA fellowship to T.T. and SRC/NATO fellowship to J.D.A.).

W-AM-Po19 ACTIVE SHORTENING DECREASES THE CALCIUM AFFINITY OF SKINNED SKELETAL MUSCLE FIBERS
J. Asayama, Y.-L. Chiu, and L.E. Ford. University of Chicago, Chicago, Illinois 60637

Skinned skeletal fibers from Xenopus laevis were activated at 3-4°C in solutions containing 10mM Caffeine, 150 mM K-propionate, 5 mM Na_2ATP, 6 mM $MgCl_2$, 10 mM imidazole at pH 7.0 and 5 mM EGTA buffered to different pCa's. Caffeine incapacitated the sarcoplasmic reticulum and steady tension levels were reached in 3-5 sec. To produce partial activation rapidly, fibers were briefly exposed to 2.5 mM free Ca^{2+} before exposure to solutions that produce less than half maximum tension(pCa6.4) By limiting contraction duration to 6 sec., 20-50 reproducible contractions could be obtained from one fiber segment. In some experiments, steadily contracting segments were suddenly shortened from one isometric length to another, making tension go slack. Time taken for force to begin to redevelop was used to assess maximum unloaded shortening velocity. In partially activated fibers, force rose very slowly, if at all. In other experiments, force-velocity relations were measured using steps to different isotonic loads. With loads less than 50% of isometric force, velocity declined progressively with shortening in all solutions. This velocity decline was greater with partial levels of activation. Greater velocity decline was seen with activation at pCa 6.2 than with pCa5.7 even though steady force levels were nearly the same in the two solutions. Results of both isometric and isotonic experiments suggest that the calcium affinity of skinned fibers is reduced during rapid shortening. This phenomenon is similar to deactivation produced by rapid shortening of intact muscle. A possible explanation is that rapid shortening decreases the number of myosin cross-bridges attached to thin filaments (Huxley(1957) Prog Biophys Biophys Chem 7:255-218) and the decrease causes decreased calcium affinity of thin filaments because of cooperativity between calcium and cross-bridge binding (Bremel & Weber (1972) Nature New Biol. 238 97-101).

W-AM-Po20 THE NECESSITY OF USING TWO PARAMETERS TO DESCRIBE SHORTENING VELOCITY: THE EFFECT OF VARIOUS INTERVENTIONS UPON ZERO LENGTH CHANGE CONTRACTION SPEED AND/OR CURVATURE.
B. Brenner* (Intr. by J. Miller), NIH, Bethesda, MD, 20205.

For the conditions studied, the length traces for long range isotonic motion (up to 20% of the initial sarcomere length of 2.5 μ) were found always to be more or less curved, although they sometimes appeared to be quite straight if only a short part of the motion was taken into account. It was shown that the velocity during isotonic motion can be described by an exponential function: $v = v_i e^{-k(SL_i - SL)}$ (SL_i: sarcomere length at the start of the release; SL: sarcomere length during motion). Thus, velocity of isotonic motion can be characterized by two parameters: v_i, the expected velocity for $SL=SL_i$ (zero length change contraction speed); and k, a constant characterizing curvature, i.e., the decrease in velocity during motion. Factors which affect the isotonic motion can do this either by affecting v_i, or by changing k, or both. Therefore, when analyzing the effects of interventions which change the isotonic motion, these two possibilities should be taken into account. Using this procedure to analyze isotonic motion, the effects of ionic strength, free [Ca^{++}], MgATP/MgADP ratio, and temperature on unloaded isotonic shortening have been studied. For the system used (single skinned rabbit psoas fibers, T= 5–15° C, 4 mM EGTA/CaEGTA, 20 mM imidazole, 10 mM NaN_3, 5 mM MgATP, 10 mM CrP, 250 Sigma U/ml CPK, KCl) it can be shown that ionic strength (μ= 0.075 M to 0.200 M) and free Ca^{++} (pCa 6.21 to pCa 5.00, μ= 0.175 M) only affect k without any significant effect on v_i, whereas MgATP/MgADP ratio (5/0 to 1/4, total nucleotide concentration 5–15 mM, no backup system) and temperature (5–15° C) have their main effect on v_i and only little or no effect on k.

W-AM-Po21 CROSS-BRIDGE FLEXIBILITY DERIVED FROM THE INFLUENCE OF LATTICE SPACING ON MECHANICAL PROPERTIES OF MUSCLE FIBERS IN RIGOR. Toshiaki Arata and Richard J. Podolsky, Laboratory of Physical Biology, NIADDK, Bethesda, MD 20205

The force-length relation of glycerinated rabbit psoas fibers was measured using length steps with rise times ranging from 3 ms to 1 s. The force-length curve shifted reversibly along the length axis, with no change in shape, when the myofilament lattice spacing was changed. Such experiments showed that a decrease in thick to thin filament spacing of 3 nm (determined by X-ray diffraction) cause the fiber to lengthen by nearly the same amount per half sarcomere. The increase in length was a non-linear function of the lattice spacing; the length increment for a given decrement in lattice spacing became smaller as the lattice spacing decreased. When the length was kept constant, a decrease in the lattice spacing produced a drop in the force, as would be expected from the shift in the force-length curves. The results were the same when lattice spacing was changed either osmotically (by adding the long-chain polymer Dextran T-500 to the bathing solution) or electrostatically (by changing the pH between 5.5 and 8.5, or the ionic strength). The simplest explanation of the results is that the cross-bridge contains a link between 3 and 10 nm in length which can swivel when the filament separation is changed. Since in rigor the orientation of S1 is stable relative to the thin filament (PNAS 78, 5559 (1981)), the short length of the cross-bridge link (< 10 nm) compared to the length of S2 (60 nm) suggests that the flexibility of the cross-bridge may originate solely from a region of the myosin molecule close to the S1-S2 junction rather than from a double hinge consisting of this region and a second flexible region at the S2-LMM junction.

W-AM-Po22 HEAT PRODUCTION IN FROG VENTRICULAR MUSCLE. Daniel M. Burchfield*, Emil Bozler*, Jack A. Rall. Using parallel fibered preparations from the frog ventricle heat production was measured with thermopiles at 0 to 10°. Because of the slowness of contraction mechanical and thermal changes could be closely correlated. In isometric twitches heat production was linear during the rising phase after the first second, then increased at the beginning of relaxation. In freeloaded isotonic twitches the time course of heat production varied with the load. At moderate loads isotonic heat was at first larger than isometric heat at the same resting length, but later became smaller. This usually occurred before the output of mechanical power had become maximal. At small loads total heat production in freeloaded isotonic twitches was smaller than in isometric twitches at the same resting length, but was larger at heavy loads. The results indicate that heat production was increased by shortening, but became smaller after the muscle had shortened significantly, even when the work produced was still large. Quick release during the rising phase of an isometric twitch caused a marked rise in temperature followed by cooling. A part of the heat was shortening heat. That the remaining heat was not, or not entirely, thermoelastic heat is shown by the observation that, at the same drop in tension, heat production greatly diminished when the rate of shortening was slowed. Supported by NIH Grants AM20048-01, AM-20792 and HL-21670.

W-AM-Po23 RADIAL COMPRESSION OF FUNCTIONALLY SKINNED CARDIAC BUNDLES ABOLISHES CALCIUM ACTIVATED FORCE. David Maughan & Michael Berman, Dept. Physiology & Biophysics, Univ. Vermont, Burlington,VT.
Fabiato & Fabiato (J. Gen. Physiol. 72:667-699, 1978) reported that a 21% reduction in the width of a single mechanically-skinned cardiac cell produces a 25% decrease of maximal calcium-activated force. A question arises whether further radial compression completely abolishes force as reported for skinned skeletal muscle fibers (Maughan & Godt, Pflugers Arch. 390:161-163, 1981). To investigate this, we functionally skinned six cylindrical bundles of cells from guinea pig left ventricle by treating the bundles with EGTA- and BRIJ-containing relaxing solutions. The bundles, stretched to approximately 2.4 μm average sarcomere length, were transferred to a series of activating solutions (pCa=5.4) containing various amounts (0-18 g/100ml) of Dextran T500. Addition of dextran reduced bundle width (w) and sharply reduced active force (F). Relative to width (w_o) and force (F_o) measured in dextran-free activating solution, least squares linear regression gives the relationship $F/F_o = 3\ (w/w_o) - 2$ at 22°C. Thus, reducing width by approximately one third abolishes force completely. However, only a 7% reduction in width would be required to produce a 25% inhibition of force, in contrast to the 21% reduction required in single skinned cells. Perhaps the myofilament lattice of a single cell swells beyond its in situ size more than that of a cell in a functionally skinned bundle, and that the reduction in filament separation required to achieve the same degree of force inhibition is similar in both cases. The similarity of these results to those seen in skeletal muscle suggests a common mechanism of force inhibition by lattice compression. Work supported by HL 21312 and American Heart 78-634.

W-AM-Po24 AXIAL STIFFNESS MODULII OF COMPRESSED-LATTICE AND SUCROSE-LOADED SKINNED SKELETAL MUSCLE FIBERS. Michael Roy Berman and David W. Maughan (Intr. by Raye Z. Litten). Department of Physiology and Biophysics, University of Vermont, Burlington, VT 05405.

We measured axial stiffness modulii of skinned single skeletal muscle fibers in which active force was reduced either by compression of the myofilament lattice or by sucrose loading. Single fiber segments (1 mm long, 2.6 μm sarcomere length) from rabbit soleus muscles were mounted between a force transducer and a displacement generator and chemically skinned in relaxing solution (pCa 9, pMg 3, pMgATP 2.523, pH 7, ionic strength 150 mM, T=22°C). Control fiber width was measured in relaxing solution containing 4% (4 g/100 ml) Dextran T500, a long-chain polymer used to reduce skinned fiber width by osmotic compression. Control active force was measured in activating solution (pCa 5.4, pMg 3, pMgATP 2.523, pH 7, ionic strength 150 mM, T=22°C) containing 4% Dextran T500. Active force was reduced by adding either 18% Dextran T500 or 1.2M sucrose to activating solution. A 2 μm (p-p) sinusoidal oscillation (10, 1, 0.1 Hz) was applied at one end of the fiber and the force oscillation was measured at the other end. Axial stiffness modulus at each frequency was calculated as stress/strain. In compressed-lattice fibers width was reduced to 70% of control and force was reduced to near 30% of control. The axial stiffness modulii did not vary significantly with frequency, being near 2×10^8 dynes/cm^2. In sucrose-loaded fibers, force was reduced to near 50% of control. The axial stiffness modulii at 10 and 1 Hz were similar, being near 4×10^7 dynes/cm^2, but at 0.1 Hz the force oscillation was undetectable, indicating a greatly reduced stiffness. Based on the differences in magnitude and frequency behavior of the axial stiffness modulii we suggest that although both lattice compression and sucrose loading reduce active force, they do so by different mechanisms. Supported by USPHS 1F32HL06543-01 (MRB).

W-AM-Po25 STRESS RELAXATION IN INTACT FROG MUSCLE. B. Collett and J. R. Milch. Physics Dept., Princeton Univ., Princeton, N. J. 08544

Length increases applied to muscle produce immediate tension increases which then decay to some new resting tension (stress relaxation). We have studied stress relaxation for length steps of 0.2% (ramp duration 10 ms) for intact frog semitendinosus muscle in relaxed and IAA-rigor states from 0 to 200 seconds after the stretch. Over the period from 10 ms to 40 seconds the data are very well fit by a relation of the form: $Y = Y_0\{1 + B \log (t_0/t)\}$ where Y is the observed tension divided by the length step, Y_0 is a rapid stiffness, B is a slope, and t_0 is the time at which Y_0 is measured. Kuhn has reported this time dependence of stress relaxation for glycerinated insect flight muscle in rigor (H. J. Kuhn, Biophys. Struct. Mech. 4, 159, 1978). The parameters (Y_0 and B with t_0 = 10 ms) were found to depend upon the state of the muscle (relaxed or rigor), the sarcomere length, and oxygenation (for relaxed muscle), but no temperature dependence has been observed (from 8°C to 23°C). Preliminary values for the parameters in states studied to date are:

	3.2μ Relaxed	4.2μ Relaxed	3.2μ Rigor	4.2μ Rigor
Y_0(g/mm)	2.8 ± 1	38 ± 4	54 ± 4	33 ± 1
B (1 decade)	0.18 ± 0.04	0.11 ± 0.01	0.16 ± 0.03	0.11 ± 0.01

A typical muscle is 22 mm long, 1.5 mm^2 in cross-section, and produces a twitch tension (at 23°C) of 14g. The structural interpretation of such a logarithmic dependence is unclear.

Supported by NSF Grant PCM-7906433.

W-AM-Po26 STEPWISE SARCOMERE SHORTENING: CONSISTENT STEP SIZE CONFIRMED BY THREE SEPERATE TECHNIQUES M.R. Denney, M.J. Delay*, F.V. Brozovich, R. Tirosh, and G.H. Pollack. University of Washington, Department of Anesthesiology and Division of Bioengineering (RN-10), Seattle, WA 98195

We reported last year at this meeting that the sarcomere length, measured with an on-line striation imaging technique, decreased in a stepwise manner. The preferred step size, defined as the sarcomere length decrement between two consecutive pauses, was 5.5 nm per half sarcomere. We report here that two other techniques give comparable results. In all experiments, single frog toe fibers were stimulated to twitch against a small load. In the first method, the microscopic image of an incoherently illuminated fiber was filmed at 4000 frames/sec. A portion of the film, corresponding to a 0.25 by 60 μm section of fiber, was projected upon a photodiode array. The sarcomere length was computed by autocorrelation. We followed the same region of the fiber, frame by frame, using a natural marker; this averts translational artifacts and ensures consistency of the sampled region. The predominant step size was 5.0 ± 0.3 nm per half sarcomere. In the second method, the two first orders of the fiber's diffraction pattern were cast upon seperate photodiode arrays, and the sarcomere length was computed on-line from alternate first orders. In some, but not all, instances similar sarcomere length traces were seen with both first orders. A predominant step size of 5-7 nm per half sarcomere was seen, consistent with, but less sharply defined than, the other methods. In conclusion, three seperate techniques, on-line image analysis, high speed cinemicrography, and laser diffraction, all show stepwise sarcomere shortening with a preferred step size at or near 5.5 nm per half sarcomere. This step size may be related to the actin monomer repeat spacing along the thin filament.

*current address: Department of Physiology, UCLA, Los Angeles, CA 90024

W-AM-Po27 LATERAL CROSS-BRIDGE FORCES IN STRIATED MUSCLE. B. M. Millman and T. C. Irving. Biophys. Interdepartmental Group, Physics Dept., Univ. of Guelph, Guelph, Ont. Canada, N1G 2W1.

Radial pressure in the A-band lattice of skinned striated muscle has been determined as a function of filament spacing in frog and rabbit skeletal muscle during relaxation and rigor using an osmotic stress technique. From these data we have calculated cross-bridge forces and the electrostatic pressure, and estimated other forces. At high pressures (>200 torr), changes in the slope of the pressure curves from rigor muscle as ionic strength was varied showed that in this regime most of the lattice pressure is electrostatic. Pressure curves from relaxed muscle at high pressure are parallel to, but at smaller spacings than the rigor curves, indicating a smaller thick filament (charge) radius. At low pressures, the curves are consistent with a force balance between attractive electrostatic and repulsive van der Waals forces. Knowing the charge radii in relaxed and rigor muscle and the shape of the relaxed muscle pressure curve, the form of the pressure curve less cross-bridge forces can be calculated for rigor muscle. Comparison of this calculated curve and the observed rigor curve gives cross-bridge pressure as a function of filament separation. Cross-bridge pressure is about 100 torr (corresponding to a lateral cross-bridge force of about 10^{-11} N), and does not vary greatly with filament spacing. Thus, when striated muscle shifts from the relaxed to the rigor state two things happen: (1) the thick filament (charge) radius increases aby about 2 nm, increasing the electrostatic pressure, and (2) cross-bridges form, giving an attractive pressure of about 100 torr. In living muscle, as it moves from the relaxed to the rigor state, the interfilament spacing is such that the increase in repulsive electrostatic pressure equals the attractive cross-bridge pressure, so there is little net change of pressure.

W-AM-Po28 INTENSITY OF FIRST ORDER DIFFRACTED LINES AFTER QUICK STRETCH/RELEASE OF SINGLE MUSCLE FIBERS. by Richard L. Lieber and Ronald J. Baskin, University of California, Davis 95616

We have completed a series of experiments which examine the nature of diffraction from single skeletal muscle fibers. (Yeh, et. al. Biophys. J. 29:509, Baskin et. al. Biophys. J. 28:45, Lieber et. al. Biophys. J. 33:223a). Based on these experiments and our previous theoretical development, we are monitoring the intensity of the first order diffraction lines after quick stretch/release from fibers which are not expected to yield significant Bragg artifacts.

In order to perform these experiments with sufficient resolution, an LSI-11 based direct memory access data acquisition system has been developed which can store the digitized data from a photodiode array in about 200 μsec. The speed of the data acquisition allows for precise experimental and closed-loop control.

The results are interpreted in terms of large scale changes in myofibrillar populations after rapid length changes. The possibility that these large scale changes may influence the tension record is being investigated.

W-AM-Po29 THE MECHANICAL EFFECTS OF MYOSIN LC_2 REMOVAL FROM RABBIT SKINNED SKELETAL MUSCLE FIBERS. Richard L. Moss*, Gary G. Giulian*, and Marion L. Greaser+, Depts. of Physiology* and Meat and Animal Science+, University of Wisconsin, Madison, WI 53706.

The physiological role of myosin LC_2 in muscle contraction remains unclear. Studies were done to determine the mechanical effects of LC_2 removal from skinned fibers from rabbit psoas muscles. Mechanical V_{max} was measured at 15°C in each fiber segment prior to and following LC_2 extraction, and following readdition of LC_2 to the segment. The segment was then subjected to SDS-polyacrylamide gel electrophoresis. The gels were silver stained and the LC_2 content of the segments determined from densitometric gel scans. An LC_2 determination was made in a control segment from the same fiber, and also in another segment following extraction in the same solutions as the experimental segment. LC_2 was partially removed by soaking the segment in a solution containing 20 mM EDTA. The value of V_{max} before EDTA treatment was 2.44 ± 0.49 muscle lengths (ML)/s and tension was 1.85 ± 0.17 kg/cm^2. EDTA treatment was found to partially extract TNC from the segments, thus necessitating readdition of purified TNC to the fiber segments following the EDTA soak. The results obtained from 6 fibers are shown in the summary table below.

	$\%V_{max}$	% Tension	$LC_2/(LC_1 + LC_3)$
Control	100	100	0.84±0.05
After EDTA	53± 9	41±15	-
After TnC	62±12	78±12	0.61±0.10
After LC_2	93± 6	89± 8	0.89±0.07

Thus, there is a distinct and reversible effect of LC_2 removal on V_{max} in mammalian skeletal muscle fibers, suggesting that LC_2 may modulate the interaction kinetics of myosin with actin. (This work was supported by grants from NIH, the MDA and the American Heart Association.)

W-AM-Po30 TENSION TRANSIENTS IN SINGLE ISOLATED SMOOTH MUSCLE CELLS(SMC): INSIGHT INTO CROSS-BRIDGE MECHANISM. D. Warshaw & F. Fay, U. Mass. Med. Sch., Physiol. Dept., Worcester, MA .

To characterize the viscoelasticity and kinetics of cross-bridges in single SMC, we studied tension transients due to step changes in muscle length ($\Delta L = 0.3\text{-}2.0\%\ L_{cell}$ in 2.0 ms). A SMC from the toad stomach muscularis (Bufo marinus) was tied to a force transducer and displacement device. The tension transients were characterized by at least three phases. Phase 1, an immediate tension change coincident with ΔL reflects properties of a linear instantaneous elastic element (IEE) with a modulus of elasticity (E_o = 131 ± 23 kg/cm^2, n=9). During activation, stiffness of the IEE scales with force being generated between $0.3\text{-}1.0F_{max}$, suggesting that the IEE is not external to the cross-bridge, rather within it. Phase 2, a rapid tension recovery (τ = 5–20 ms) was detected during ΔL as a nonlinearity in the IEE. Phase 3, beginning after completion of ΔL, involved a further biphasic recovery of tension comprised of two exponential components (τ_{fast} = 5–20 ms; τ_{slow} = 50–300 ms). The phase 3 recovery rate ($t_{1/2}$) was dependent upon the direction and size of ΔL as well as the state of the cell. The $t_{1/2}$ became progressively shorter going from 2.0% releases ($t_{1/2}$ = 231 ± 93 ms, n=4) to 2.0% stretches ($t_{1/2}$ = 17 ± 7 ms, n=4) in cells maintaining peak force (P_o=1.8 ± 0.3 Kg/cm^2, n=9). During force development $t_{1/2}$s become longer and after prolonged peak contraction the cells were incapable of shortening reflected by $t_{1/2}$s greater than 1.0 s. The dependence of $t_{1/2}$ on the cell's contractile state suggests that Phase 3 reflects cross-bridge turnover. Since the $t_{1/2}$s are longer in SMC and exhibit a Δl dependence opposite to that in striated muscle, these results may reflect kinetics that are slower and unique to cross-bridges in SMC. (Supported by: DMW, HL05770 & MDA; FSF, HL14523.)

W-AM-Po31 STIFFNESS OF CONTRACTED AND RELAXED VASCULAR SMOOTH MUSCLE. S.P. Driska, Physiology Dept., Medical College of Virginia, Virginia Commonwealth University, Richmond, VA 23298.

Smooth muscle stiffness measurements should be useful in determining if there is any relationship between myosin light chain phosphorylation and the number of attached cross-bridges. Hog carotid artery smooth muscle stiffness was calculated from the force changes measured in response to rapid (<2ms) length changes of various amplitudes imposed on relaxed and contracting tissues as 10 Hz square waves. The stiffness depended on the size of the length steps, with the smallest length changes (0.05% of muscle length, peak-to-peak) resulting in the largest values of stiffness in contracting muscles. Expressed as a Young's modulus, they were about 120 X 10^5 N/m^2, or about 56 F_o/L_o, where F_o is the maximum active force and L_o is the muscle length at which it is developed. With amplitudes of 2% of muscle length, ptp, the stiffness was less, about 29 F_o/L_o. The time-average active force of muscle being subjected to small square wave length changes was the same as the unperturbed isometric force. With larger amplitude length changes it was less. When large amplitude length changes were imposed on a contracting muscle and then stopped, isometric force often increased slightly. These facts suggest that larger stretches were inhibiting cross-bridge function, perhaps by breaking cross-bridges. Stiffness during the development of force and during the subsequent relaxation was proportional to force. This proportionality between force and stiffness was identical to that obtained when force was varied by changes in the extracellular Ca^{2+} concentration. Supported by NIH HL 24881 and HL25383.

W-AM-Po32 MECHANICS OF THE LEFT VENTRICLE: R.S. Chadwick. Intr. by M. Eden, Biomedical Engineering and Instrumentation Branch, Division of Research Services, National Institutes of Health, Bethesda, MD. 20205.

A theory of the mechanics of the left ventricle is presented. A linear continuum description of the myocardium is developed which accounts for anisotropic elastic behavior due to the fiber direction field. The constitutive relation between fiber tension and fiber strain incorporates the essential features of the behavior of papillary muscles in length-tension experiments, and is also shown to be consistent with the geometrical structure of the sarcomere. The ventricular cycle is analysed as a sequence of four mechanical equilibrium states: end isovolumic relaxation, end diastole, peak isovolumic contraction, and end systolic ejection. The degree of activation of the fibers is simplified to be totally "off" during the former two states, and totally "on" during the latter two states. Boundary value problems are formulated and solved analytically for each of these states for a ventricle modelled as a thick walled finite cylinder. The fibers spiral on cylindrical surfaces and have a helical pitch angle which varies continuously through the wall in accordance with anatomical measurements. Key quantities are tabulated which permit a simple determination of all geometrical changes for each state of the cycle, e.g. wall thickness, as well as ejection fraction and stroke work performance calculations for a wide class of parameter changes. It is shown that the physiological distribution of fiber helix angles maximizes the peak isovolumic chamber pressure. Also it is shown that either isovolumic sphericalization or ellipticalization could be normal contraction patterns depending on the precise distribution of fiber angles.

W-AM-Po33 EXAMINATION OF HALDANE'S FIRST LAW FOR THE PARTITION OF CO AND O_2 TO HEMOGLOBIN A_0: J. Wyman, G. A. Bishop, B. Richey, R. L. Spokane, and S. J. Gill Department of Chemistry, University of Colorado, Boulder, CO. 80309

A study of the oxygen replacement reaction of carbon monoxide saturated hemoglobin (HbA_0) was carried out using spectroscopic, calorimetric and pH titration methods. Under fully saturated conditions the replacement reaction can be defined by a single partition constant over all ratios of bound oxygen to carbon monoxide. This indicates that under saturating conditions Haldane's first law for the ligand binding of gas mixtures holds for any CO/O_2 ratio. It further shows that there is no appreciable difference in relative $CO\text{-}O_2$ affinity between the α and β chains. The same partition coefficient was found to hold for different pH, buffer and allosteric effector (IHP) conditions. The lack of any pH dependence of the partition coefficient was confirmed by the absence of proton changes for the replacement reaction. The temperature dependence of the partition coefficient and calorimetric results yield a value for the enthalpy of the reaction of $3.65 \pm .29$ kcal/mole-heme.

Supported by NIH Grant HL 22325 and NSF PCM 772062.

W-AM-Po34 FLUORESCENCE RELAXATION STUDIES OF PYRIDOXAMINE-5-PHOSPHATE LABELED APOHEMOGLOBIN. Janusz Kowalczic and Enrico Bucci, Department of Biological Chemistry, University of Maryland, School of Medicine, Baltimore, Maryland 21201. The fluorescence of human apohemoglobin labeled at the Val β1 with pyridoxamine-5-phosphate was investigated. At $4^{\circ}C$ the lifetime of the excited state was found to be 4.6 and 3.5 ns at pH 6.5, and 7.5 respectively. The intensity of fluorescence at pH 7.5 was two times lower than at pH 6.6. The quantum yield at $5^{\circ}C$ at pH 7.0 was 0.21. Correlation times (τ_c) were evaluated from steady state fluorescence anisotropy and lifetimes measurements under quenching by KI. It was found that the major component of τ_c at pH 6.5 was 40 ns and at pH 7.5 was 5.1 ns. Singlet-singlet energy transfer between the label as a donor and ANS as acceptor (ANS binds indside the heme-pocket) was about 26 Å between the randomly oriented fluorophores. In the tridimensional model of crystalline deoxyhemoglobin the distance between Val β1 and the iron atom of the nearest heme is about 22 Å.

W-AM-Po35 SYNTHESIS AND CHARACTERIZATION OF BIS-OXINDOLYLALANINE-7,14-MYOGLOBIN. Jeffrey A. Radding and Frank R. N. Gurd, Department of Chemistry, Indiana University, Bloomington, IN 47405.

The stability of sperm whale myoglobin results from the contributions of electrostatic, hydrophobic and other forces. Hydrophobic residues, such as tryptophan, contribute to the stability of proteins through entropic forces by burial within the protein matrix, thereby excluding water. Cetacean myoglobins contain two invariant tryptophan residues at positions 7 and 14, in the A-helix of the molecule. Both tryptophans occupy relatively buried positions in the protein. To probe the contribution of these hydrophobic residues, the tryptophans in sperm whale myoglobin were specifically oxidized to oxindolylalanine by reaction with dimethyl sulfoxide and concentrated hydrochloric acid in glacial acetic acid. Characterization of the modified bis-oxindolylalanine-7,14-myoglobin was performed by amino acid analysis, cellulose acetate electrophoresis, isoelectric focusing, and absorbance spectrophotometry of several ligand complexes. The physical properties of the derivative were determined by measurement of acid stability at constant ionic strength and potentiometric titration. Results indicate a significant decrease in the overall stability of the protein with minimal changes in its gross electrophoretic behavior. Further work directed at relating this decreased stability to changes in hydrophobic and/or electrostatic stabilization is being pursued. (Supported by U.S. Public Health Service Research Grant HL-14680.)

W-AM-Po36 MOSSBAUER STUDIES OF 57Fe ENRICHED CYTOCHROME c_1aa_3 FROM Thermus thermophilus.
W. R. Dunham, W. F. Filter, K. L. Findling, J. A. Fee, Biophysics Research Division, The University of Michigan, Ann Arbor, MI 48109 and T. A. Kent and E. Munck, Gray Freshwater Biological Institute, University of Minnesota, P. O. Box 100, Navarre, MN 55392.

Previous studies of cytochrome c_1aa_3 from T. thermophilus have shown that those spectral properties assignable to the aa_3 component were, in general, identical to those of beef heart cytochrome oxidase (J. A. Fee, M. G. Choc, K. L. Findling, R. Lorence, and T. Yoshida (1980) Proc. Nat'l. Acad. Sci. 77, 147-151). More recent comparisons of x-ray absorption properties (L. Powers, Unpublished) and S-band EPR (W. R. Dunham, Unpublished) suggest that the Cu atoms in c_1aa_3 reside in virtually identical environments to those of beef heart oxidase. The resting state of c_1aa_3 has now been examined by Mossbauer spectroscopy. We find three iron environments in the protein: two low-spin ferric sites attributable to the hemes a and c_1. A third site has a quadrupole splitting $\Delta E_Q \sim 1.2$ mm/s and an isomeric shift, $\delta \sim 0.43$ mm/s, parameters typical of high-spin ferric hemes; this spectral component is assigned to heme a_3. When studied in an applied field of 6 Tesla and in the temperature range 4.2-20 °K the observed effective field at the iron nucleus was found to be of equal magnitude to the applied field. As would be predicted from previous models of cytochrome oxidase, our results are consistent with heme a (and heme c_1) being isolated centers within the complex. However, the observed magnetic hyperfine interactions associated with the a_3 site are much smaller than would be expected from the reported magnetic susceptibility measurements of beef heart cytochrome oxidase. These results suggest that either the heme a_3 has an unusually large zero field splitting or that the (spin-coupled) system has a diamagnetic electronic ground state.

W-AM-Po37 AN EXAFS INDICATION OF STRUCTURAL CHANGE IN THE CARBOXYMYOGLOBIN PHOTOLYSIS AT LOW TEMPERATURE.
B.Chance, R.Fischetti, A.Sivaram, Johnson Res.Fnd., U.ofPA, Phila, PA, and L.Powers, Bell Laboratories, Murray Hill, NJ. Spons. by T. Yonetani

In a previous communication(1), we described an apparatus for measuring EXAFS by fluorescence detection of the photolysis and recombination of carboxymyoglobin at 4-100°K. Complete photolysis of highly concentrated MbCO samples (4-20mM) was obtained by Xenon flash illumination. EXAFS of the photo product (Mb*) resembles closely that of the intact MbCO; the maximum change of EXAFS is observed at 7150 eV with an amplitude of 0.8% of the edge jump. When recorded by 4 min EXAFS scans, the amplitude of the effect falls to half its value at 30°K, in agreement with Iizuka et al(2). The structure change on illumination is complete at 10°K within 2 sec, the resolving time currently available. Analysis of EXAFS data suggests that the total change due to core expansion and displacement of the CO on photolysis is ≤ 0.05 Å. It appears that the scalar displacement of CO from myoglobin in low temperature photolysis is minimal (although tumbling of the CO is possible) and that important changes may occur at the iron atom itself. Restitution of a ground state of the iron atom may be the rate-limiting process in the tunneling reaction pictured by Alberding et al (3).
1. R.Fischetti et al. Abstract Vol, Intl.Biophys.Congress Mexico City, p.322(1981). 2. T.Iizuka et al. Biochim.Biophys.Acta 371:126-139(1974). 3. N.Alberding et al. Science 192:1002-1003(1976).
Supported by NIH grants GM 27308, GM 27476, GM 28385, HL-SCOR-15061 and SSRL Project 423B (NSF,DDR, DOE).

W-AM-Po38 EDGE AND EXAFS STUDIES OF LOW SPIN LIGANDED HEMOGLOBINS
Korszun, Z. R. and Moffat, K.
Section of Biochem., Mol. and Cell Biol., Cornell University, Ithaca, NY 14853

EXAFS and K-absorption edge spectra were obtained on various hemoglobin derivates at CHESS (the Cornell High Energy Synchrotron Source), including imidazole, CN^-, N_3^-, ferric and NO, CO, O_2 ferrous species. All of these species, except NO, yield bond lengths which are quite similar to their respective model hemes. In NO hemoglobin, the nitrosyl -Fe bond refines to a value of 1.85 Å instead of 1.75 Å, otherwise the coordination geometry is consistent with that of the 6-coordinate model heme. The shapes of the K-edge spectra are diagnostic of the ligand geometries of these molecules. Imidazole, CN^-, and CO (linear ligands) hemoglobins fall into one class, while O_2, NO and N_3^- (bent ligands) hemoglobins fall into another. It appears that these spectra will be of diagnostic value in predicting ligand geometries of heme proteins whose detailed structures are not known.

W-AM-Po39 MIXED VALENCY ASYMMETRIC HYBRID HEMOGLOBINS AS MODELS FOR INVESTIGATING THE INTERMEDIATE STEPS DURING THE LIGATION OF HEMOGLOBIN. Shigetoshi Miura, Susan F. Dosch, and Chien Ho. Department of Biological Sciences, Carnegie-Mellon University, Pittsburgh, PA 15213.

The structure-function relationship in human adult hemoglobin (Hb A) has been a subject of intense investigation during the past decade. However, the detailed molecular mechanism for the cooperative oxygenation of Hb A is not fully understood. This, in part, is due to a lack of understanding of the structures and properties of the intermediate species formed during the oxygenation process, i.e., Hb with 1, 2, or 3 O_2 molecules bound. Of special interest are the quaternary structure of each intermediate species and the stage when the quaternary structural transition takes place. We have prepared the following mixed valency asymmetric and cross-linked hybrid hemoglobins from Hb C (β6 Glu→Lys) and symmetric valency hybrid hemoglobins [$(\alpha^{+CN}\beta)(\alpha^{+CN}\beta)$ and $(\alpha\beta^{+CN})(\alpha\beta^{+CN})$] from Hb A as models for the intermediate structures during the ligation process: $(\alpha^{+CN}\beta)_A(\alpha\beta)$; $(\alpha\beta^{+CN})_A(\alpha\beta)_C$; and $(\alpha^{+CN}\beta^{+CN})_A(\alpha\beta)_C$, where the subscripts A and C denote that the subunits are from Hb A and Hb C respectively. Hb C and the symmetric valency hybrid hemoglobins from Hb A are cross-linked in the CO form by bis(3,5-dibromosalicyl) fumarate according to the procedure of Walder et al. [Biochemistry 18, 4265 (1979)]. The site of cross-linking by this bifunctional reagent has been shown by X-ray crystallography to be from Lys82β_1 to Lys82β_2, spanning the 2,3-diphosphoglycerate binding site [Walder et al., J. Mol. Biol. 141, 195 (1980)]. The hyperfine shifted and exchangeable proton resonances for these hybrid hemoglobins over the spectral region from 5 to 25 ppm downfield from H_2O as a function of experimental conditions are being obtained. From these results, we plan to deduce the structural states of these hybrid hemoglobins and to relate them to the nature of the intermediate structures of Hb A during the oxygenation process. (Supported by research grants from the NIH and NSF).

W-AM-Po40 LIGAND-LINKED ASSEMBLY OF NORMAL AND MUTANT β CHAINS OF HUMAN HEMOGLOBIN. M. C. Farmer and Gary K. Ackers, Dept. of Biology, The Johns Hopkins University, Baltimore, MD 21218

We have studied the self-assembly of isolated β chains in three human hemoglobins (A_o [normal], Kempsey[β99 asp → asn], and S[β6 glu → val]) in both their unliganded and fully-oxygenated states (conditions: 0.1 M Tris-HCl, 0.1 M NaCl, 1mM Na_2EDTA, pH 7.4, 21.5°C). The studies by analytical gel chromatography indicate association of monomers to form tetramers in all three systems, but with significant differences in the abundance of intermediate dimers. Oxy β_A and β_S assemble with only insignificant proportions of intermediate dimers. By contrast oxy β Kempsey chains exhibit as much as 50% dimers under these experimental conditions. The data for unliganded chains in all three cases indicate significant fractions of intermediate dimers. All three systems exhibit quaternary enhancement - i.e. subunit assembly into quaternary structures leads to an enhancement of oxygen binding affinity (Valdes and Ackers; P.N.A.S. 75, 311; Mills and Ackers, P.N.A.S. 76, 273). The results imply that (1) there are at least two energetically-distinct classes of noncovalent bonding interactions within tetrameric β chains, and (2) a ligand-linked structure change within tetrameric β chains leads to alteration in the relative strengths of the intersubunit bonds. Supported by grants from the NIH and NSF.

W-AM-Po41 Functional Properties of Glucose-6-Phosphate Hemoglobin. Shyh-Horng Chiou, Laura M. Garrick and Melisenda J. McDonald. Department of Medicine, Harvard Medical School, Boston, MA.02115

A covalent adduct of D-glucose-6-phosphate (G6P) and human adult hemoglobin was prepared by in vitro incubation of the phosphorylated sugar and carbonmonoxy-hemoglobin. Structural analysis indicated that G6P was specifically attached to the α-amino groups of the β chains by a ketoamine linkage. In the absence of phosphate, stripped G6P Hb possessed a low oxygen affinity (P_{50} = 12 mm Hg at pH 7, $[Cl^-]$=0.1 M), a slightly decreased value of n (n = 2.3) and a substantially reduced alkaline Bohr effect ($-\Delta \log P_{50}/\Delta$ pH = 0.36) when compared to normal adult hemoglobin. The addition of inositol hexaphosphate did not significantly alter the properties of this modified protein. The sugar phosphate groups, which are covalently bound to the hemoglobin, mimic the effect of free organic phosphate in stabilizing the deoxy form and consequently lowering the oxygen affinity of the molecule. The lack of effect of inositol hexaphosphate on the functional properties of G6P Hb indicates that this organic phosphate and the G6P moiety are competing for the identical binding sites on the hemoglobin molecule. Rapid mixing experiments revealed a slow rate of carbon monoxide combination which was unaltered by the addition of phosphate. Furthermore, a rapid, biphasic oxygen dissociation time course was observed suggesting enhanced α,β chain differences in the liganded form of this protein. A sugar phosphate covalently bound would have an effective concentration that is very large and would significantly bind to the hemoglobin regardless of the state of ligation. Thus, this modified hemoglobin may be a good model to examine the role of organic phosphate in regulating the oxygen binding of liganded as well as unliganded hemoglobin.

W-AM-Po42 The Effect of pH on the Rate of Dissociation of the Oxygenated Beta Chain Tetramer of Hb A. Susan M. Turci and Melisenda J. McDonald (Intro. by Joseph R. Shaeffer). Department of Medicine, Harvard Medical School, Boston, MA. 02115.

The kinetic profile of the subunit assembly process of hemoglobin is affected by the oligomeric nature of the non-α-subunit. McDonald (J.B.C. 256:6487-6490, 1981) has shown that the rate of beta tetramer dissociation to monomer is the limiting step in the overall formation of oxygenated Hb A at 20° and pH 7 in 0.1M potassium phosphate buffer. The presence of phosphate appears to stabilize the tetrameric structure of these isolated heme chains. Since it is known that protons, as well as, phosphate ions, stabilize the tetrameric structure of hemoglobin, an investigation of the effect of pH on the stability of the chain tetramer (as monitored by its rate of dissociation to monomer) was undertaken.

The rate of beta tetramer dissociation was followed spectrophotometrically in 0.1M potassium phosphate buffer at 20°. As the pH was raised from 6 to 8 apparent first order kinetic profiles were observed. Preliminary results yielded rate constants of 0.015, 0.046 and 0.21 min^{-1} at pHs 6,7 and 8 respectively. These findings indicate a substantial effect of protons on the stability of the beta chain tetramer and hence, on the overall hemoglobin tetramer assembly process. Furthermore, this pH dependence is in a direction opposite to that reported for the tetramer to dimer dissociation constant of liganded Hb A.

W-AM-Po43 NMR RELAXATION STUDIES OF THE BINDING OF AMINO ACIDS TO HEMOGLOBIN

Hussein M. K. Zeidan

The University of Michigan-Flint Chemistry Department Flint, Michigan 48503

The mechanism of the binding of amino acids which exhibit some antisickling activity to hemoglobin and sickle hemoglobin has been investigated by NMR proton relaxation time measurements. Upon addition of phenylalanine to hemoglobin and sickle hemoglobin solutions a larger increment in relaxation rate of the aromatic moiety was found than for the side chain methyl groups of either alanine or valine. These results suggest that this aromatic moiety has rapid accessibility to the binding sites, and that the binding occurs essentially by hydrophobic interactions through the aromatic portions of the amino acid. Identical results were obtained by using sickle hemoglobin, which suggests that the binding sites of phenylalanine to hemoglobin and sickle hemoglobin are the same. Site directed paramagnetic nitroxide radicals (spin labels) have been used to perturb the nuclear magnetic resonance spectra of amino acids binding to hemoglobin and sickle hemoglobin. The results of this investigation showed an increase in the relaxation rate of the protons of the aromatic moiety of these antisickling agents. This finding suggests that the binding sites of phenylalanine to hemoglobin and sickle hemoglobin is close to the cysteine residue.

(Supported in part by an NIH research grant to Dr. M. E. Johnson, University of Illinois at the Medical Center)

W-AM-Po44 FLUORESCENCE RELAXATION STUDIES OF PYRIDOXAMINE-5-PHOSPHATE LABELED APOHEMOGLOBIN.Janusz Kowalczic and Enrico Bucci,Dept of Biological Chemistry, University of Maryland School of Medicine,Baltimore MD 21201. The fluorescence of human apohemoglobin labeled at the Val β1 with pyridoxamine-5-phosphate was investigated. At 4° C the lifetime of the excited state was found to be 4.6 and 3.5 ns at pH 6.5 and 7.5 respectively. The intensity at pH 7.5 was two times lower than at pH 6.6. The quantum yield at 5°C at pH 7.0 was 0.21. Correlation times (τ_c) were evaluated from steady state fluorescence anisotropy and lifetimes measurements under quenching by KI. It was found that the major component of τ_c at pH 6.5 was 40 ns and at pH 7.5 was 5.1 ns. Singlet-singlet energy transfer between the label as donor and ANS as acceptor (ANS binds inside the heme pocket) was about 26 Å between the randomly oriented fluorophores. In the tridimensional model of crystalline deoxyhemoglobin the distance between Val β1 and the iron atom of the nearest heme is about 22 Å.

W-AM-Po45 MULTIPLE CONFORMERS IN HEMEPROTEINS. EVIDENCE FROM INFRARED SPECTRA FOR CARBONYL, OXYGENYL, AND CYANO LIGANDS. W.S. Caughey, H. Shimada, M.P. Tucker, and S. Yoshikawa, Department of Biochemistry, Colorado State University, Ft. Collins, CO 80523.

Four CO stretch bands near 1950 cm^{-1} which can be ascribed to four discrete protein conformers in dynamic equilibrium are found to be a general property of myoglobin carbonyls. Relative intensities of IR bands are sensitive to changes in temperature, pH, and protein structure. Detection of only one resonance in ^{13}C NMR spectra indicates interconversions among conformers are more rapid than the NMR time scale. Hemoglobin carbonyls also exhibit multiple bands but only two or three have been detected for a given subunit. OxyMbs and oxyHbs exhibit multiple IR bands for bound O_2 near 1130 cm^{-1}. Although more difficult to establish accurately than for carbonyls, 5 or 6 bands are typically detected for bound O_2. Protein structure affects band frequencies and intensities as do changes in pH and temperature. Multiple conformers for Mb and Hb oxygenyls are thus indicated although some band splitting due to Fermi resonance may occur. Cytochrome c oxidase (CcO) exhibits CO bands $\sim$1964 cm^{-1} for $Fe^{2+}CO$ with 1 to 4 electron reduced species; the presence of a minor band $\sim$1959 cm^{-1} suggests two conformers at each oxidation state. Cyanide binding to CcO is highly dependent on oxidation state. With fully-oxidized species the only band found is at 2152 cm^{-1}, consistent with $Cu^{2+}CN$. One electron reduction results in two bands at 2131 and 2152 cm^{-1} as expected for $Fe^{3+}CN$ and $Cu^{2+}CN$, respectively. With either 2 or 3 electrons added, there is only one band ($Fe^{3+}CN$ at 2131 cm^{-1}). Fully-reduced CcO gives $Fe^{2+}CN$ at 2060 cm^{-1}. Thus, during the sequential addition of electrons to fully-oxidized CcO the metal sites accessible to CN^- are altered and appropriate changes in protein conformation must accompany the changes in oxidation state. Furthermore, band asymmetry gave evidence of multiple C-N conformers at a given site. (Supported by U.S.P.H.S. grant No. HL-15980.)

W-AM-Po46 INFLUENCE OF STRONG OR WEAK FIELD TRANS LIGANDS UPON THE STRENGTH OF IRON-CARBON BOND IN CARBONMONOXY IRON "PICKET FENCE" PORPHYRIN AS DETECTED BY RESONANCE RAMAN SPECTROSCOPY, E. A. Kerr, H. C Mackin and Nai-Teng Yu (Intr. by D. B. Dusenbery), School of Chemistry, Georgia Institute of Technology, Atlanta, GA 30332.

The change in the iron-carbon bond strength brought about by altering the properties of the fifth heme ligand is of intrinsic interest and importance in understanding the phenomenon of cooperativity and the mechanism of protein control of heme reactivity. Such information is now obtainable via resonance Raman spectroscopy.

The ν(Fe-CO) frequency is a direct measure of the iron-carbon strength (in the absence of CO distortion). We report here the ν(Fe-CO) frequencies in the CO complexes of iron(II) "picket fence" porphyrin, Fe(II)TpivPP, with trans ligands of varying strength. With a strong ligand such as 1-MeIm or pyridine, the ν(Fe-CO) in benzene appears at ~489 cm^{-1} which is 23 cm^{-1} lower than that of MbCO despite of the much higher CO affinity for the model hemes. With a weak ligand such as tetrahydrofuran the ν(Fe-CO) is located at 526 cm^{-1} which is 37 cm^{-1} higher than that in strong ligands. X-ray crystallographic data indicate that the Fe-C bond length in Fe(TPP)(CO)(Py) and Fe(deutero)(THF)(CO) is 1.77(2) and 1.706(5)A, respectively.

Binding affinity is not directly correlated with the strength of the Fe-C bond. The CO affinity of Fe "picket fence" (1,2-diMeIm) is known to be ~400 times lower than that of the unconstrained complex (1-MeIm). However, the ν(Fe-CO) for the former (496 cm^{-1}) is higher than that for the latter (489 cm^{-1}). This implies that to account for the difference in ΔG° of CO binding between the two complexes more than one bond must be considered (supported by NIH GM18894).

W-AM-Po47 INVESTIGATION OF STRUCTURAL DIFFERENCES RESPONSIBLE FOR MAGNETIC HYPERFINE INTERACTION CHANGES AT NITROGEN LIGANDS IN HEME SYSTEMS. K. Mishra, T.P. Das, and C.P. Scholes, Dept. of Physics, SUNYA, Albany, NY 12222.

1. Electron nuclear double resonance (ENDOR) of metmyoglobin single crystals shows a 5% inequivalence between the hyperfine couplings of diagonally opposite heme nitrogens. Our molecular orbital (MO) computations show such a hyperfine difference can be explained by $\pm$0.01 Å Fe-N bond length changes between diagonally opposite heme nitrogens. However, small distortions in heme nitrogen coordinates in a direction perpendicular to the Fe-N bond cause no change in hyperfine couplings. We have summed the overall filled MO energies; the change in them resulting from the Fe-N bond length change is less than 100 cal/mole. The underlying cause of the electronic distortion which alters the Fe-N bond length could be asymmetrically arranged heme side chains or asymmetric protein environment.

2. From the mutant Hemoglobin M-Milwaukee, ENDOR has previously been obtained for the proximal histidine Nε of the ferric Beta subunits. When the ferrous Alpha subunits go from deoxy to oxy ligation, there is a 2.5% increase in the histidine hyperfine coupling at the Beta subunits. In our computations we determined that a$\sim$0.03 Å decrease in the Fe-his bond length would account for the hyperfine difference. The decrease in overall MO energy localized at the heme was about 100 cal/mole. This change is much less than the 3 kCal/mole interaction energy that represents the difference of oxygen binding affinity per heme between R and T conformation. This finding is consistent with the view that the quaternary conformational interaction energy is not localized at the heme but is distributed throughout the protein. (Supported by NIH grants AM-17884 and HL-15196).

W-AM-Po48 CHEMICAL POTENTIAL MEASUREMENT OF SICKLE CELL HEMOGLOBIN IN SOLUTIONS AND GELS. M.S.Prouty, V.A.Parsegian, and A.N.Schechter, N.I.H., Bethesda, MD 20205

Using osmotic stress, we have measured the chemical activity of deoxy sickle cell hemoglobin (HbS) between 3° and 37°C over concentrations from 0 to > 50g/dl. We find this method to be practical for determining thermodynamic parameters governing assembly and phase transitions in a large class of protein systems. In the present experiments we immerse dialysis bags containing HbS into large-volume dextran solutions of known osmotic pressure (Prouty et al. 1981. Biophys. J. 33:304a). We determine HbS concentration vs. pressure at 3°, 20°, 30°, and 37°C. In each case, at a specific osmotic stress, the concentration vs. pressure curve suddenly increases slope and the HbS suspension shows a sudden increase in viscosity. These changes occur at HbS concentrations where others have found the onset of gelation. Higher stresses are required at lower temperatures. The change with temperature of the osmotic stress required to effect gelation, when converted into a change of HbS chemical potential with temperature, gives transition entropies and enthalpies in excellent agreement with determinations made by other methods (Ross. 1980. Biophys. J. 32:79). After the onset of gelation, concentration rises dramatically with applied pressure over a concentration range that increases with increasing temperature. Then, in a hitherto-thermodynamically-inaccessible regime of the HbS gel, protein concentration increases gradually with applied stress with a slope that is insensitive to temperature. We expect that the compressive stress of this high concentration region reveals the work of concentrating HbS fibers, while the abruptly changing intermediate region denotes transformation from single-molecule to polymer form. The pressure vs. concentration behavior qualitatively resembles that of a condensing gas.

W-AM-Po49 CHARACTERIZATION OF DCT-TEMPAMINE SPIN LABELLED HEMOGLOBIN AS A PROBE OF THE MOLECULAR DYNAMICS OF THE SICKLING PROCESS. L. Lee, M. N. Kossak, and L. W.-M. Fung, Wayne State University, Chemistry Department, Detroit, Michigan 48202.

The reaction of the spin label 4-(4,6-dichlorotriazinyl)amino-2,2,6,6-tetramethylpiperidine-1-oxyl (DCT-Tempamine) with hemoglobin (Hb) provides an additional means of probing the environment of some of the surface residues of Hb and their role in Hb-membrane interactions. The conventional EPR spectrum of the spin labelled protein indicates that the label exhibits multicomponent motion. Results indicate that the label binds to Hb at a spin label to protein ratio of 1 or 2, depending on the labelling conditions. In order to ascertain the role of specific protein positions in Hb-membrane interactions, we are characterizing the site of the protein to which the spin label covalently attaches by a number of different methods. We have determined that the nitroxide radical enhances the relaxation rate of nearby surface histidine residues by observing the spin echo NMR spectra of the aromatic resonances of labelled Hb. Histidines are also known to mediate the hydrolysis of p-nitrophenylacetate by esterases such as Hb (D. Elbaum and R. L. Nagel, J. Biol Chem. 256, 2280, 1981). The decreased activity of the spin labelled hemoglobin further indicates that the site of chemical modification is histidine. Our initial results indicate that the β chains of Hb are labelled. Using protein chemistry techniques, we are attempting to determine the precise location of the probe in the protein. Furthermore, we are using this spin labelled hemoglobin to probe the structure of sickle Hb and its role in membrane-protein interactions and in the molecular dynamics of the sickling process. (Supported by the Michigan Heart Association (MHA) and NIH; LL is a Res. Fellow of MHA; LF is an NIH Res. Car. Dev. Awardee).

W-AM-Po50 ANALYSIS OF NUCLEATION RATES IN SICKLE HEMOGLOBIN POLYMERIZATION. F. A. Ferrone (Department of Physics and Atmospheric Science, Drexel University, Philadelphia, Pa. 19104), J. Hofrichter and W. A. Eaton (Laboratory of Chemical Physics, NIADDK, NIH, Bethesda, Md. 20205)

Although a large body of kinetic information on Hb S polymerization can be rationalized in terms of a simple homogeneous nucleation model, this model fails to explain the extreme autocatalysis observed in the polymerization progress curves. Recent experiments using laser photolysis to initiate polymerization have suggested a mechanism to explain the autocatalysis by invoking a heterogeneous nucleation process in which new polymers are formed on the surface of existing polymers (Ferrone et al., Biophys. J. 32, 361, 1980). Numerical integration of the coupled differential equations describing this model demonstrated its plausibility, but did not permit the parameters which describe the free energy barriers to nucleation to be determined from the kinetic data. Linearization of the kinetic equations, however, permits them to be analytically integrated and provides a particularly simple form for the initial portion of the kinetic progress curve, viz. $f(t) = A(\cosh Bt - 1)$, where $f(t)$ is the fractional extent of the reaction. Values of the parameters A and B have been determined from least-squares fits of this equation to the experimental data. Using these results, the concentration and temperature dependence of the homogeneous and heterogeneous nucleation rates can be separately determined. Both nucleation rates exhibit a high concentration dependence (>10), which appear to exclude fragmentation of polymers to produce additional nuclei as the origin of the extreme autocatalysis. The results of the analysis can now be used to test statistical thermodynamic models for the free energy barriers to homogeneous and heterogeneous nucleation.

W-AM-Po51 TRANSIENT OPTICAL SPECTRA OF MYOGLOBIN AND HEMOGLOBIN. J. Hofrichter, E. R. Henry, J.H. Sommer, and W. A. Eaton. Laboratory of Chemical Physics, NIADDK, NIH, Bethesda, Md. 20205.

Absorption spectra of Hb and Mb have been measured following photolysis of the CO complex with a Nd:YAG laser (532 nm, 10 ns fwhm). The source for spectral measurements was the fluorescence of a dye with a nanosecond lifetime excited by a second Nd:YAG laser (355 nm, 10 ns fwhm), and the transmitted intensity was detected with a vidicon and optical multichannel analyzer. Difference spectra in the Soret region (400-460 nm) were measured as a function of the time delay between photolysis and probe pulses from -10 ns to +100 μs. Spectra with S/N ratios greater than 100 were obtained by averaging 10 laser shots. For Hb at 21^0C the geminate recombination yield, observed rate of rebinding, spectral changes of the deoxy photoproduct, and rate of these spectral changes were similar to those previously reported by others. For Mb at 21^0C the spectrum of the deoxy photoproduct was identical at all times from -7 ns to +100 μs, suggesting that the heme and surrounding globin achieve their equilibrium conformations in less than about 3 ns. The geminate recombination yield for Mb was 0.06 with an observed rate constant of $1x10^7$ s^{-1}, compared to 0.48 and $2x10^7$ s^{-1} for Hb. In the simplest kinetic model the photolysed CO either rebinds to the heme or escapes from the protein. These data would then require that the higher geminate recombination yield for R-state Hb result from a more rapid formation of the Fe-CO bond, and that movement of the ligand out of the heme pockets of the two proteins occur at about the same rate. Since both the geminate recombination yield and bimolecular combination rates (k_{on}(Hb) = $6x10^6$ $M^{-1}s^{-1}$ and k_{on}(Mb) = $4x10^5$ $M^{-1}s^{-1}$) are about 10-fold higher for R-state Hb, the model implies that the rate of entry of the ligand from the solvent into the heme pocket is about the same in the two proteins as well.

W-AM-Po52 KINETICS OF HEMOGLOBIN S POLYMERIZATION IN SINGLE RED CELLS. M. Coletta, J. Hofrichter, F. A. Ferrone, and W. A. Eaton. Laboratory of Chemical Physics, NIADDK, NIH, Bethesda, Md. 20205. (present addresses; M.C., U. of Rome, Italy; F.A.F., Drexel. U., Phila., Pa.)(Intr. by D.R. Davies).

We have developed a laser-photolysis, light scattering technique to investigate the kinetics of Hb S polymerization in single red cells from patients with sickle cell disease. Deoxy Hb S is prepared in about 1 ms by photolysis of the carbon monoxide complex, using an argon ion laser focussed to a diameter of 3 μm. Polymerization is detected by an increase in the scattered laser light. As in solutions of purified Hb S, there is a marked delay prior to the onset of polymerization. The kinetic progress curves for polymerization in cells are the same as those observed in solution, except in cases where cell shape changes contribute to the change in light scattering. As expected from solution studies, there is a broad distribution of delay times in a cell population, ranging from a few milliseconds to tens of seconds, with a most probable delay time of about 30 ms. Also stochastic behavior is observed for cells with delay times longer than about 1 s. All of the results so far indicate that polymerization inside sickle cells proceeds by the same nucleation mechanism as in solutions of purified Hb S. Using the concentration dependence of the delay time found for solutions, the distribution of intracellular Hb S concentrations can be calculated from the distribution of delay times. This concentration distribution, together with solution data, can then be used to calculate the cell data on oxygen binding, morphologic sickling, extent of polymer formation, and polarized optical absorption. It is clear that this new experimental technique will be extremely useful for studying the relation between delay time of polymerization and clinical severity of sickle cell disease and for assessing the effect of potential therapeutic inhibitors.

W-AM-Po53 STOCHASTICS OF HOMOGENEOUS NUCLEATION IN HEMOGLOBIN S POLYMERIZATION. J. Hofrichter, W. A. Eaton (Laboratory of Chemical Physics, NIADDK, NIH, Bethesda, MD 20205) and F.A.Ferrone (Dept. of Physics and Atmospheric Sciences, Drexel U., Philadelphia, PA 19104) (Intr. by T. L. Hill)

In a series of experiments in which the polymerization kinetics were studied by initiating the reaction by laser photolysis of very small volumes ($<10^{-9}cm^3$) of CO hemoglobin S, a continuous increase in the variability of the delay time was observed for delay times longer than about 10 sec (Ferrone et al., Biophys J.,32,361(1980)). To systematically study this phenomenon we have developed a computer-controlled experiment in which large numbers of progress curves can be measured sequentially on a single sample. For delay times below 1 sec roughly gaussian distributions having a width equal to approximately 5% of the delay are observed. For samples having delay times >20 sec we observe a minimum delay time and a broad distribution, skewed toward short times, for which the standard deviation is comparable to the mean value of the delay. Although the delay times may vary by over a factor of 10, the shape of the polymerization progress curves is identical once polymerization is detected. These results are readily interpreted using a double nucleation model in which polymerization is initiated by nucleation of individual polymers in the solution phase (homogeneous nucleation) and autocatalysis is produced by nucleation of additional polymers on the surface of existing ones (heterogeneous nucleation). The stochastic behavior is interpreted as arising from the low probability per unit time, λ, of homogeneously nucleating a single polymer in the small sample volume. Assuming steady state nucleation, λ can be obtained by fitting the function $\exp(-\lambda t)$ to the observed distribution function after correcting for the time required to detect polymerization after the nucleation event. The initial portion of the individual progress curves additionally yields a product of the heterogeneous nucleation rate and the rate of polymer growth.